Titre: Title:	Steel Truss Moment Frames with Seismic Energy Dissipation Elements and Self-centering Capacity
Auteur: Author:	Keyhan Faraji
Date:	2025
Type:	Mémoire ou thèse / Dissertation or Thesis
Référence: Citation:	Faraji, K. (2025). Steel Truss Moment Frames with Seismic Energy Dissipation Elements and Self-centering Capacity [Thèse de doctorat, Polytechnique Montréal]. PolyPublie. https://publications.polymtl.ca/65789/

URL de PolyPublie: PolyPublie URL:	https://publications.polymtl.ca/65789/
Directeurs de recherche: Advisors:	Robert Tremblay
Programme: Program:	Génie civil

POLYTECHNIQUE MONTRÉAL

affiliée à l'Université de Montréal

Steel Truss Moment Frames with Seismic Energy Dissipation Elements and Self-centering Capacity

KEYHAN FARAJI

Département des génies civil, géologique et des mines

Thèse présentée en vue de l'obtention du diplôme de *Philosophiæ Doctor*

Génie Civil

Janvier 2025

POLYTECHNIQUE MONTRÉAL

affiliée à l'Université de Montréal

Cette thèse intitulée :

Steel Truss Moment Frames with Seismic Energy Dissipation Elements and Self-centering Capacity

présentée par **Keyhan FARAJI**

en vue de l'obtention du diplôme de *Philosophiæ Doctor*

a été dûment acceptée par le jury d'examen constitué de :

Bruno MASSICOTTE, président
Robert TREMBLAY, membre et directeur de recherche
Richard SIMON, membre et co-directeur de recherche
Pierre LÉGER, membre
Jeffrey EROCHKO, membre externe

DEDICATION

Dedicated to my family,

ACKNOWLEDGEMENTS

I wish to extend my deepest gratitude to my dear family for their unwavering support and encouragement along this journey. I am eternally indebted to them for their endless patience, and love.

RÉSUMÉ

L'application des éléments de dissipation d'énergie combinée au mécanisme d'auto-centrage dans les nouveaux systèmes structurels a fait l'objet de nombreuses études réalisées au cours des trois dernières décennies pour améliorer la résistance sismique et la résilience des structures et développer des systèmes durables à utiliser dans les zones vulnérables à des tremblements de terre intenses et fréquents.

Cette recherche a proposé deux types de cadres de moment en treillis parasismique et réparables, notamment 1) des cadres de moment en treillis équipés d'amortisseurs de friction et de tendons en acier (FT-TMF) et 2) un cadre de moment en treillis avec amortisseurs de friction et noyau basculant post-tendu. (RF-TMF). Ces systèmes sont conçus pour subir peu ou pas de dommages et rester opérationnels après un séisme de niveau de conception, nécessitant aucune ou une réparation minimale.

Le système FT-TMF est un cadre de moment en treillis en acier avec des amortisseurs de friction installés entre la corde inférieure du cadre et les colonnes adjacentes et une paire de tendons élastiques dans chaque travée qui relient la corde inférieure du cadre aux colonnes. Lors d'un événement sismique, une partie considérable de l'énergie sismique se transforme en chaleur et est dissipée par les amortisseurs à friction tandis que les tendons confèrent au système une capacité d'auto-centrage qui atténue les dérives résiduelles. Des poutres au niveau de support sont installées dans les TMFs à proximité des bases des colonnes pour protéger les colonnes contre les dommages sismiques.

Le deuxième système, RF-TMF, est un système hybride composé de deux cadres en treillis équipés d'amortisseurs à friction, avec un rôle et une position similaire à ceux des FT-TMF, et d'un cadre à bascule rigide avec des tendons post-tendus entre les deux qui sont interconnectés via les poutres de liaison.

Le noyau basculant supprime l'effet des modes supérieurs lors d'un tremblement de terre et régule le mouvement latéral de l'ensemble du système pour se conformer au modèle de déplacement du premier mode, tandis que les tendons post-tendus installés dessus assurent la stabilité et offrent au système une capacité d'auto-centrage qui réduit les dérives.

Un ensemble de joints de connexion résistant aux moments et réparables avec des détails spécifiques ont été installés dans les joints reliant les poutres de liaison et le noyau basculant et de la même manière dans les joints reliant les poutres de niveau de support et les colonnes dans les TMFs pour contrôler les dommages et participer au processus de dissipation d'énergie.

Comme objectif principal des systèmes proposés, l'absorption d'énergie fournie par les dispositifs de friction principalement et le mécanisme d'auto-centrage offert par les tendons élastiques, ou le noyau basculant post-tendu, sont utilisés pour créer un système structurel résilient à faible dommage et rapidement réparable pour l'application dans les zones sujettes à des tremblement de terre fréquents et forts.

Les deux systèmes proposés ont été étudiés en deux phases. La première phase poursuivie dans cette recherche était axée sur l'étude de la réponse sismique du système FT-TMF conçu conformément aux normes canadiennes et américaines. Pour évaluer la performance du système et vérifier la méthode de conception proposée conformément à la pratique canadienne, le système FT-TMF est modélisé et analysé comme système structurel résistant aux charges latérales pour des bâtiments de 4, 7 et 12 étages conçus pour un site à Vancouver, en Colombie-Britannique, conformément au Code national du bâtiment du Canada (CNBC 2015) et à la norme pour la conception des structures en acier au Canada (CSA S16-19). Des modèles structurels des structures archétypales ont été simulés dans les logiciels OpenSees et SAP2000 et une série d'analyses spectrales, statiques non linéaires et dynamiques non linéaires ont été utilisées pour évaluer leurs réponses sismiques. Le nouveau système a présenté un comportement hystérétique fiable, des dérives sismiques résiduelles triviales et est resté intact lors des tremblements de terre de conception, garantissant un niveau de performance d'occupation immédiat, comme en témoignent les résultats de l'étude.

Ensuite, pour approfondir les performances du système et vérifier l'efficacité de la méthode de conception proposée conformément à la pratique américaine, le processus de chargement et de conception de la structure a été réalisé à nouveau, en respectant les normes et spécifications ASCE 7-22, AISC 360-16 et AISC 341-16. Ensuite, une suite de 44 enregistrements sismiques de champ lointain suggérés dans la norme FEMA P-695 a été utilisée pour effectuer l'évaluation du risque d'effondrement de la structure et les courbes de fragilité correspondantes ont été obtenues pour les points d'effondrement prévus. Les capacités d'effondrement médianes, qui indiquent que la moitié

des enregistrements entraînent un effondrement, ont été utilisées pour mesurer les taux de marge d'effondrement (CMR) des archétypes. Les ratios de la marge d'effondrement ajustés (ACMR) répondent aux critères d'acceptation FEMA P-695, comme le montrent les résultats.

Dans la deuxième phase de la recherche, l'accent a été mis sur l'étude du comportement sismique du système hybride RF-TMF proposé. À cet égard, le nouveau système RF-TMF a été étudié comme système de résistance latérale d'un ensemble de bâtiments archétypaux de 7, 9 et 12 étages considérés comme étant situés dans une zone sismique élevée avec des failles actives dans la région de Los Angeles. Californie, États-Unis. Des modèles structurels numériques du système ont été développés dans OpenSees et analysés sous l'effet de 22 enregistrements sismiques en champs lointain de FEMA P-695 pour étudier leurs performances sismiques. Les données analytiques obtenues ont montré que les TMF et le noyau basculant s'adaptaient bien et fonctionnaient comme un système hybride, de sorte que le système présentait une réponse hystérétique stable, un mouvement latéral conforme au premier mode, un faible dommage contrôlé et des dérives latérales limitées qui ont vérifié le niveau de performance sismique satisfaisant et la réparabilité viable post-événement attendue. Enfin, les résultats analytiques satisfaisants ont vérifié la fiabilité de la procédure proposée utilisée dans l'analyse et la conception du nouveau système hybride.

Dans l'ensemble, les systèmes FT-TMF et RF-TMF proposés ont démontré des performances sismiques robustes et ont accompli les objective de conception.

.

ABSTRACT

Application of energy dissipation elements combined with self-centering mechanisms, in novel structural systems has been the subject of many studies over the past three decades to improve seismic resistance and resilience of the structures and develop sustainable systems to be utilized in the areas vulnerable to intense and frequent earthquakes.

This research proposed two types of earthquakes-resistant and repairable systems based on steel truss moment frames including 1) truss moment frames equipped with friction dampers and steel tendons (FT-TMF) and 2) truss moment frame with friction dampers and post-tensioned rocking core (RF-TMF). These systems are intended to experience no or low damage and remain in service after a design-level seismic event requiring no or minimum repair.

The FT-TMF system is a steel truss moment frame with friction dampers installed between the bottom chord of the truss and the adjacent columns at the end panels and a pair of elastic tendons in each span which connects the bottom chord to the columns. During a seismic event, a considerable portion of the seismic energy is transformed into heat and dissipated by the friction dampers while the tensile force developed in the tendons provide the system with self-centering capacity and mitigates the residual drifts. Support-level grade beams are accommodated close the columns' feet to protect the columns against seismic damage.

The second system, RF-TMF is a hybrid system composed of two truss frames equipped with friction dampers, with a similar role and position they have in FT-TMFs, and a post-tensioned rigid rocking core (frame) in between that are interconnected via link beams. The rocking core suppresses the effect of higher modes during an earthquake and regulates the lateral movement of the whole system to conform the first mode displacement pattern, while the post-tensioned tendons, installed through their height, provides the system with stability and self-centering capability that reduces the drifts. A set of repairable moment resisting connection joints with specific details are installed in the joints connecting the link beams and the rocking core, and similarly in the joints connecting the support-level grade beams and the columns in the TMF, to control damage and participate in the energy dissipation process. As a main objective in the proposed systems, the energy absorption provided by the friction devices and elastic tendons, or the post-tensioned rocking core are employed to create a resilient low damage and quickly restorable structural system for application in areas prone to frequent and strong ground motions.

The two proposed systems were investigated in two phases. The first phase pursued in this research was focused on the investigation of the seismic response of the FT-TMF system designed in accordance with the Canadian and the U.S. standards.

To evaluate the performance of the system and verify the proposed design method in accordance with Canadian practice, the FT-TMF system were modeled and analyzed as the lateral load resisting structural system for a 4-, 7- and 12-storey archetypal buildings which were designed for a typical active seismic site in Vancouver, British Columbia. The buildings were designed in accordance with the National Building Code of Canada (NBCC 2015) and the standard for the design of steel structures in Canada (CSA S16-19). Structural models of the FT-TMFs in the representative buildings were simulated in OpenSees and SAP2000 software and a series of spectral, nonlinear static, and nonlinear dynamic analyses were employed to capture their seismic responses. The new system exhibited reliable and stable hysteretic behaviour, trivial seismic residual drifts, and remained undamaged under design earthquakes, warranting immediate occupancy level of performance, as evidenced by the study outcomes. Then To further investigate the system performance and verify the efficacy of the proposed design method in alignment with American practice, the design of the structure was performed again, adhering to the U.S. standards and specifications of ASCE 7-22, AISC 360-16 and AISC 341-16. Following the design, a suite of 44 far-field ground motion records from FEMA P-695 was used to conduct the collapse risk assessment of the structures and the corresponding fragility curves were derived. The median collapse capacities, the intensity that half of the records result in collapse, were employed to measure the Collapse Margin Ratios (CMRs) of the archetypes. The adjusted collapse margin ratios (ACMRs) were found to meet the FEMA P-695 acceptance criteria.

The second phase of the research was focused on the investigation of seismic behavior of the hybrid RF-TMF system. In this regard the RF-TMF system was studied as the lateral resisting system of a set of 7-, 9- and 12- storey archetypal buildings that were considered to be located at a high seismic hazard zone with active faults in Los Angeles Area, CA, USA. Numerical structural models of the system were developed in OpenSees and analyzed under 22 far-field ground motion records from FEMA P-695 to investigate their seismic performance. The obtained analytical data showed that the TMFs and the rocking core adapted well and functioned as a hybrid system, resulting in a stable hysteretic response, lateral movement consistent with the first mode, controlled low damage, and limited lateral drifts. These findings validated the satisfactory seismic performance level and

the expected post-event viable repairability. Finally, the satisfactory analytical results verified the reliability of the proposed procedure used in the analysis and design of the new hybrid system.

Overall, the proposed FT-TMF and RF-TMF systems exhibited robust seismic performance and accomplished the design objectives.

.

Table of Contents

LIST OF TABLES

LIST OF FIGURES

LISTE OF SYMBOLS AND ABBREVIATIONS

Abbreviations:

2D 2-Dimensional

AISC American Institute of Steel Construction

ASCE American Society of Civil Engineers

BRB Buckling Restrained Brace

CSA Canadian Standards Association

EQ Earthquake

FEMA Federal Emergency Management Agency

F-TMF Truss Moment Frame equipped with Friction damper

FT-TMF Truss Moment Frame equipped with Friction damper and steel Tendons

IDA Incremental Dynamic Analysis

MCE Maximum Considered Earthquake

NBCC National Building Code of Canada

NTHA Nonlinear Time history Analysis

PT Post-Tensioned

R Rocking

RC Rocking Core

RSA Response Spectrum analysis

RF-TMF Post-Tensioned Rocking Truss Frame

SC-SPSW Self-centering Steel Plate Shear Wall

SESBF Segmental Spine Braced Frame

STMF Special Truss Moment Frame

TMF Truss Moment Frame

Symbols:

A	Cross Section
δ	Elongation
Δ	Displacement
E	Modulus of Elasticity
h_s	Storey Height
h	Height
K	Stiffness
L_R	Lever Arm
$M_{P-\Delta}$	P-Δ Moment
M_v	Seismic Moment
P	Gravity Load
R_d	Ductility Factor
R_o	Overstrength Factor
R	Response Modification Factor
T	Tensile Force
V	Base Shear

CHAPTER 1 INTRODUCTION

1.1 Background

Truss moment frame (TMFs) is an economic system to construct single and multi-storey long span structures covering large areas such as arenas, shopping malls, aircraft hangers, warehouses, office buildings and industrial facilities. These frames, which consist of open web truss form girders and solid web columns, are designed to resist both gravity loads, and lateral forces applied by winds and or seismic events. This system outperforms moment frames (MFs) in various dimensions, such as economic efficiency for long spans, fabrication convenience, installation speed, and connection simplicity. Moreover, in TMFs the installation and placement of the wiring, piping, ductworks, and other electrical and mechanical equipment through web openings in its girders is more convenient compared to MFs with solid web beams that leads to better use of the interior space from an architectural perspective (Basha & Goel, 1994; Goel & Itani, 1994). Additionally, in this system, the structural components and connections are largely visible and readily accessible, thus structural and fireproofing inspections, repair and retrofit can be conveniently executed. Based on current design codes, TMFs are normally designed to experience no and low damage during minor and moderate seismic shakings, while when subjected to strong earthquakes they are expected to suffer damage in their structural elements, however they must remain stable and provide life safety level of performance. Conventional TMFs in various architectural forms, shapes and dimensions have been used in many countries throughout the world. The exploratory inspections after the 1985 Mexico City earthquake revealed that conventional TMFs had acted as a weak column-strong girder system and exhibited poor seismic response which had resulted in uncontrolled damage in the trusses as well as columns. Local buckling in columns, fractures and local failure in the girders were some of the reported deficiencies that had led to significant strength and stiffness degradation in the buildings constructed with ordinary TMFs, resulting in critical structural damage in many and collapse in some cases (Itani & Goel, 1991; Ger et al., 1993).

To enhance the seismic behavior of TMFs, comprehensive research on this system carried out in the 1990s that culminated in the development of an advanced TMF system, termed Special Truss Moment Frame (STMF), that has superior performance against severe earthquake due to its special detailing based on the strong column-weak girder approach. Accordingly, the research on the earthquake resilient STMFs led to better understanding about its behavior and development of

seismic design criterion for this system that have been incorporated into the AISC seismic provisions since 1997. Currently, the seismic requirements, which also cover STMF, are included in CSA standard and in many design codes in other countries. In STMF system, subjected to severe ground motions, controlled inelastic deformations are provided in chord members within central special ductile segments of the trusses. Other truss members and columns are designed to remain essentially elastic. This ductile system is expected to demonstrate a good energy dissipation capacity and strength under strong seismic events. Further studies led to the introduction of more advanced types of STMFs such as truss moment frames with buckling restrained knee braces (BRBs) accommodated at their end panels to control the seismic plastic deformations. Less damage and easier post event maintenance is expected for the latter STMF system.

Despite the efficacy of STMFs in ensuring the life safety of the occupants under strong ground motions, owing to lengthy post-event repair process, they are still vulnerable to further damage that could compromise their stability under doublet earthquakes or intense aftershocks. Moreover, the large plastic deformation in the special segments could lead to large drifts and increase the risk of damage in the other structural and non-structural elements (e.g., roof elements). Therefore, development of no or low damage TMF systems, with a sustainability approach, that could provide higher level of seismic resistance and facilitate post-event restoration and realignment process can be a considerable advancement in STMF systems. In this regard, at first phase of this research a novel earthquake resistant TMF systems named FT-TMF is proposed and studied. In this system, which is considered as an advanced STMF system, the ductile segments are replaced by friction dampers, accommodated in the bottom chords of the girders at the end panels to dissipate a portion of the kinetic energy imposed in the system during a strong seismic event and limit the seismic force induced in the rest of the structure. A pair of elastic tendons, installed in parallel with the dampers, connects the bottom chords to the adjacent columns. These tendons act simultaneously with the friction dampers and endows the system with positive stiffness that limit the lateral drift in post-slip range, resulting in obviation of drift-induced damage in the structural and non-structural elements.

In the second phase of this research, two TMF system equipped with friction devices (F-TMF) are paired with a post-tensioned rocking core (R) installed in the between to form a hybrid structural system, named RF-TMF, that can exhibit a satisfactory seismic behavior with viable after event repairability. The superior performance of post-tensioned rigid rocking systems with various

configurations in suppressing the higher mode effects and eliminating the residual drifts have been validated in several numerical studies and experimental tests in the past Moreover, the former studies and experimental tests showed that the post-tensioned rocking cores, upgraded with energy dissipation elements, can represent an optimal flag-shape force-displacement response during ground motion (Ajrab et al., 2004; Deierlein et al., 2011; Grigorian et al., 2017; Steele et al., 2017).

The aim of this system was to combine the advantages of a post-tensioned rocking core (R) and a truss frame enhanced with friction dampers (F-TMF) to create an advanced structural system that could exhibit satisfactory seismic response and feasible post-event repairability.

In this hybrid system (RF-TMF), the rigid rocking core mitigates higher-mode effects and regulates lateral movement during earthquakes, ensuring that the entire system follows the first-mode movement pattern. Meanwhile, the post-tensioned tendons installed in the rocking core play a crucial role in stabilizing the system, while also applying a re-centering moment, limiting lateral displacements and mitigating residual drifts. In parallel a large portion of the seismic energy is dissipated by the friction dampers installed in the F-TMFs.

In this research the structural models of the introduced FT-TMF and RF-TMF systems were simulated in finite element software including OpenSees and SAP2000 to analyse their seismic behavior and develop appropriate design procedures for this system.

1.2 Research methodology

The methodology utilized to attain the research objectives comprises the following steps:

1- Past studies led to the development of different types of STMFs, and the pertinent design procedures were reviewed. Moreover, the seismic design requirements for the STMFs included in the design codes: CSA S16-19 (The Canadian Standards Association, 2019) in Canada and AISC 341-16 (The American Institute of Steel Construction, 2016a) and AISC 360-16 (The American Institute of Steel Construction, 2016b) in the U.S. were studied.

2- A number of structural elements such as connections and braces with energy dissipation capacity and re-centering mechanisms that have been developed and studied by various researchers in the past two decades were studied.

3- The different configurations of the rocking and strong back structural systems, that have been proposed and investigated by various researchers during the past two decades, were reviewed.
4- A number of relevant technical documents that have been produced by the manufacturers representing the specifications of different types of friction devices, friction ring springs, elastic springs and high-strength tendons were studied to attain a profound comprehension of their empirical attributes and capabilities.
5- The configurations of the two innovative FT-TMF and RF-TMF systems were proposed. A simple and practical analysis and design procedure was developed for each system.
6- The structural models of the proposed systems as the lateral resisting system of multi-storey archetypal buildings were simulated in OpenSees (Mckenna, 2020) and SAP2000 (Computers&Structures Inc., 2023) software. Special efforts and considerations devoted to select, calibrate and or combine the appropriate material and elements in the utilized software to properly simulate the real behavior and characteristic of some special elements including friction dampers, tendons, plastic hinges and fuse connections. Two different software were utilized in the numerical modeling process to compare the analytical result and minimize the computational calculation errors to achieve more precise and reliable results.
7- The archetypal buildings were subjected to a set of non-linear static analyses (pushover), to have a better understanding of the proposed systems' global behavior of the system and the functionality of the special elements such as friction dampers and the steel tendons, under the lateral loading condition.
8- The structural models of the FT-TMF system, as lateral resisting system in a set of 4-, 7- and 12-storey typical buildings in Vancouver area in Canada, were designed in accordance with Canadian standards including NBCC 2015 (National Research Council of Canada, 2015) and CSA S16-19 (The Canadian Standards Association, 2019). The seismic behavior of the archetypal buildings and the functionality of the friction dampers and self-centering steel tendons were tested by means of non-linear time history analyses. The captured responses were used to evaluate the seismic performance level of the representative buildings.

9- The loading condition (gravity and seismic) on the modeled FT-TMF were modified for Los Angeles area in the western U.S. in accordance with ASCE 7-22 (The American Society of Civil Engineers, 2022) and redesigned in accordance with AISC 341-16 (The American Institute of Steel Construction, 2016a) and AISC 360-16 (The American Institute of Steel Construction, 2016b)guidelines. Then they were subjected to Incremental dynamic analyses (IDA) under a set of 44 FEMA P-695 (Federal Emergency Management Agency 2009) ground motions, to explore their seismic performance, resilience and collapse capacity. The effect of tendon size on the system's strength and capacity was also studied.
10- The structural model of the RF-TMF system, as the lateral load resisting system in a set of 7-, 9- and 12-storey archetypal buildings in Los Angeles area, were designed in accordance with AISC 341-16 and AISC 360-16. Then they were subjected to a set of dynamic time history analyses under a set of 22 earthquake records to explore their global seismic behavior and performance level, the compatibility of the truss frames with the rocking core and the functionality of the friction dampers and the post-tensioned tendons.

1.3 Objectives and scope of the study

The principal objective of this research is to introduce novel and practical earthquake-resistant and sustainable structural systems, FT-TMF and RF-TMF, for seismically active areas. These systems are intended to exhibit a satisfactory seismic resistance and maintain their operability after intense earthquakes with minimal or no need to post-event repair and realignment.

The main goal of the research is delineated as follows:

1- To develop two novel earthquake resistant no or low damage systems, FT-TMF and RF-TMF, with viable post-event repair and realignment capability.
2- To develop a simple and practical analysis and design procedures for the proposed systems and verify the efficacy of the suggested procedure in a set of multi-storey archetypal buildings subjected to a series of numerical non-linear static and dynamic analyses.
3- To validate the functionality of friction dampers and steel tendons during ground motions in FT-TMF and RF-TMF systems.

4- To validate the compatibility of the rocking system paired with the truss frames and its competence in mitigating the higher mode effects and improving the seismic response in the hybrid RT-TMF system.

The scope of this study is limited to numerical simulations and computational analyses of three multi-storey prototypes for each proposed system.

1.4 Organization and thesis structure

This PhD dissertation is prepared and presented in seven (7) chapters. Three (3) journal articles that have been derived from the findings of this study are incorporated as the three (3) body chapters of this thesis.

Chapter 1 Introduces the main topic of this inquiry, providing relevant background information and outlining the methodology employed in this study.

Chapter 2 Reviews the past studies, experimental tests and technical effort performed by other researchers. This chapter encompasses a discussion on the prior investigations pertaining to TMFs and the evolution of the special segment concept for energy dissipation in STMFs. Furthermore, a review of several self-centring connections and an advanced bracing system equipped with energy dissipating components that have been previously devised is presented. Additionally, a brief overview of elastic spine (strongback) systems and controlled rocking frame is provided.

Chapter 3 Provides a detailed technical description of the developed systems and elucidates the methodology and approaches adopted to accomplish the objectives of this research.

Chapters 4, 5, 6 Include the following three articles that have been submitted for publication in scientific journals:

1) Advancement in truss moment frames' seismic behaviour with friction dampers and tendons
2) Seismic collapse assessment of truss moment frame with friction dampers and steel tendons
3) Truss moment frame system with friction dampers and post- tensioned rocking core

Chapter 7 Concludes and finalizes the doctoral dissertation emphasizing the main novel contributions. A set of suggestions for future studies is also provided in this chapter.

CHAPTER 2 LITERATURE REVIEW

2.1 Special Truss Moment Frames (STMFs)

Special Truss Moment Frames, named STMFs, are earthquake resistant truss moment frames that were introduced in 90's after the poor performance of conventional TMFs revealed during the 1985 Mexico City earthquake. As a representative case, the 22-storey Pino Suárez complex, which included five steel-frame buildings experienced such significant combination of seismic damage in the open web frames (trusses) that they became unstable and collapsed. Buckling of columns in lower floors, local failure occurred in nearly all girders and failure in braces were some of the observed damages. The collapse mechanism that occurred in this complex verified the detrimental effect of weak column-strong girder combination in the employed ordinary open web frames that led to formation of soft storey mechanism and failure (Peterson, 1986; Osteraas & Krawinkler, 1989; Ger et al., 1993; Goel & Itani, 1994).

Accordingly, Goel and Itani (1990) carried out an extensive study including numerical analyses and laboratory tests on ordinary truss moment frames (OTMF) to investigate the damage propagation mechanism and improve seismic design practice in these systems. In this way they fabricated a number of full-scale sub-assemblages containing a column and half-span floor Warren truss taken from a 4-storey building in each sample, which were designed in accordance with UBC 1988, applying the load combination of 1.25D+0.5L+1.5E on them. It should be noted that they selected Warren system, because of the widespread use of this type of truss frame in construction projects. Then they applied large cyclic deformations to the prototypes to approximately simulate the behaviour of the truss moment frames during severe earthquakes.

The test resulted in the occurrence of buckling and early fractures in diagonal members similar to the damages developed in truss moment frames during the Mexico City earthquake (Goel & Itani, 1994). A typical fracture, observed in the mentioned test, is illustrated at Figure 2-1.

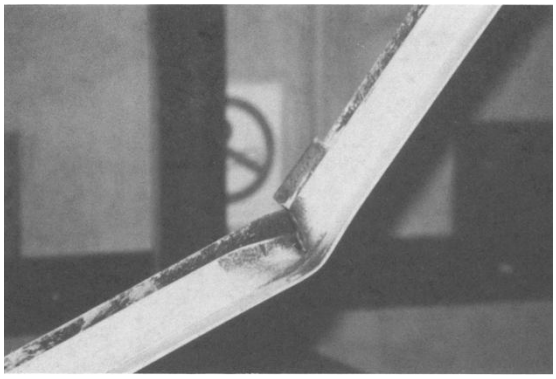

Figure 2-1 : Fracture in diagonal web member (Goel & Itani, 1994)

Goel (1994) also observed that the buckling of diagonals due to compression caused shear force strength decrease that led to reduction in lateral force resisting capacity. In addition, when the diagonals were subjected to compressive forces, they buckled, and the adjacent tension diagonals created unbalanced forces on the chord members leading to squashing phenomenon in the truss and local buckling in diagonal members built of non-compact single angles (Goel & Itani, 1994).

The force-displacement hysteresis loops of the tested conventional TMF that indicate its severely poor performance under lateral loading conditions, are exhibited at Figure 2-2. In these cyclic loops loop, the decline in lateral load and substantial diminution in the strength and stiffness is evident.

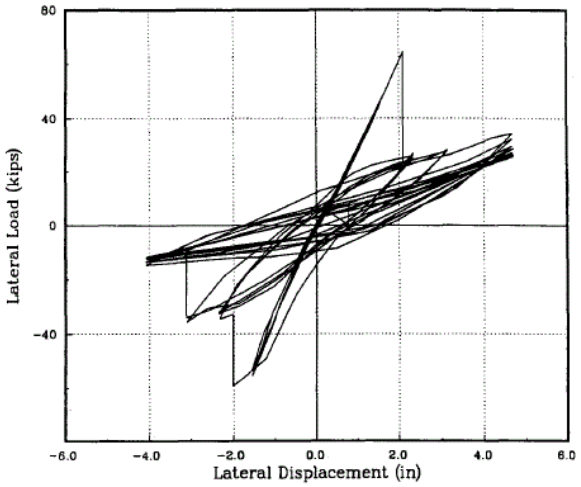

Figure 2-2 : Hysteretic loop in a conventional truss frame under quasi static cyclic loading (Goel & Itani, 1994)

As a consequence of the investigations on the conventional truss moment frames, there emerged a pressing need for a daring endeavor to revise and enhance this system and apply a new design procedure. Finally, the studies led to the development of a new type of truss moment frames including a ductile special segment in the mid panel of girders. In this new system, which is considered a strong column-weak girder combination, a limit state design approach is applied to ensure that, during intense seismic events, the plastic behaviour is confined to the ductile segment, while the remainder of the structure would essentially preserve its elasticity (Goel & Itani, 1994). This seismically resilient TMF system was termed Special Truss Moment Frame (STMF).

The seismic design provisions of truss moment frames have been developing during the last three decades, and seismic design requirements for STMFs have been in force in the AISC seismic provisions since 1997. They are also currently included in the design codes of other countries such as CSA S16-19 in Canada.

In accordance with the current seismic provision, the following main criteria are accepted in design of seismic resilient structures including structures built of truss moment frames:

- In minor earthquakes, structures should remain intact without any damage
- In moderate earthquakes some damage in non-structural elements can occur
- In severe earthquakes, structures must not collapse but they can experience some non-structural and structural damage.

Presently, in accordance with seismic provisions such as CSA S16-19 and AISC-341-16 the truss moment frames can be designed with special segments. Special Truss Moment Frames (STMF) with X-diagonal and Vierendeel special segments, developed in 90s are reviewed below. Subsequently, the STMF system with Buckling-Restrained Knee Bracing special segments (BRKB) , developed a decade later, are briefly discussed.

2.1.1 Truss moment frames with ductile X-diagonals and Vierendeel segments

Truss moment frame with X-diagonal special segment is the first generation of STMF developed in the 1990s. In this system the special segments are composed of X-diagonals and chords in mid span where the shear forces, caused by gravity loads, are minor (Figure 2-3). The X-diagonal web

members are normally built of double compact sections to eliminate local buckling and increase ductility of the system.

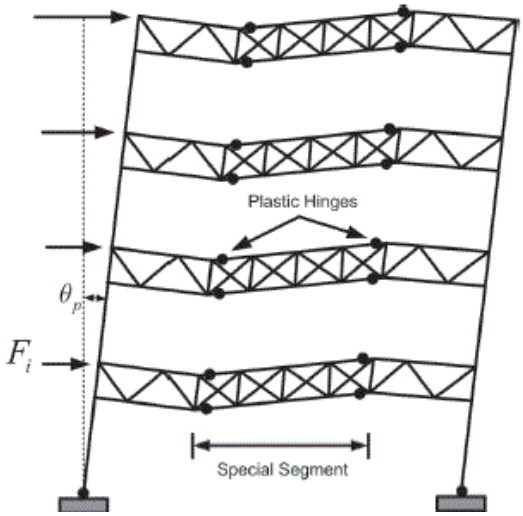

Figure 2-3 : A typical STMF system with X-braced special segments (Goel & Itani, 1994)

As it is shown in the free body diagram (Figure 2-4), in this system the lateral forces such as earthquake loads, induce vertical shear force in the special segment which is resisted and dissipated by the diagonal and the chord members (Goel & Itani, 1994; Goel et al., 1997).

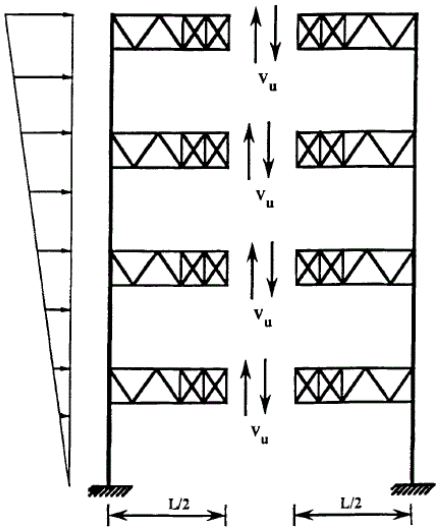

Figure 2-4 : Free body diagram of a truss moment frame with X-diagonal special segment, subjected to lateral forces (Goel & Itani, 1994)

During a severe earthquake the induced vertical shear forces cause yielding and buckling of the diagonal members that culminate in the formation of plastic hinges at the extremities of the chord members in the special segment, endowing the truss moment frames with requisite ductility and seismic energy dissipation capacity through regulated inelastic deformations.

In design of this system, it should be considered that when the special segment is fully yielded, the truss frame's lateral drift should be limited to less than 3 percent, and the seismic moment induced in beam to column connections should be less than their flexural yield strength to prevent brittle failure in the connections. Because the seismic damage in this system is concentrated in the ductile special segments with replaceable elements, it is considered as a low damage and restorable system. However, the replacement and repair process could take considerable time and result in a temporary suspension of the structures' occupancy.

The performance of this STMF system was verified by a set of experimental tests, including quasi-static cyclic loading on a one-storey sub-assemblage that comprised a full truss frame with an X-diagonal special segment (Goel et al., 1997). Development of the controlled damage and formation of plastic hinges in the X-diagonal special segment during the experimental test are illustrated in Figure 2-5.

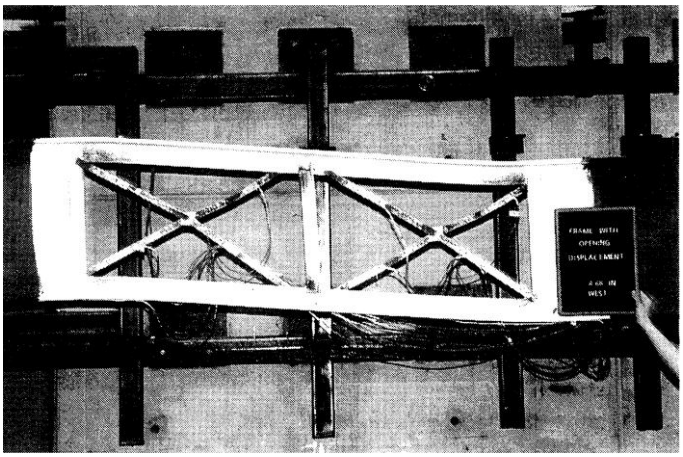

Figure 2-5 : Yielding, buckling and plastic hinges in the opening (Goel et al., 1997)

The stable hysteresis behaviour of this system with a satisfactory energy dissipation capacity under quasi static cyclic loading test is shown in Figure 2-6.

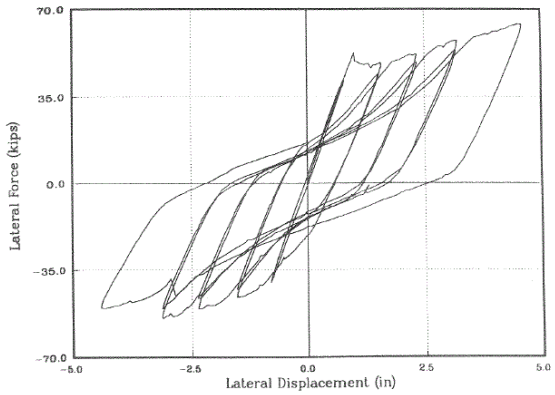

Figure 2-6 : Hysteretic loop of a truss moment frame with X-diagonal special segment under quasi static cyclic loading (Goel et al., 1998)

Later studies on the STMFs, mainly conducted by Basha and Goel (1994-1995), led to development of a truss moment frame with a Vierendeel special segment located in mid panel of the girder (Figure 2-7).

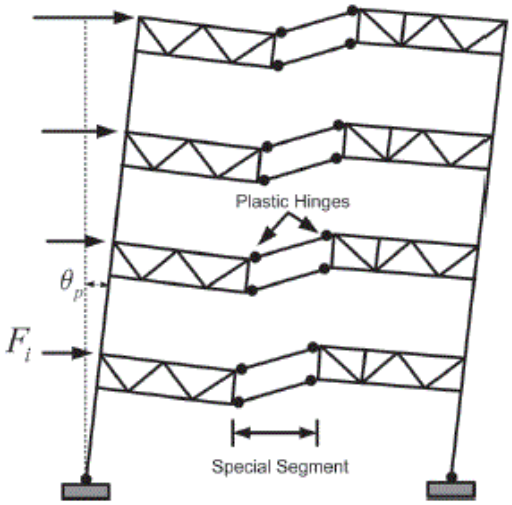

Figure 2-7 : A typical STMF system with Vierendeel special segments (Basha & Goel, 1995)

Compared to X-diagonal special segments, the Vierendeel type special segment is more flexible and exhibits a more stable hysteresis behaviour with a favorable energy dissipating capacity. In this system the lateral force such as earthquake loads develop vertical shear in the Vierendeel

special segment, which is resisted by chords of this segment (Basha & Goel, 1994; Basha & Goel, 1995; Chao & Goel, 2008).

To investigate the behaviour of this system, they studied a four-storey truss moment frame with Vierendeel special segment numerically and performed experimental quasi-static cyclic tests on four one storey full-scale truss-column sub assemblage with ductile Vierendeel segment as a simplified simulation of the behaviour of this system during seismic events (Basha & Goel, 1994; Basha & Goel, 1995). The deformation of the Vierendeel segment in a typical tested sub-assemblage is represented at Figure 2-8.

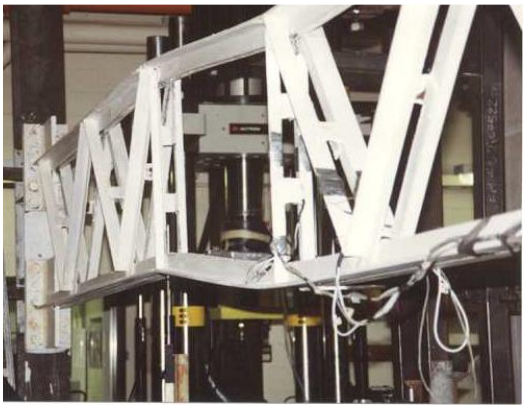

Figure 2-8 : Deformation in the Vierendeel special segment (Basha & Goel, 1994)

Under the quasi-static cyclic tests, this structural system exhibited full and stable hysteretic loops which confirmed its excellent seismic response with a favorable energy dissipation capacity (Figure 2-9).

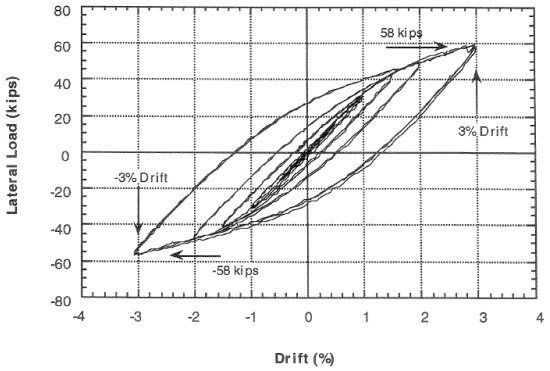

Figure 2-9 : Hysteretic loop of a truss moment frame with Vierendeel special segment (Basha & Goel, 1995)

Chao and Goel (2008) continued the studies and developed a Performance-Based Plastic Design procedure (PBPD) for truss moment frames with special segments to accomplish more predictable seismic behaviour and controlled damages in these structural systems (Chao & Goel, 2008). Moreover, special segments incorporating double HSS chord members, diagonal viscous dampers and buckling restrained braces were proposed to improve the seismic behaviour of the system (Kim et al., 2016; Jiansinlapadamrong et al., 2019; Chao et al., 2020).

2.1.2 Truss moment frames with Buckling Restrained Knee Bracing special segments (BRKB-TMF)

Continuing research on STMFs led to development of another STMF system called, Buckling-Restrained Knee-Braced Truss Moment Frame (BRKB-TMF) which employs Buckling Restrained Braces (BRBs) as energy absorbing elements in the truss frames, this system was introduced circa one decade ago.

In this system the bucking restrained knee bracings are accommodated between bottom chords and adjacent columns at end panels to dissipate seismic energy (Figure 2-10).

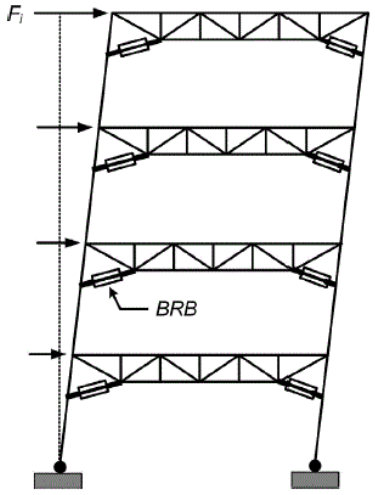

Figure 2-10 : A typical Buckling-Restrained Knee-Braced Truss Moment Frame (Wongpakdee et al., 2014)

These BRBs can sustain inelastic deformations in severe earthquakes whereas the other elements in the truss remain essentially in elastic range (Wongpakdee et al., 2014; Yang et al., 2015).

In a BRB, the steel core is restrained against global buckling then it can represent a stable yielding in tension and compression providing the truss moment frame with excellent ductility.

Following severe earthquakes, compared to conventional moment frames, BRKB-TMF represents less and controlled damage, less repair costs, and lower probability of collapse despite using less steel (Yang et al., 2015).

2.1.3 Truss moment frame enhanced with pre-compressed friction ring springs

A new version of truss moment frame enhanced with pre-compressed friction ring springs was introduced and developed by Tremblay and Faraji (2019).

In this system , named RS-TMF the pre-compressed ring spring is installed between the columns and the tips of the truss bottom chord extensions at the end panels (Tremblay & Faraji, 2019). The ring spring is composed of a pre-compressed assembly of precisely machined outer and inner rings which are working in compression (Figure 2-11).

The size and number of the rings that can be sized and arranged to develop the desired activation load and post-activation stiffness properties in the system in both directions. During a seismic event, when axial compressive force induced in the ring spring column installed in the bottom chords of the RS-TMF system, the conical inner rings slide inside the outer ones resulting in axial displacement with frictional resistance in the spring column. Simultaneously, the inner and outer rings experience circumferential compressive and tensile stresses, respectively, which resists against the external compression and tends to return the system back to its original position. When the compressive force disappears the friction direction reverses, causing a sudden drop in strength. However, if the inner and outer rings remain fully elastic, the produced self-centering force reverts the system to its original position.

Figure 2-11 : Typical assemblies of pre-compressed friction ring springs from the manufacturer: Ringfeder Power Transmission GMBH web site (2024), (www.ringfeder.com).

Tremblay and Faraji (2018) examined the seismic performance of a long span (20m) RS-TMF in a numerical model. The tested model was considered as the lateral load resisting system of a model single-storey industrial building assumed to be constructed on a class C site in Vancouver, British Columbia (Figure 2-12).

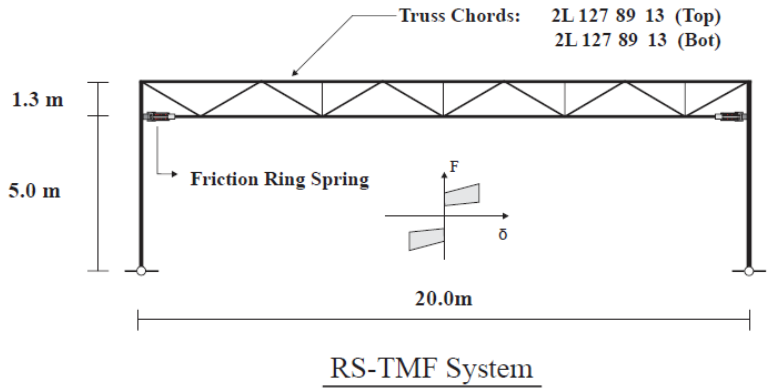

Figure 2-12 : Schematic of the studied RS-TMF prototype (Tremblay & Faraji, 2019)

This study also developed a force- based method to design the ring springs which resulted from the static equilibrium of the applied gravity and seismic loads in the RS-TMF. The controlled force displacement (pushover) analyses on the prototype model showed the lateral stiffness in system in pre-slip and post-slip ranges. The positive post-slip stiffness in the system provided by the pre-compressed friction ring springs refers to the self-centering capacity (Figure 2-13).

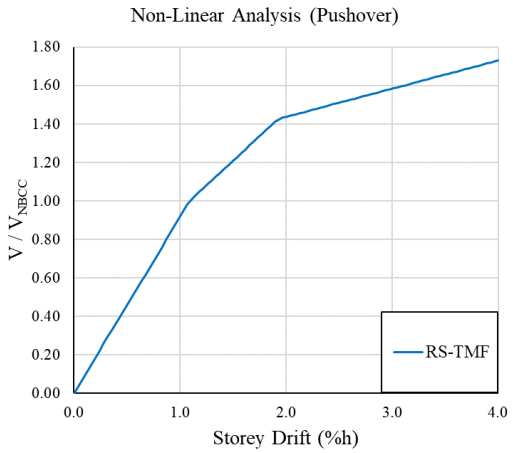

Figure 2-13 : Variation of stiffness in pre- and post-slip ranges in the studied prototype (Tremblay & Faraji, 2019)

The seismic performance of the prototype examined by application of dynamic non-linear time history analyses was conducted under three suites of 5 ground motion records, one suite for each sources of earthquakes contributing to the seismic hazard at the site: crustal earthquakes, subduction in-slab earthquakes and subduction interface earthquakes. The ground motion records were selected and scaled in accordance with the NBCC 2015.

Subjected to the applied ground motion records, the prototype RS-TMF system exhibited a satisfactory self-centering capacity with a symmetrical flag-shape hysteretic response that entirely eliminated the residual drift. The time history and global hysteretic response of the prototype under a typical IS5 subduction interface ground motion record is illustrated at Figure 2-14.

(a) (b)

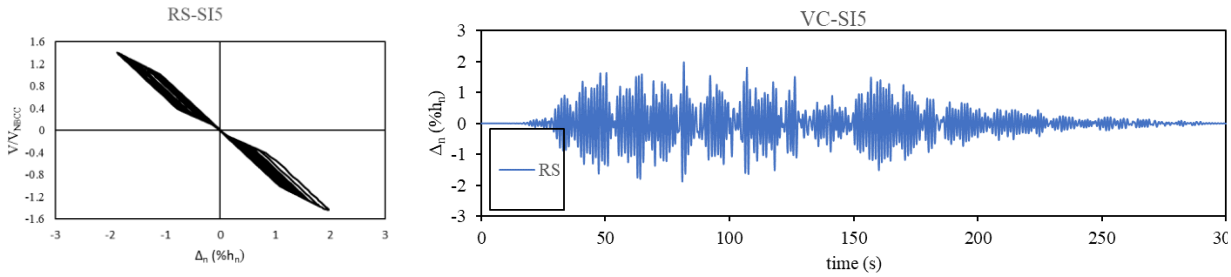

Figure 2-14 : a) Hysteretic and b) Time history response of the RS-TMF prototype under SI5 ground motion record (Tremblay & Faraji, 2019)

Although the pre-compressed ring springs theoretically provided the prototype with an excellent self-centering capacity, they showed a low energy dissipation capacity. Moreover, the real performance of the system and the feasibility of its application are subjects that need to be investigated experimentally. Studying the RS-TMF system was a prelude to the FT-TMF system in this thesis.

2.2 Self-centering mechanism with energy dissipating systems in moment frames

After 1994 Northridge earthquake, the inspections revealed that many structures which were expected to show ductile and resilient seismic behaviour, experienced brittle fractures, especially in connections. In addition, inspections showed that a large number of structures exhibited such large deformations that they could not stay in service (Mahin, 1998). Further investigations disclosed that the majority of the failures occurred due to low plastic capacity of welded connections (Christopoulos et al., 2002).

The post-Northridge earthquake studies helped the researchers and engineers to better understand the seismic response of bolted and welded connection and revise design guides, practices and provisions. Since then, revised seismic provisions require that the structures should be designed in a way that in severe earthquakes, inelastic deformations occur in specified members such as ductile connections in MFs and special segments in TMFs dissipating seismic energy while the other elements should remain in elastic range. This practice could resolve the problem of brittle and pre-mature fractures in these structures by reducing the seismic force demand, controlling the damage and limiting it to the specified elements. On the other hand, these structures could become vulnerable to large seismic deformations and drifts due to the large deformation in the ductile elements. To overcome the problem, self-centering mechanisms, that can provide the structures with the required lateral stiffness in the non-linear range to bring them back to their original position, seem a good solution to control the deformations and reduce the seismic residual drifts. Therefore, structural engineering researchers tried to innovate and propose structural systems enhanced with practical and reasonable self-centering mechanisms as well as energy dissipating segments, elements and or devices. Practical design, ease of fabrication and installation, repairability and cost-efficiency are key factors in the development of these innovative systems.

The following sections review various self-centering and energy-dissipating systems for steel structures, including connections, shear walls and braces, which are proposed over the past two decades.

2.2.1 Self-centering moment resisting connection with post-tensioned tendons and energy dissipating top and seat angles

Ricles et al. (2001) proposed a moment resisting post-tensioned steel connection consisting of bolted top and seat angles, with high-strength strands running parallel to the beam and anchored outside the connections (Ricles et al., 2001). The high-strength strands, which are post-tensioned after installation of the top and set angles, compress the beam flanges against the column flanges in the connection and contribute to the moment capacity of the connections by developing contact stresses at the beam-to-column interface (Figure 2-15).

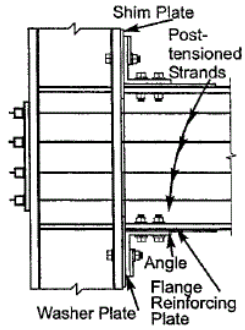

Figure 2-15 : A typical self-centering energy moment resisting connection with energy dissipating top and seat angles (Ricles et al., 2001)

In this connection, the friction at the beam-to-column contact interface resists transverse beam shear. In addition, the top and seat angles also resist moment and transverse beam shear. Following seismic loads, this connection behaves similarly to a rigid connection until the decompression in the post-tensioned tendon occurs and the separation of the beam tension flange from the column leads to gap opening at the beam-column interface. The gap opening provides an elastic restoring force that returns the frame to its pre-earthquake position while the inelastic deformation of the angles dissipates the input energy. Analytical modeling has shown that seismic response of the connection, illustrated by moment-rotation curves, exhibits an excellent flag-shaped hysteretic behaviour. This response results from the combination of the elastic behaviour of post-tensioned tendon and plastic behaviour of the angles (Figure 2-16).

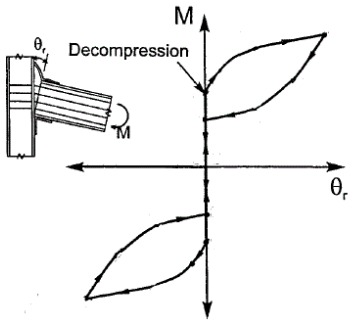

Figure 2-16 : Schematic of the moment-rotation hysteretic curve of the self-centering moment resisting connection with energy dissipating top and seat angles (Ricles et al., 2001)

In frames fabricated with this connection, since the seismic damage is limited to the angles, the system is considered as a low-damage and cost-effective system. To investigate the behaviour of this connection, Ricles et al. (2001) developed an analytical model in the computer program Drain-2DX to simulate its behaviour. Then, they performed laboratory tests on a set of specimens of cross-shaped beam-to-column sub-assemblages with the proposed connection representing interior joints in a moment frame. The comparison between the lateral force-displacement hysteretic curves of the connection from the analytical model and the experimental tests confirmed the accuracy of the analytical model (Figure 2-17).

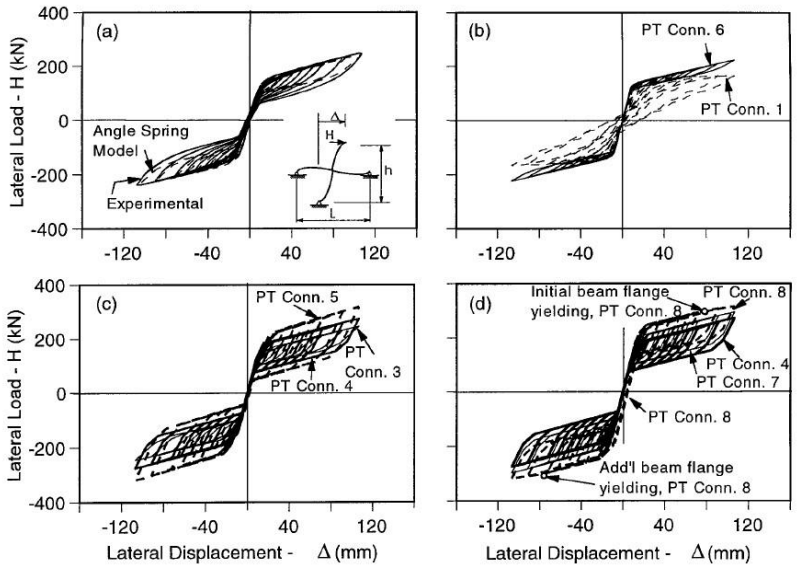

Figure 2-17 : A typical comparison between the lateral force-displacement hysteretic curves acquired from analytical models and experimental tests in the tested specimens (Ricles et al., 2001).

Then, to investigate the performance of the connection using a macro approach, they modeled a 6-storey steel TMF. The results of non-linear time history analysis showed that a typical frame with the post-tensioned energy dissipating connection exhibited self-centering capacity with satisfactory stiffness, strength and ductility. As a result, it represented superior seismic response compared to similar moment frames with conventional welded connections (Figure 2-18).

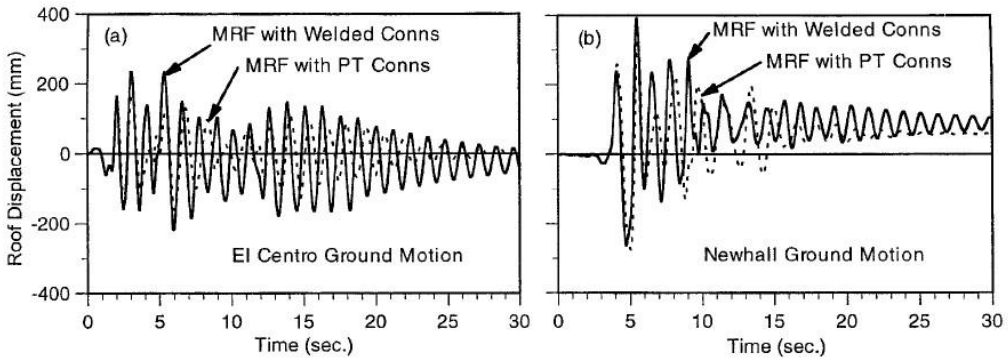

Figure 2-18 : Roof displacement time history analysis results: (a) El Centro ground motion; (b) Newhall (Northridge) ground motion (Ricles et al., 2001)

2.2.2 Self-centering connection with post-tensioned and energy dissipating bars

Christopoulos et al. (2002), proposed a Post-Tensioned Energy Dissipating connection, called (PTED), for moment resisting frames and developed an analytical model and a design procedure for it. In this beam-to-column connection, a high-strength post-tensioned steel bar (PT) is installed at mid-depth of the beam on each side of the web, compressing the beam against the column. The PT bar connects the web of the beam to the backside of the column through two holes in the column's flanges. On each side of the beam's web, two energy dissipating buckling restrained bars are inserted into the holes in the column's flanges and connected to the couplers welded to the column's flanges and continuous plates. These parallel energy dissipating bars are confined by steel housings to prevent them from buckling in compression. Therefore, the energy dissipating bars can show stable yielding in tension and compression (Christopoulos et al., 2002).

The post-tensioned energy dissipating connection, its geometry and free body diagrams are shown in Figure 2-19.

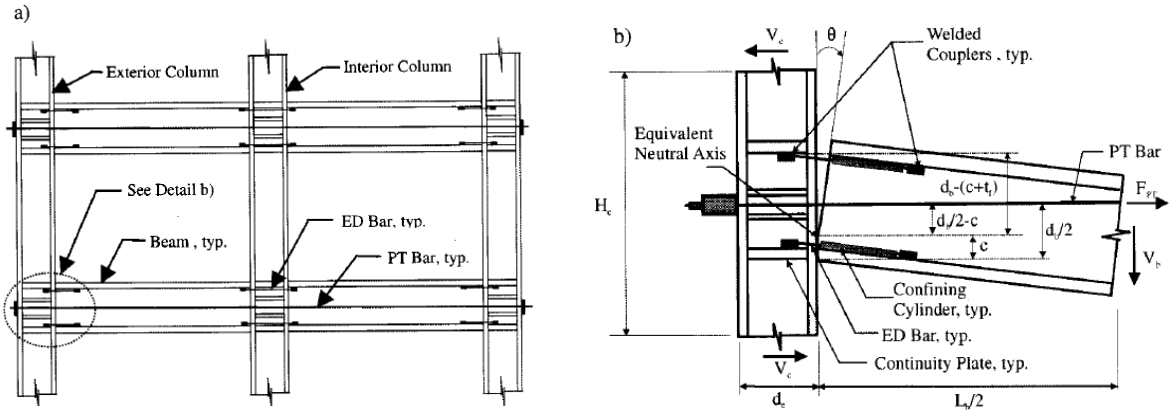

Figure 2-19 : a) Steel frame with post-tensioned energy dissipating connections; b) Geometric configuration and free-body diagram of exterior post-tensioned energy dissipating connection (Christopoulos et al., 2002)

The analytical studies by Christopoulos et al. (2002) showed that under a defined lateral force and the corresponding displacement, a gap opening at the beam-to-column interface occurred, and the post-tensioned bar provided the connection with excellent self-centering capacity, as was demonstrated by a flag-shaped moment-rotation curve. Simultaneously, inelastic deformation in the ED bars dissipated the lateral force, resulting in stable moment-rotation hysteretic curves (Figure 2-20).

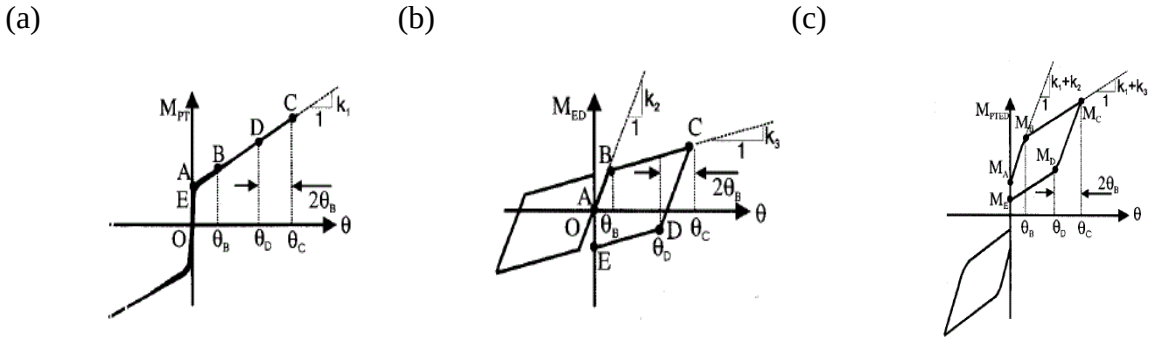

Figure 2-20 : Idealized hysteretic behaviour of PTED beam-to-column connection : a) contribution of PT bars; b) contribution of ED bars; and c) moment-rotation of the connection (Christopoulos et al., 2002)

Although the vertical shear resistance in this connection is provided by friction at the beam-to-columns interface, which can be adjusted by the proper compressive force in the post-tensioned bar, additional shear resistance capacity can be achieved by installing shear-resistant elements,

such as flexible long seat angles below the beam, which can deform without any moment resistance. Christopoulos et al also performed a large scale cyclic test on the proposed connection which verified the accuracy of the analytical results and the design procedure (Figure 2-21).

Based on the analytical and experimental results, the authors showed that this connection can achieve the characteristics of conventional welded connections plus self-centering and energy dissipating capacity. Moreover, the experimental tests proved that under large inelastic deformations, the damage occurred in replaceable ED bars while the other structural elements experienced no damage, hence this system is considered a low-damage structural system. They also showed that this connection can practically sustain large displacements representing excellent self-centering and energy dissipating capacities (Christopoulos et al., 2002).

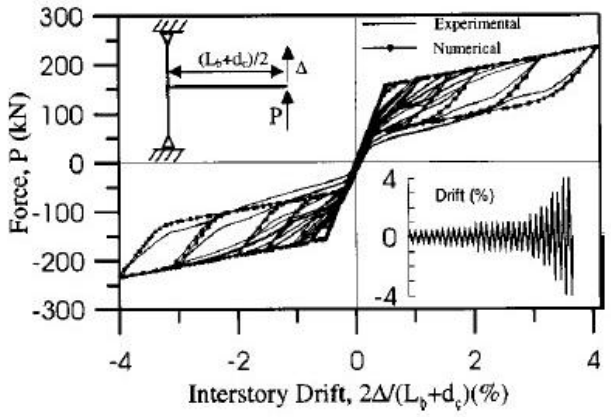

Figure 2-21 : A typical comparison between the numerical and experimental force-displacement hysteretic curves of PTED connection (Christopoulos et al., 2002)

2.2.3 Self-centering Steel Plate Shear Walls (SC-SPSW)

This system (SC-SPSW), represented in Figure 2-22, is built of a self-centering steel moment frame with post tensioned (PT) rocking connection which is infilled by a thin steel web plate as energy dissipating element (Clayton et al., 2016; Dowden & Bruneau, 2016). When the frame is subjected to lateral forces, the storey shear forces apply compressive and tensile forces in diagonal directions in the steel web plate. Although low compressive forces will lead to buckling of the thin web plate, it can resist large tensile forces up to yielding. Therefore, the primary lateral resistance in the system is provided by tension capacity of the thin steel web plate. In this system, high strength

post-tensioned steel strands are anchored to the web of the beam and the exterior flange of the column, compressing the beam against the column. These strands are placed into holes in the inside and outside column flanges. A shear tab with no moment resistance is placed between the beam web and the column inside flange to transfer developed shear in the connection to the column. Following lateral displacements in the nonlinear range, gap opening at the beam-to-column interface happens while the inelastic deformations in the thin web plate dissipate the lateral force. The elongation of the strands caused by gap opening provides the required compression force to close the gap and bring the frame to its original position to mitigate residual drifts. Two different types of PT rocking connections include 1) flange-rocking (FR) which can rock about both flanges of the beam and 2) New Z-BREAKSS (NZ) which only rocks about the top flange suggested for this system. In the second connection the boundary frame extension during lateral movement, that happens in FR connection, is eliminated. The schematic of the two connections is displayed at Figure 2-22.

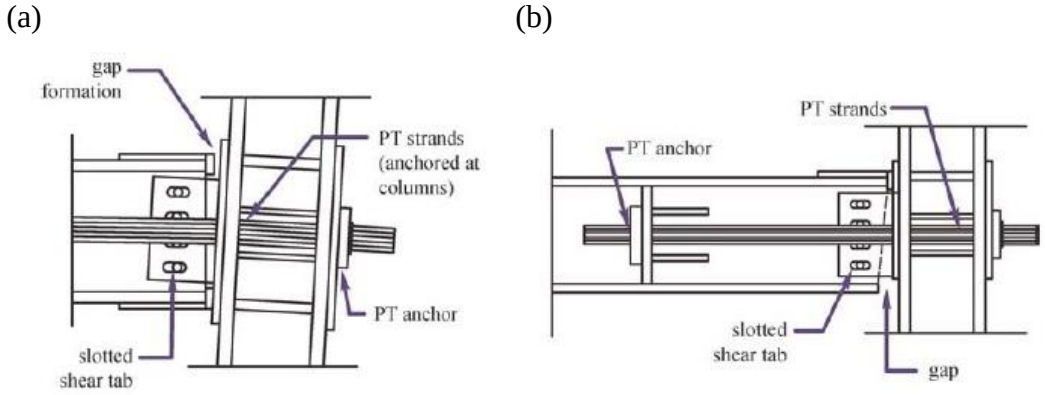

Figure 2-22 : (a) FR and (b) NZ connections (Clayton et al., 2016)

Clayton et al. (2016) investigated the performance of this system with two alternative steel web plates including full infill web plate and strip infill plates in a series of numerical analyses and experimental tests (Clayton et al., 2016).

In the analytical parts of the study, they used performance-based design procedure for a model frame and performed non-linear time history analyses applying ground motion records with different intensities, including events with low, medium and high probability of occurring in 50 years to it in order to predict its seismic behaviour subjected to different seismic hazard levels. The

experimental tests included quasi static cyclic and shake table tests on one third scaled three-storey SC-SPSW specimens SC-SPSW performed in University of Washington (Figure 2-23).

(a) (b)

Figure 2-23 : Test set-up for (a) quasi-static and (b) shake table tests (Dowden & Bruneau, 2016)

Typical force-displacement hysteretic curves obtained from the shake table test on the specimens with FR and NZ connections under a simulated earthquake, with 10% probability of exceedance in 50 years (medium level) in Los Angeles area, are illustrated in Figure 2-24.

The result showed that during severe earthquakes, this system can experience yielding damage, which was concentrated in the replaceable thin web plate, while the other structural elements including beams, columns and post tensioned strands remain elastic with no damage. However, some residual drift remained in the system following the earthquake, limiting the potential resilience of this system.

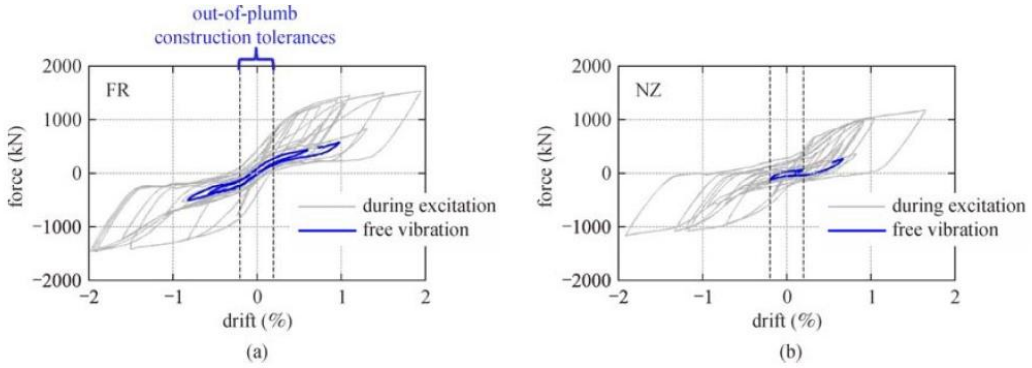

Figure 2-24 : Results from medium excitation for specimens (a) FR and (b) NZ (Dowden & Bruneau, 2016)

2.2.4 Self-centering Energy Dissipating bracing system (SCED)

This system (SCED) is an earthquake resilient, and damage-free bracing system developed for moment frames. This system comprises of two main inner and outer tubular bracing members, a set of elastic tendons and energy dissipation devices which are fixed with a series of connecting, guiding and encasing elements. The schematic of this system is illustrated at Figure 2-25.

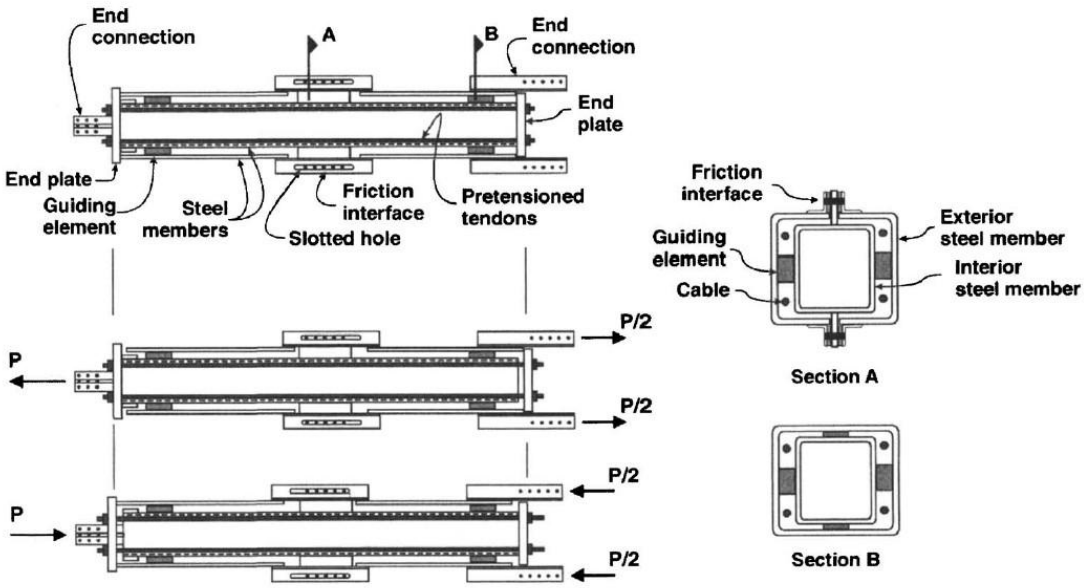

Figure 2-25 : Schematic of SCED system with steel tubes, tendons, and friction devices (Christopoulos et al., 2008)

Subjected to lateral loads when the bracing element start to move against each other, the tensile force developed in the tendons imposes a self-centering capacity in the frame that tends to return it back to its original position; in parallel the energy dissipation system, such as friction dampers, dissipate a portion of the induced kinetic energy in the system.

A post-tension force in the tendons can considerably improve the self-centering capacity in the system and mitigate the residual drifts. Similar to structural systems with self-centering and energy dissipation capacities, This passive system is intended to be adjusted in such a way that it shows an elastic response under minor to moderate, and a non-linear response subjected to intense ground (Christopoulos et al., 2008).

The stable hysteretic response combined with self-centering capacity in this system were verified by a set of cyclic quasi-static and dynamic analyses tests on a full scale moment frame prototype

performed at the Structural Engineering Laboratory of École Polytechnique of Montreal. Typical hysteretic responses of the system to the experimental test are illustrated in Figure 2-26.

(a) (b)

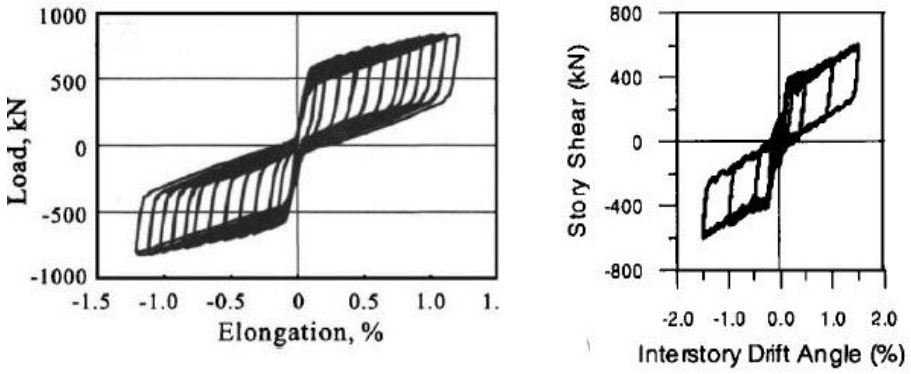

Figure 2-26 :a) Response of SCED prototype under quasi-static axial loading, b) Response of SCED prototype under dynamic loading (Christopoulos et al., 2008)

Further studies on this concept led to introduce an advanced version of this system in which one or more floating intermediate members with a set of tendons are accommodated in parallel with the existing members in a telescoping format (Figure 2-27).

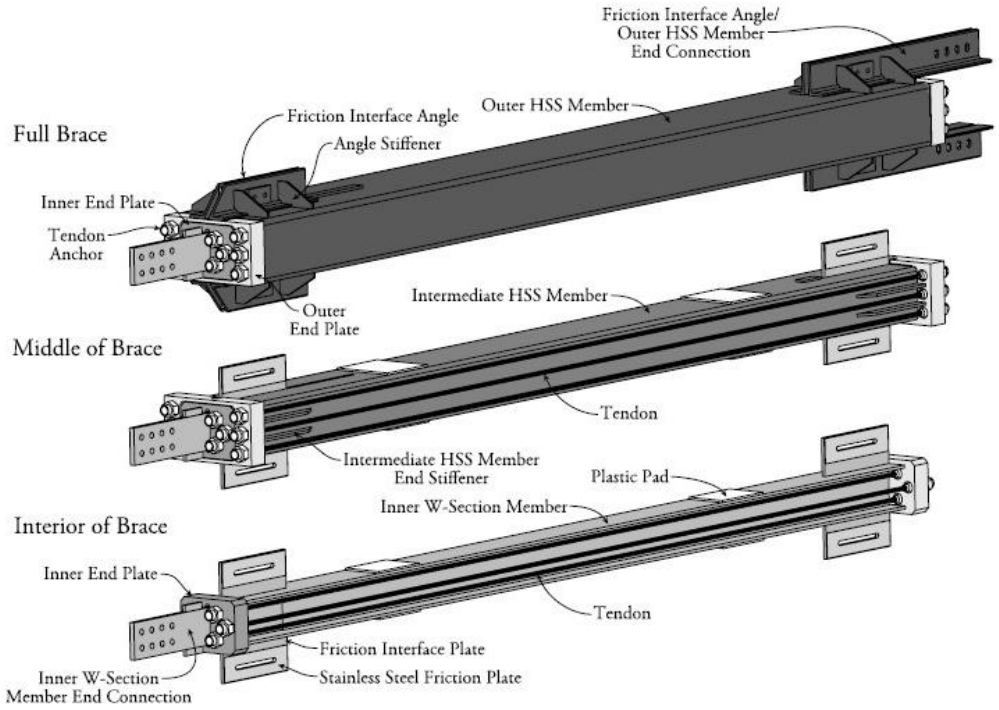

Figure 2-27 : Schematic of a T-SCED brace system (Erochko et al., 2015)

A set of quasi static and dynamic tests on a full scale T-SCED installed in a single storey frame were conducted at the University of Toronto. In the dynamic tests, two ground motions including 1) a Cascadia subduction zone earthquake and 2) an MCE level earthquake with 2% probability of exceedance in 50 years for Los Angeles area were simulated and applied to the specimen. The results from the experimental tests verified that the T-SCED system experienced no buckling and can noticeably achieve higher ductility and self-centering capacity compared to SCED due to the enhanced -elongation capacity (Erochko et al., 2015).

2.3 Elastic spine (strongback) systems

Following strong earthquakes, conventional multi-storey braced frames are vulnerable to damaging concentration in one or few stories which can lead to soft-storey mechanism. Elastic back spine system, which is also referred to as a strongback system, is a hybrid earthquake resilient system composed of a traditional steel frame and a strong mast such as a vertical truss or a shear wall. It can be a solution to mitigate the formation of soft-storey for steel braced frames. In the

strongback system, the mast, such as a vertical elastic truss spanning the full frame height, acts as a strong spine for the system to prevent or delay the formation of soft storey and reduce peak deformation demands in individual braces. In addition, in braced frames improved with a strongback system, the seismic drifts become uniform through the height. The other advantage of the system is that it can be utilized to retrofit existing steel braced frames. Then it can also be considered as an economic solution for retrofit projects.

2.3.1 Steel braced elastic spine systems with BRBs

The utilization of buckling-restrained braces (BRBs) in structures has significantly enhanced the inelastic behaviour of bracing systems. In order to study the seismic performance of strongback systems equipped with BRBs, Lai and Mahin (2015) performed a series of analytical studies including monotonic and cyclic non-linear static as well as nonlinear time history analyses under ten earthquake records on a six-storey building model with different configurations of seismic resistant systems including conventional systems such as inverted V and X braced frames as well as elastic strong spine system with BRB braced frames (Figure 2-28). It should be noted that the truss elastic spines were shifted from the center of the beams to better proportion the loads in the elastic spine members. The results showed formation of weak stories in the conventional braced frames while the braced frames modified with the strongback system prevented the formation of weak stories. Moreover, they showed that BRB members improved the deformation capacity of the strongback system (Lai & Mahin, 2015).

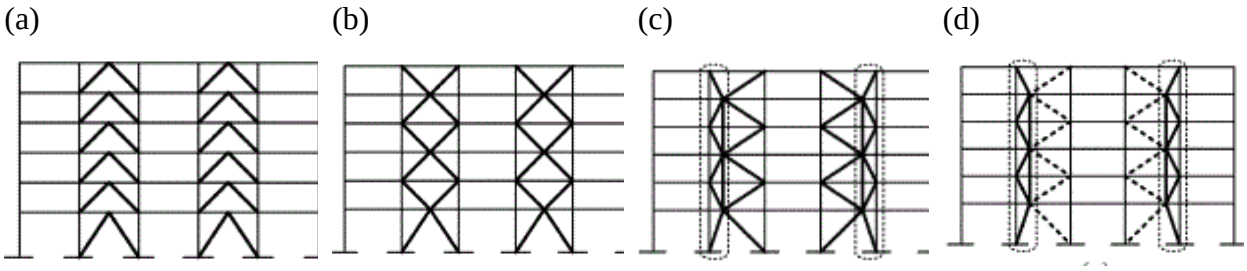

Figure 2-28 : Conventional frames and modified elastic spine frames a) inverted V braced frame; b) X braced frame; c) elastic spine frame with traditional braces; d) elastic spine frame with BRB braces (Lai & Mahin, 2015)

Further studies conducted by Simpson and Mahin (2018) numerically simulated the cyclic behaviour of a two-storey one bay steel frame with BRB bracing with centered and offset configurations of the strongback (Figure 2-29).

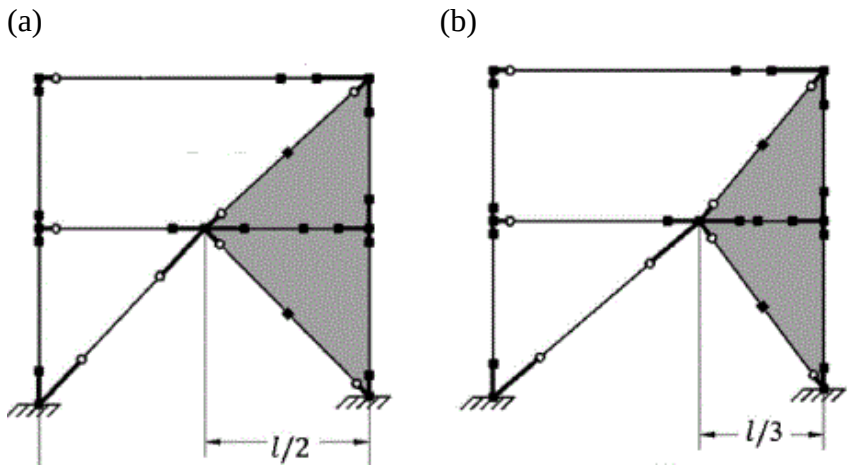

Figure 2-29 : Numerical model schematic: a) centered scheme; b) offset scheme (Simpson & Mahin, 2018)

The global base shear-roof displacement and brace axial force-axial deformation hysteretic curves of the studied models obtained from numerical results, represented in Figure 2-30, showed that the model with the offset configuration of the strongback exhibited smaller elastic stiffness and ultimate strength but slightly larger deformation capacity for the BRB members compared to the model with centered strongback.

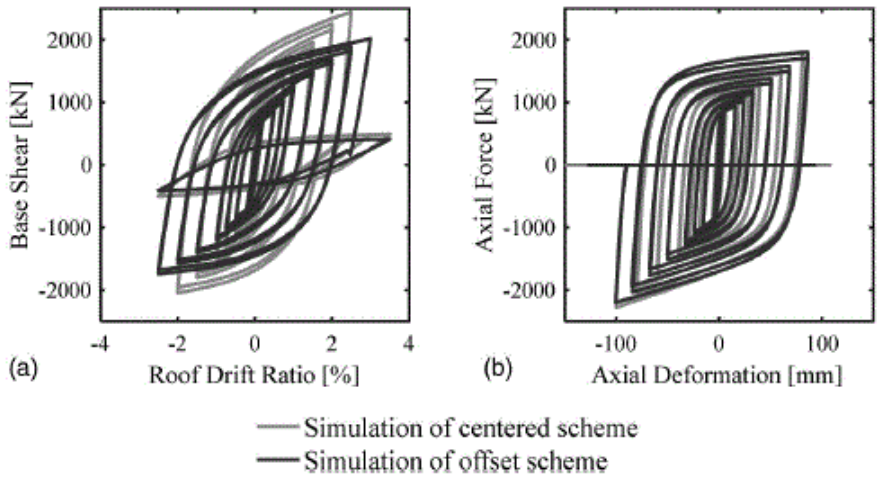

Figure 2-30 : Numerical comparison of centered and offset schemes: a) global hysteretic comparison; b) brace hysteretic comparison (Simpson & Mahin, 2018)

They also performed a cyclic test of a nearly full-scale specimen of the studied two-storey one-bay steel frame with BRB bracing members in a centered strongback configuration. The comparison

between hysteretic curves verified the compliance of the numerical and experimental results for the model (Figure 2-31).

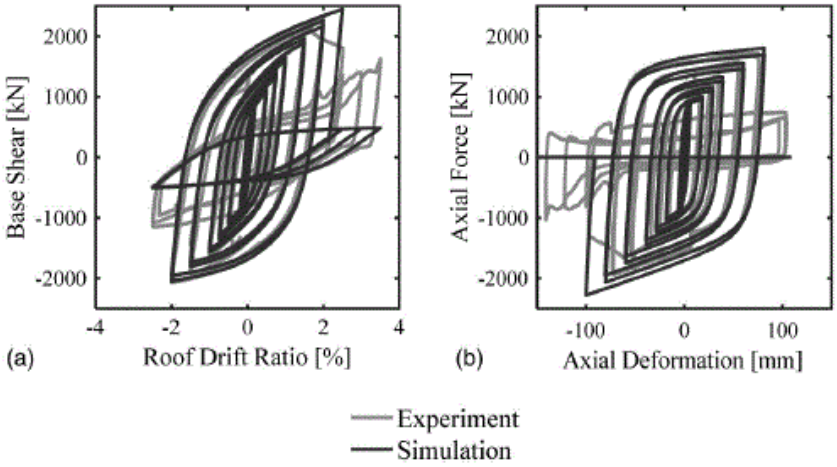

Figure 2-31 : Comparison of numerical and experimental results for centered system a) global hysteretic; b) brace hysteretic (Simpson & Mahin, 2018)

The results of the experimental test also showed that the strongback system behaved as intended and predicted in the numerical simulations: it avoided the formation of a soft storey, even after the degradation of the BRB members, and it was observed that, after the rupture of the BRB members, the other elements provided considerable strength, stiffness and energy dissipating capacity for the frame (Simpson & Mahin, 2018).

2.3.2 Segmental Spine Braced Frames (SESBF)

Although employing elastic spine system in braced frames can efficiently mitigate weak storey mechanism and achieve nearly uniform lateral drifts over the frame height, during severe ground motions, the contribution of higher modes develop large axial forces in members of the truss spine, which can lead to inelastic deformation and damage in the system. Although the increase of member size in the spine can keep the members in the elastic range, it can cause higher seismic acceleration in the system due to larger mass and also negatively affect the economic viability of the system.

Segmental elastic spine (Figure 2-32) can be a solution to solve the problem. In this system, the elastic spine is built of elastic truss segments with pinned bases that are installed over the height. The flexural discontinuity of the segmented spine can significantly reduce force demands while it can still prevent soft-storey mechanism and concentration of force demand in members.

Chen et al proposed a tall, braced frame composed of two parallel segmental spine braced frames (SESBF) that were connected with link beams. The link beams within each elastic truss segment are intended to yield simultaneously (Chen et al., 2019).

They also proposed a practical analysis method to design this system to achieve the intended performance including uniform drift through high and limited force demand.

This method predicts the force demand developing from yielding of the ductile elements plus the forces developing from higher mode effects through the height of the frame with equivalent static and spectrum methods, respectively.

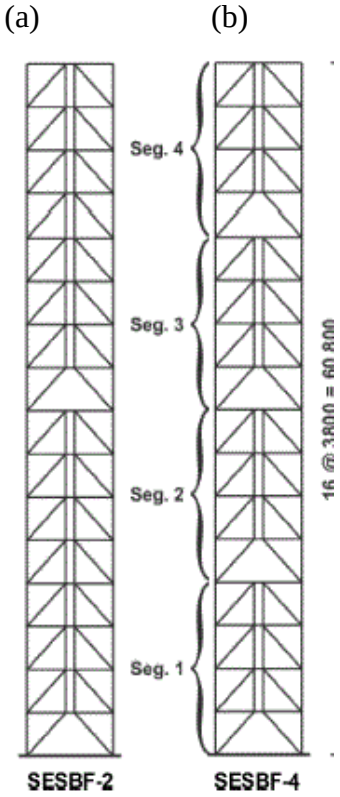

Figure 2-32 : Schematic of 16 storey segmental spine braced frames - a) spine with two elastic segments of spine b); spine with four segments (Chen et al., 2019)

They then performed nonlinear time history analyses on 8- and 16-storey buildings with different configurations of 1, 2 and 4 elastic truss segments to validate the accuracy of the design procedure. The earthquakes records employed for nonlinear time history analyses were a set of crustal, subduction in slab and interface ground motion records scaled for a hazard level corresponding to a probability of 2% in 50 years in Canada.

The analytical results showed that the segmental system performed as intended and verified the accuracy of the design procedure by validating some parameters such as peak storey shears, drifts, and axial forces in braces, columns, and ties in the studied models (Figure 2-33).

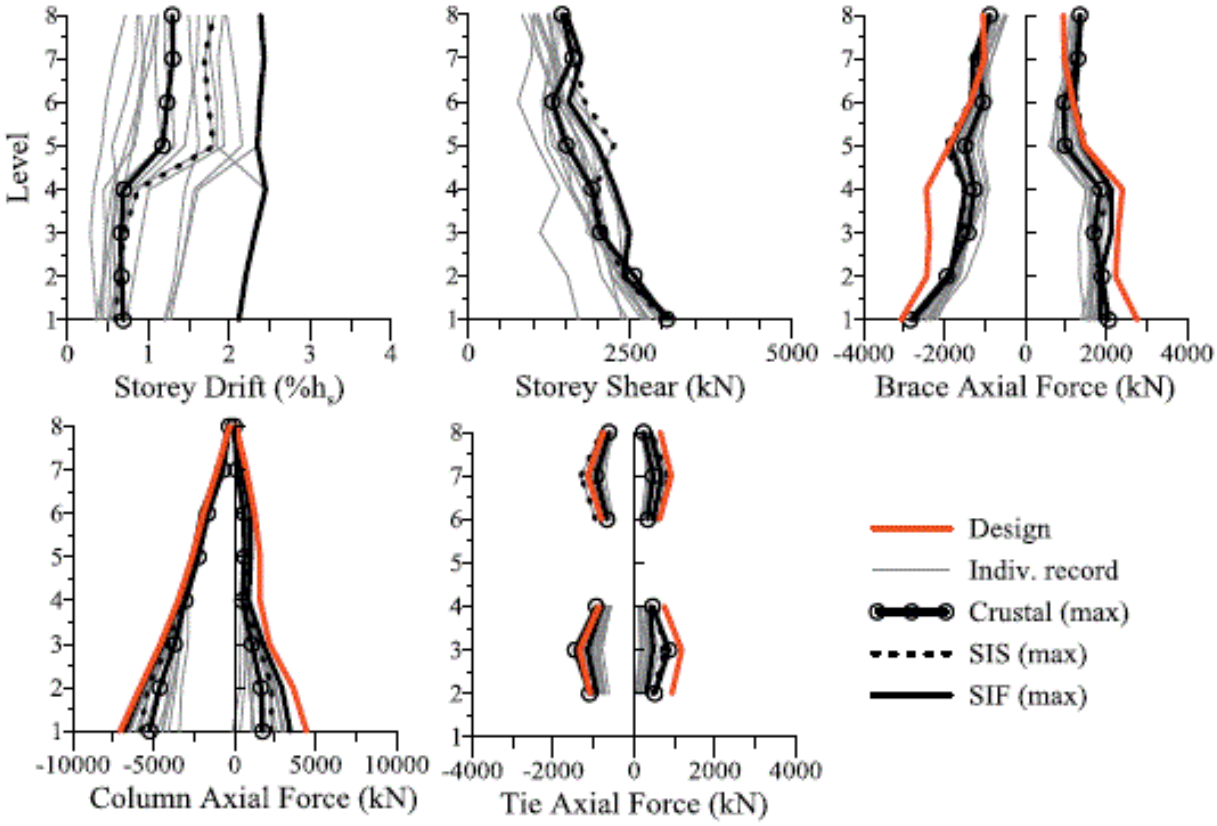

Figure 2-33 : Peak values of storey shears, drifts, and axial forces in braces, columns, and ties along the height of the 8-storey SESBF with two elastic segments of spine (Chen et al., 2019)

2.4 Rocking systems

In 1963, Housner studied the concept of rocking structures by exploring the free vibration response of a rigid rocking block. Later, in 1975, response characteristics of a system including structural flexibility coupled with rocking were examined by Meek (Grigorian & Grigorian, 2015).

This concept was utilized to develop a new type of self-centering system called controlled rocking system that can be applied in structures such as concrete bridge piers, prestressed concrete walls and steel frames to mitigate seismic structural damage and residual drifts, but in this research, the focus is on controlled rocking steel frames which have been developing since 2000s.

The controlled rocking steel frame is a rigid frame that is designed to rock off its foundation and following a specific lateral load, the base of each columns in this frame can uplift rather than develop tension. This system is anchored to ground with post-tensioned tendons to provide it with extra overturning resistance and positive stiffness after uplifting of the frame. Moreover, energy dissipation elements can be installed in this system to decrease seismic force demand and improve the seismic response (Aslam, 1978; Ajrab et al., 2004; Grigorian & Grigorian, 2015).

A rigid rocking system employed in the structures acts as a robust backbone representing a near-linear first mode shape pattern and mitigates the influence of higher modes during seismic events. Therefore, it endows the entire system with a predetermined and consistent lateral movements and storey drift distribution along the height. Consequently, the possibility of soft storey formation and premature failures will be reduced. In recent years, researchers have been developing different configurations of rocking steel frames to optimize the seismic performance of the system. In the following section, a number of recently developed rocking steel frames will be reviewed and discussed.

2.4.1 Steel braced frames with controlled post-tensioned rocking frame and energy dissipating shear fuses

An advanced self-centering frame composed of steel braced frame, high strength tendons and shear yielding fuses was studied analytically and experimentally in a research project by Deierlein et al developing a performance based design procedure for it (Ma, 2010; Deierlein et al., 2011).

In this braced frame, the initial overturning resistance is provided by the resistant moment caused by gravity load of the frame, vertical post-tensioned tendons and energy dissipating fuses. When this frame is subjected to strong ground motions, the rocking action occurs and gap opening at the base of the frame causes elongation of the tendons providing the frame with self-centering restoring force which is added to the overturning resistant moment caused by the weight of the frame.

Meanwhile, inelastic deformations take place in the shear fuses dissipating seismic force (Ajrab et al., 2004; Deierlein et al., 2011; Eatherton, Ma, Krawinkler, Mar, et al., 2014; Martin et al., 2019).

Deierlein et al. introduced two different configurations: a single frame in which the shear fuse can be installed along the centerline or column line and a dual frame in which the fuses are placed between two frames to maximize their energy dissipation (Figure 2-34).

(a) (b)

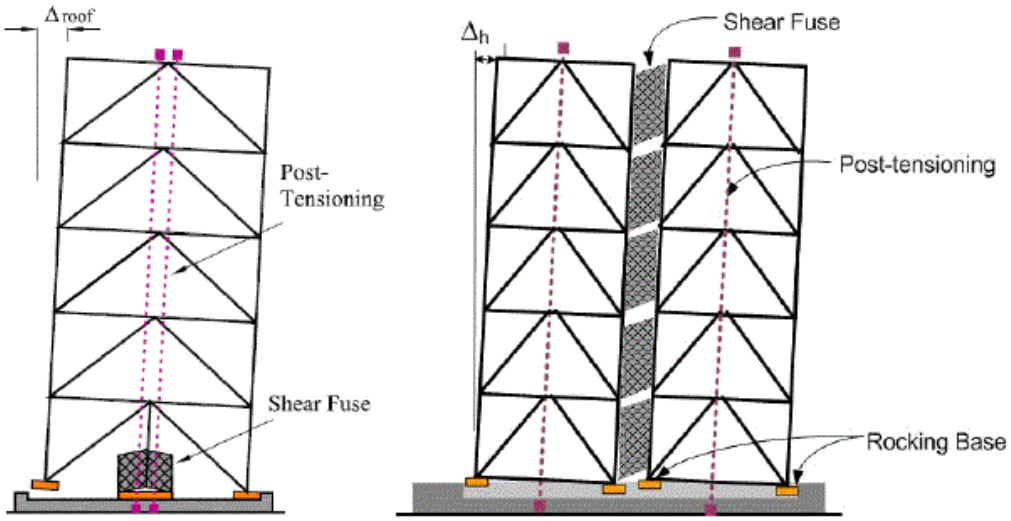

Figure 2-34 : Controlled rocking frame configurations; a) Single rocking frame b) Dual rocking frame (Deierlein et al., 2011)

During their research program, they also developed and employed replaceable butterfly shape steel fuses as the energy dissipation elements in the rocking system (Figure 2-35).

(a) (b)

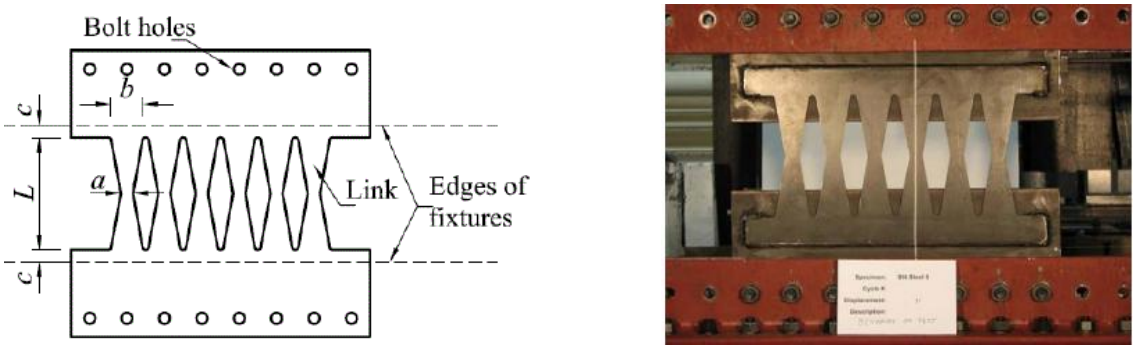

Figure 2-35 : a) Schematic and a b) photo of butterfly shaped shear fuse (Ma et al., 2010; Deierlein et al., 2011)

It is expected that these frames will remain completely undamaged in mild and moderate earthquakes.

Under intense earthquakes, seismic damage concentrates only in the shear fuses that can be easily replaced, while the other structural members remain undamaged.

The schematic of self-centering response, energy dissipation response and combined response of the rocking system is represented in Figure 2-36.

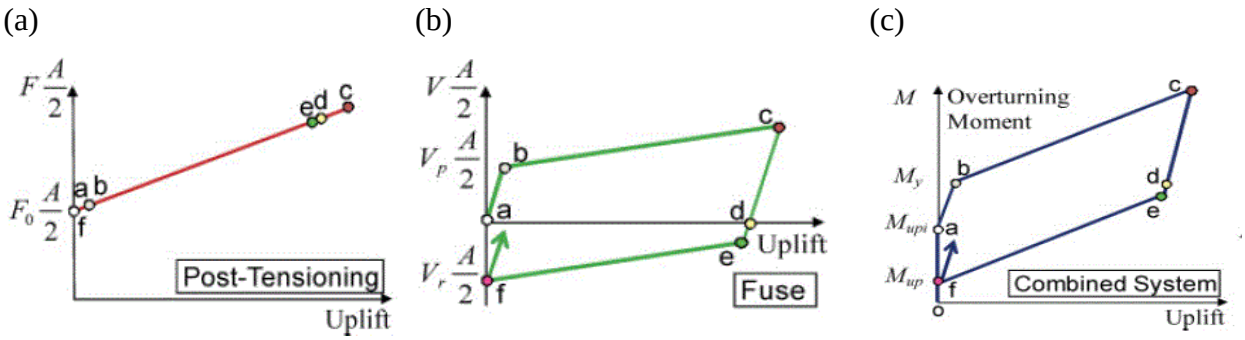

Figure 2-36 : a) Self-centering response of the Rocking frame b) energy dissipating response of the fuse c) Combined response of the system (Deierlein et al., 2011)

To further investigate the performance and behaviour of the introduced rocking system, a series of large-scale experimental tests were conducted by Deierlein et al., in collaboration with the NEES laboratory at University of Illinoise and E-Defense facility in Japan.

The first experimental program, conducted at NEES laboratory, included a set of nine quasi-static cyclic and hybrid simulations on a half-scale single dual rocking frame prototype. The tests provided valuable insights into the system, such as its overall behaviour, the balance between the fuse elements and post-tensioned tendons to achieve the desired self-centering response and the effects of fuse degradation (Deierlein et al., 2011).

The tested rocking frame along with its overall hysteretic response and the individual components contributing to the hysteretic behaviour observed in one of the nine tests, are illustrated at Figure 2-37.

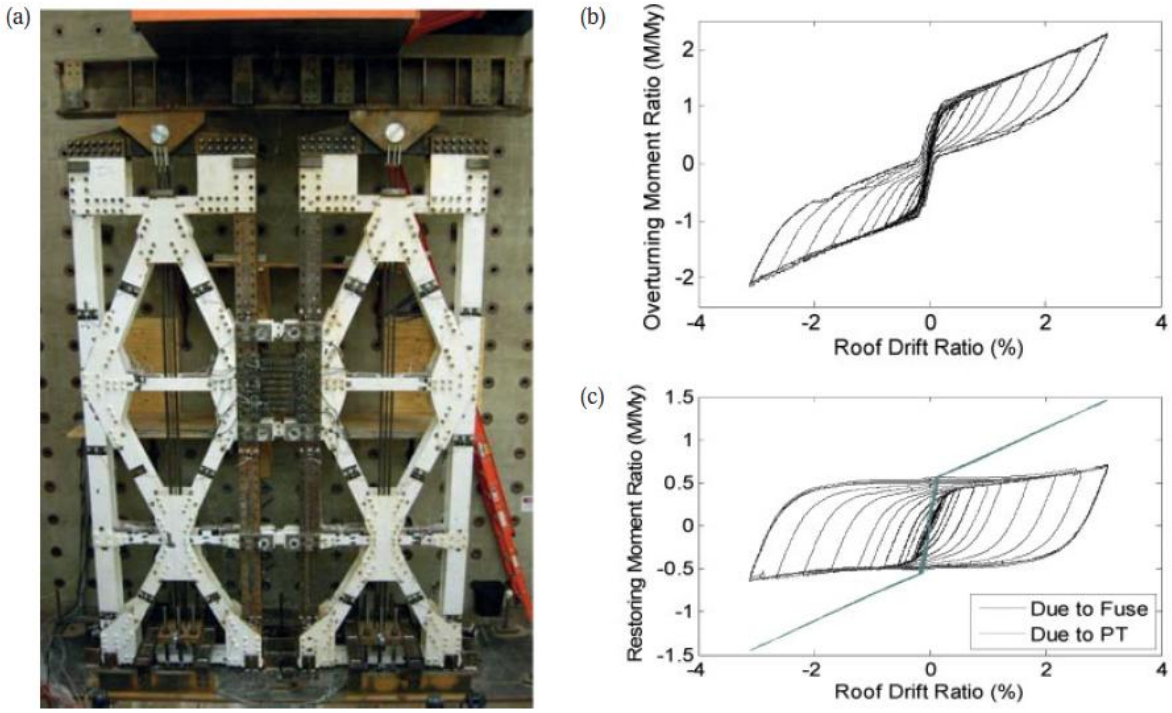

Figure 2-37: Quasi-static cyclic testing of dual frame specimens; a) test specimen, b) overall hysteretic response, c) components of hysteretic response (Deierlein et al., 2011).

The experimental findings from the quasi static cyclic test on the rocking frame, were supported by a shake table test program conducted at the E-Defense facility in Japan.

In the shake teble test program, a three-storey rocking frame was subjected to a set of simulated ground motions scaled to MCE level earthquake.

Overall, the shake table tests confirmed the viability of the rocking frame concept and the expected behaviour of the system. Furthuremore they provided valuable insights into design, installation ond repair of this system (Deierlein et al., 2011).

The three-storey prototype along with the experimental responses obtained from the application of simulated JMA-Kobe motion on the prototype, are illustrated in Figure 2-38.

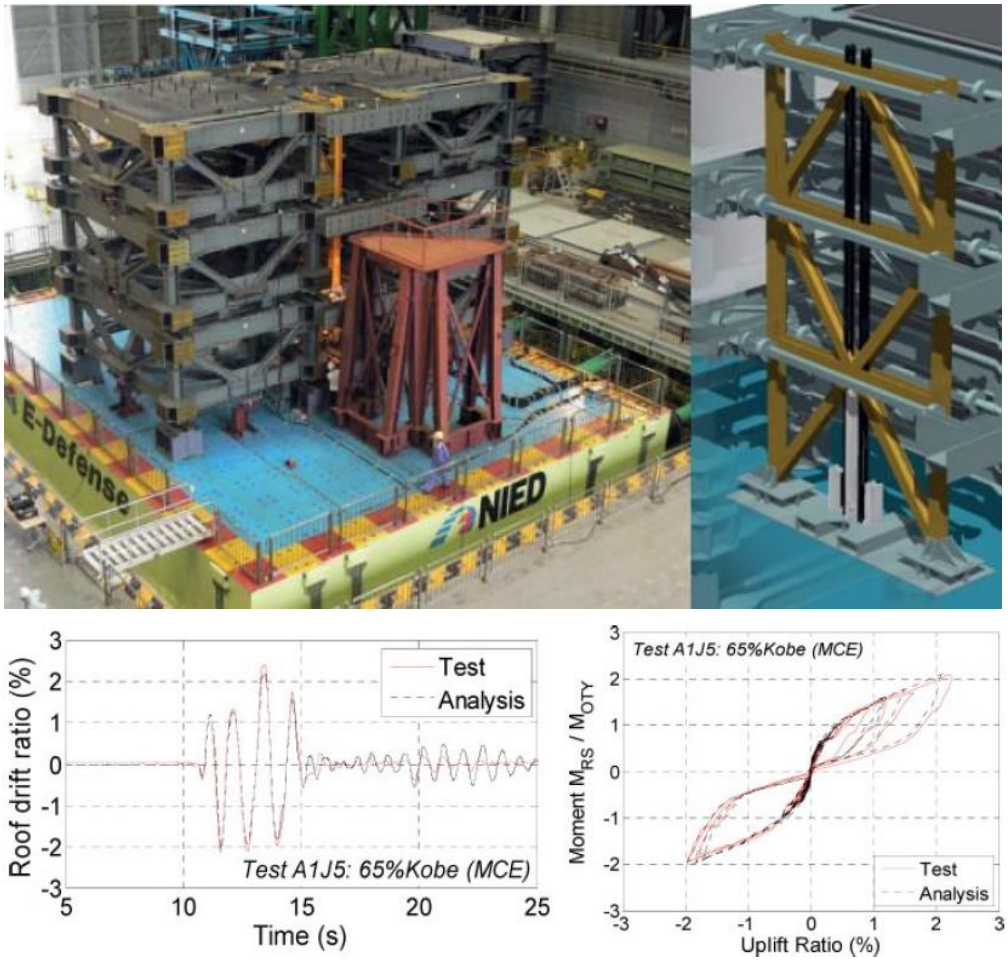

Figure 2-38 : Top - 3-storey single frame prototype, Bottom -Shake table results under JMA Kobe motion, scale to MCE intensity (Deierlein et al., 2011)

2.4.2 Post-tensioned rocking system with multiple frames and nonlinear brace

Further studies on controlled rocking frames revealed that although in this system lateral seismic displacements follow first mode shape pattern; the contribution of higher mode effects increases the force demand in rocking frame members. Moreover, the increase in earthquake intensity can increase the developed shear force in the system that can lead to larger force demands. Therefore, the rocking frame members that are intended to remain in the elastic range, are vulnerable to nonlinear deformations. Although increasing the member sizes can guarantee their elastic behaviour, it will also increase the weight of the rocking frame, which can lead to higher seismic acceleration in the rocking frame during earthquakes. Furthermore, using larger sections to fabricate the rocking frame members will increase the construction cost. To address this issue,

Wiebe et al. (2009) proposed a segmental rocking system, called multiple rocking frame, in which one or more controlled rocking joints are placed above the rocking base. This configuration reduces the overturning moment near the added joints and can proportionally decrease the peak shear throughout the frame. Notably, these improvements do not significantly increase the magnitude, or the variability of the lateral peak displacement compared to a similar system with a single rocking joint at the base. (Wiebe & Christopoulos, 2009; Wiebe et al., 2013).

They then proposed another controlled rocking frame in which they included a nonlinear brace in the first storey level. In this system, the nonlinear brace limits the storey shear envelope through the height of the frame, leading to a reduction in the overturning moment envelope and peak storey accelerations. The concept of the higher mode mitigation mechanism in the proposed segmental rocking frame with the energy dissipating brace in the first storey, is shown at Figure 2-39 (Wiebe et al., 2013).

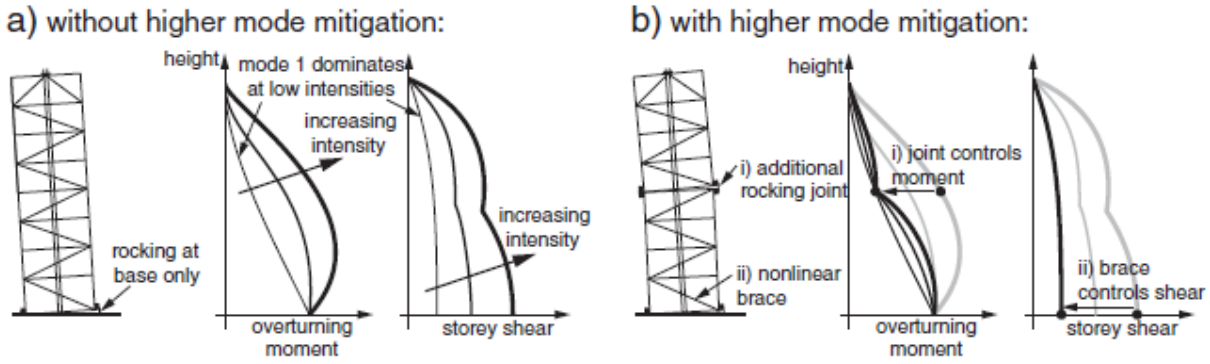

Figure 2-39: Concept of higher mode mitigation mechanisms: (a) system and response without higher mode mitigation and (b) system and response with higher mode mitigation(Wiebe et al., 2013).

To further investigate the performance of this system, they conducted an experimental testing program, which included a series of shake table tests on a 30% scaled 8-storey segmental rocking prototype with a self-centering energy-dissipating (SCED) brace at the first storey level, conducted at the Hydro-Québec Structures Laboratory at Polytechnique Montréal. The tested frame and its setup is shown at Figure 2-40.

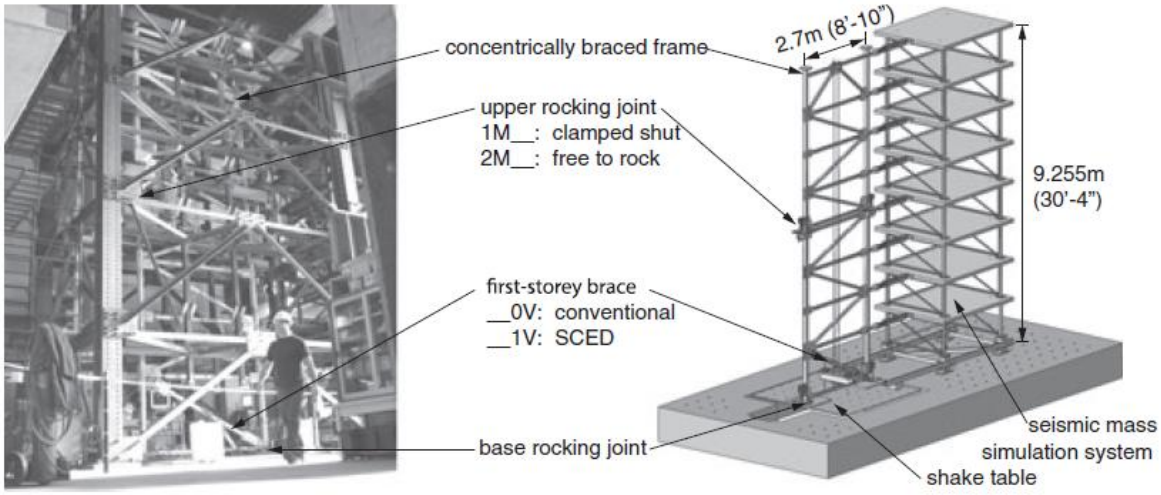

Figure 2-40: Controlled rocking steel frame shake table test setup (Wiebe et al., 2013).

The experimental tests demonstrated the satisfactory response of the system and confirmed its effectiveness in reducing peak storey shears and overturning moments. Furthermore, the results confirmed the agreement between the numerical simulations and experimental findings (Wiebe et al., 2013).

CHAPTER 3 DEVELOPEMENT OF THE PROPOSED STRUCTURAL SYSTEMS

3.1 General

Past three decades have witnessed remarkable progress in advancing the seismic design codes, developing novel seismic resistant structural systems and enhancing the quality of construction owing to the lessons from past earthquake, the comprehensive research on structural systems, the developments in structural software, and the advancement of technology. Accordingly, the design methods based on entire elastic behaviour in structures has been giving way to the ductile design approach using limit state criteria to control the seismic damage mechanism and limit it to pre-selected elements. In addition, the incorporation of various types of energy dissipation devices and re-centering mechanisms in structures has been attracted the interest of researchers and motivated numerous studies, briefly reviewed in Chapter 2, to devise novel earthquake resistant and resilience structural systems. Such advanced systems are expected to undergo no or minimal damages in the pre-selected elements or devices, be feasibly restorable and demonstrate superior seismic performance and resilience compared to conventional structural systems.

Special truss moment frames with ductile segments (STMF), which were developed after a comprehensive study on poor seismic performance of ordinary truss frames in 90s, was a typical structural system developed based on ductile design approach and considered a significant evolution in truss moment frame systems. Since then, several modifications such as application of viscos dampers or BRB diagonal members in the ductile panel have been suggested to improve its seismic resilience.

Although during severe earthquakes, the STMF system can exhibit a stable and reliable seismic response with a controlled damage mechanism limited to the special system, it is anticipated that this system will undergo large permanent residual deformations intensified by P-Δ effects that result in further damage in other structural and non-structural elements and negatively affect the serviceability of the structure. Due to considerable after event repair time required to replace the ductile segments and the damaged elements, such affected structures could be vulnerable to further damages and excessive drifting under doublet earthquakes and the potential strong after shocks, that can put them in the risk of instability issues.

To resolve the mentioned potential shortfalls in the STMF systems, this research focuses on development of novel earthquake resistant truss moment frames with a very robust and reliable seismic performance that adhere to the principles of sustainability. The concept of sustainability implies that the structures can remain operational after severe earthquakes with minimal or no repair demand.

This study introduces two category of seismic-resistant systems that employ energy dissipation devices and self-centering mechanisms to enhance the structural performance under strong seismic events. The first category of the developed earthquake resistant special truss moment frames is a truss moment framing system enhanced with friction dampers and self-centering steel tendons. The second category includes a hybrid system composed of truss moment frames with friction dampers linked to a post-tensioned rocking core acting as a united system. Under intense ground motions, these advanced systems are expected to exhibit a reliable seismic response with no or low damage and intended to adequately lend themselves to a viable and quick post-event repair and static realignment procedure. The development process and performed studies in the mentioned novel systems are discussed as follows:

3.1.1 Truss moment frame enhanced with friction dampers and steel tendons

The first system is composed of a truss moment fame enhanced with friction dampers and steel tendons. In this system the friction dampers are accommodated between the columns and the ends of the truss bottom chord extensions. Friction dampers can be designed and detailed to provide a predictable and uniform slip resistance over the predefined range of deformations in the system. Their reliable performance and effective functionality to dissipate seismic input energy has been proven in numerous experimental tests and actual buildings. A pair of tendons built of high-strength strands are installed along the bottom chord which connect the bottom chords to the adjacent columns. Steel tendons have been incorporated in many self-centering systems such as self-centering connections and rocking systems, which were developed and studied in the past two decades. In the proposed system the dampers can efficiently limit the lateral overstrength as the forces they impose to the columns and adjacent truss members. Moreover, no seismic damage is expected in these elements, and they can maintain their operability after intense seismic events. The system equipped with friction damper without tendon has no post-slip lateral stiffness to resist against the movement and therefore it is very susceptible to progressive drifting intensified by P-

Δ effects. In the proposed FT-TMF system this problem is eliminated by installation of the elastic tendons. Under lateral forces, as the frame deforms and friction dampers begin to slip, the tendons act in parallel with the dampers and the tensile force developed in the tendons results in a self-centering capacity within the system that helps return the frame to its original position. While this does not produce a fully self-centering response with a flag-shaped force- displacement curve, it enhances system stability, effectively controls and limits the seismic drifts, and improves the system's overall behaviour. In this system the dampers can be adjusted for a desired slip force and the cross-section area of the tendons can be regulated to achieve the required post-slip lateral stiffness to suppress P-Δ effect and realise a suitable response. The tendon length in this system can span the entire truss length, ensuring that the tendon strains remain within the elastic range of the material behaviour under the maximum expected inter-storey drifts. The seismic resilience of this system can be more enhanced by incorporating a set of replaceable support level grade beams near the column bases, which can reduce the seismic demand and inhibit the potential damage propagation in these elements.

As a first attempt to study the FT-TMF system, a single-storey prototypes truss frames were detailed with friction dampers and elastic tendons (Figure 3-1). The seismic performance of the prototype was examined under a series of 15 ground motions scaled for Vancouver area in accordance with NBCC 2015. The results were represented by Tremblay and Faraji at 12th Canadian conference on earthquake engineering in 2019 (Tremblay & Faraji, 2019).

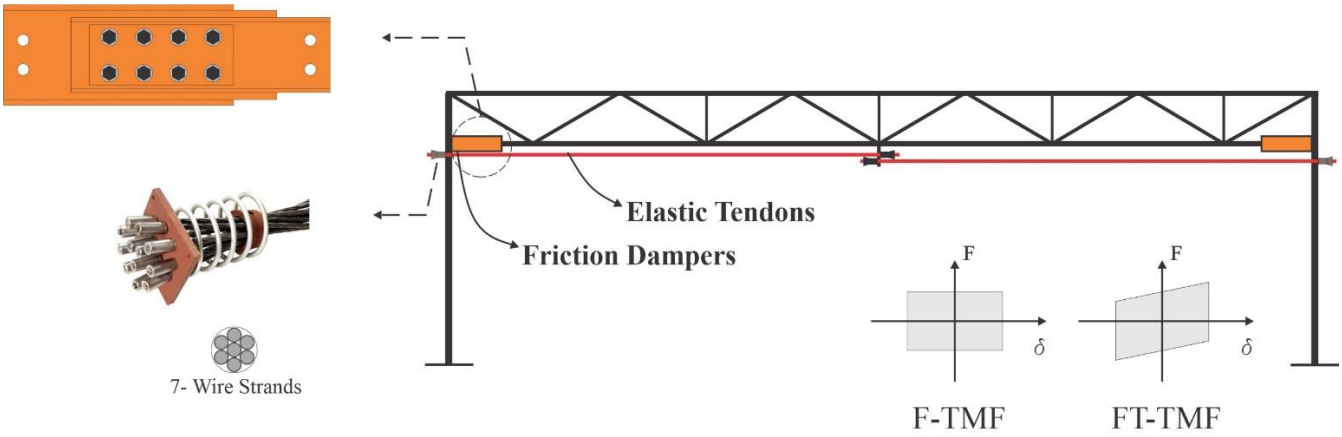

Figure 3-1 : Schematic and configurations of a single storey FT-TMF

In this thesis, the FT-TMF system is the subject of the first two article represented in Chapters 4 and 5.

In Article 1, the system FT-TMF is more discussed and employed as the lateral resisting system of three 4-, 7- and 12-storey typical commercial buildings with steel structure located in Vancouver, BC, a high seismicity zone in Canada. A force-based analyses and design procedure is developed to design the FT-TMFs in accordance with Canadian practice by application of NBCC 2015 and CSA S16-19 requirements.

The global seismic behaviour and performance level of the archetypal buildings is investigated by means of non-linear static and dynamic time history analyses performed under 15 ground motion specified for Vancouver area. Moreover, the behaviour of the structural element and the functionality of the employed friction devices and steel tendons are studied.

Article 2 focuses on collapse risk assessment of three 4-, 7- and 12-storey model commercial buildings with steel structure designed with FT-TMF lateral resisting system. The studied prototypes are considered to be located in the high seismicity Los Angeles area, CA, USA. Therefore, they are designed based on American practice with respect to standards of ASCE 7-22, AISC 360-16 and AISC 341-16. The Incremental Dynamic Analyses (IDA), under a set of 44 FEMA P-695 ground motion records, is applied to investigate the seismic performance of the archetypes, estimate collapse capacity and examine the employed design method.

3.1.2 Truss moment frame enhanced with post-tensioned controlled rocking core and energy dissipating friction devices

The studies on the FT-TMF systems led to development of the other proposed earthquake resistant system (RF-TMF). This structural system is composed of two F-TMFs inter-connected to a post-tensioned rocking core in between through linking beams. The rocking core is built of a stiff braced frame which can rock on its hinged support on the foundation. During an intense seismic event, when the rocking core uplifts and the gap opening occurs at the column-foundation connection, the post-tensioned force plus the additional tensile force developed in the tendons (strands) provide a resistant moment (self-centering capacity) in the system that tends to return the truss frame back to its original position while the friction devices dissipate a considerable part of the seismic force

simultaneously. Additionally, the tendons play a crucial role as stabilizers, ensuring the stability of the rocking frame throughout the event. As another vital competence in this hybrid system, the rigid rocking frame acts as a strong back for the entire system and suppresses the effect of higher modes during an earthquake providing the system with a pre-regulated lateral movement with a uniform (linear normalized) storey drift pattern over the height. Therefore, the risk of damage concentration of damage in one or few stories, that can lead to formation of soft-storey and brittle failure, is eliminated. This system can notably represent a flexible and stable seismic response with capability of resisting larger deformations compared to conventional system. A set of support-level replaceable grade beams, installed in columns' feet, can efficiently protect columns from the formation of plastic hinges and enhance the system's seismic resilience. Replaceable moment connections are accommodated in both link and grade beams to absorb the potential seismic damage and facilitate the post event repair programs. The schematic of the proposed system and detailing of the replaceable connection in a 9-storey frame is illustrated in Figure 3-2.

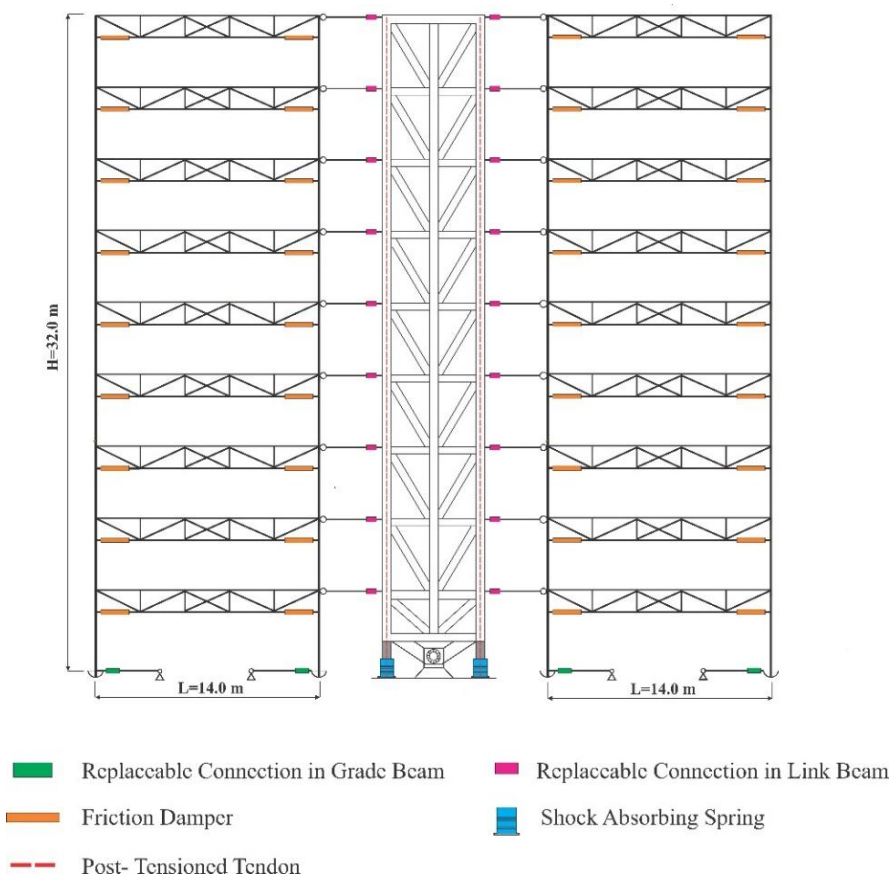

Figure 3-2 : Schematic of a 9-storey RF-TMF system

The subject of Article 3, which is assigned as Chapter 6 of this thesis, is the advantages, efficiency and seismic performance of the novel RF-TMF system. In this regard, this lateral load resisting system is applied and examined in a set of 7-, 9- and 12-storey model commercial buildings in Los Angeles area, CA at the western U.S. which are loaded and designed in compliance with American standards.

A force-based design method is proposed for the system and applied to the prototypes. The global seismic performance of the representative buildings is examined with non-linear static and dynamic time history analyses under 22 strong ground motion. Moreover, the captured results are used to interpret the functionality of the friction dampers and post tensioned rocking frame in this system. A type of replaceable fuse connection, which is accommodated in the linking and grade beams to control the internal forces and enhance the system's resilience, is also detailed and discussed.

CHAPTER 4 ARTICLE 1: ADVANCEMENT IN TRUSS MOMENT FRAMES' SEISMIC BEHAVIOUR WITH FRICTION DAMPERS AND TENDONS

This article is submitted to: Journal of Constructional Steel Research on 27th October 2024
Manuscript Number:JCSRES-D-24-02050

Keyhan Faraji [a], Robert Tremblay[a] and Joshua Woods[b]

a Department of Civil, Geological and Mining Engineering, Polytechnique Montréal, Montréal, QC, Canada
b Department of Civil Engineering, Queen's University, Kingston, ON, Canada

Corresponding Author: Keyhan Faraji, Email: keyhan.faraji@polymtl.ca

Abstract

This paper proposes a novel steel truss moment frame system equipped with friction dampers and elastic tendons (FT-TMF). The new structural system is intended to improve the seismic performance of conventional TMF structures. Three archetypal structures, designed with the FT-TMF system, were modeled and studied as the lateral load resisting structural system for a 4-, 7- and 12-storey buildings which were designed for a site in Vancouver, British Columbia in accordance with the National Building Code of Canada (NBCC 2015) and the standard for the design of steel structures in Canada (CSA S16-19). Numerical models of the archetypal structures were developed in OpenSees and SAP2000 software and a series of spectral, nonlinear static, and nonlinear dynamic analyses were employed to capture their seismic responses. Results of the study demonstrated that under design earthquakes the new system had a reliable hysteretic behaviour, experienced negligible residual drifts, and was undamaged and would remain in service.

Keywords: Truss moment frame, Friction damper, Elastic tendon, dynamic analysis

4.1 Introduction and Research Objective:

Truss moment frames (TMFs) are economic structural systems that are easy to fabricate and install in a timely manner. This type of structural system, in the form of different multi-span and multi-storey frames, can be easily employed to accommodate long spans and cover large areas. Consequently, it has been an ideal system that has commonly been used in the construction of malls, arenas, warehouses, and industrial structures. Truss moment frames are also a favorable

system from an architectural perspective, because mechanical and electrical systems can be installed through or inside the open web space in the girders, resulting in reduced storey heights (Goel & Itani, 1994; Jiansinlapadamrong et al., 2019).

After poor seismic performance of TMFs during Mexico City earthquake in 1985, a significant amount of research was conducted on TMFs, which led to the introduction of special truss moment frames (STMFs). STMFs are designed with a replaceable ductile panel (special segment), in the form of X-diagonal or open Vierendeel, located in mid span to act as a fuse and dissipate seismic energy through controlled inelastic deformations (Hanson et al., 1986; Basha & Goel, 1994; Goel & Itani, 1994; Basha & Goel, 1995; Ireland, 1997). In this system, the concentration of plastic deformation is in the ductile panel, and the resulted stable hysteretic behaviour of the frame mitigates the risk of brittle fractures in the surrounding structural elements, including the columns, chords, verticals and diagonal members. Theoretical and experimental research on this low damage system resulted in a better understanding of its seismic performance and improved the design procedure over the past three decades (Goel & Itani, 1994; Chao & Goel, 2008; Pekcan et al., 2009).

More recent research on STMFs, including the combination of open web steel truss frames and buckling restrained braces (BRBs) led to development another low damage truss moment frame system, commonly referred to as a Buckling Restrained Knee Braced Truss Moment Frame (BRKB-TMF), in which buckling resisting knee braces are installed between bottom chords and adjacent columns. In this system, which is designed with a performance based plastic design approach (PBPD), the BRBs play the role of special segments in STMFs acting as a replaceable fuse which dissipates the seismic energy through cyclic deformation of the BRBs (Wongpakdee et al., 2014; Yang et al., 2015).

TMFs with ductile fuses are expected to have controlled flexible seismic response with no risk of progressive collapse and are normally designed to meet life safety performance criteria. However, during large earthquakes, STMFs could experience significant residual drifts, intensified by dynamic P-Δ effect, due to large plastic deformations in the ductile segments or BRBs. Since it may not be possible to replace the damaged fuses immediately after an earthquake, potential aftershocks similar to those that frequently occurred after the 2010 Canterbury earthquake in New Zealand (Potter et al., 2015) or the complex doublet earthquakes that happened after the 2012 Ahar-

Varzaghan earthquake in Iran (Momeni et al., 2019) would make the damaged frames vulnerable to permanent damage in elements not designed to resist earthquake loads and negatively affect their stability. Such damaged structures would require repair and rehabilitation before they could return to service, resulting in significant costs and disruptions in functionality.

As a response to the need for economical and resilient structural systems, the main objective of this research was to develop a new type of earthquake resistant and resilient steel truss moment frame that can be employed in multi-storey buildings in high-seismic zones. The system was intended to experience no or low damage and remain in service following a large earthquake and any aftershocks.

The proposed system, denoted FT-TMF, is a steel truss moment frame with friction dampers installed between the bottom chord of the truss and the adjacent columns and a pair of elastic tendons in each span which connect the bottom chord to the columns (Faraji & Tremblay, 2019; Tremblay & Faraji, 2019). In this system, the friction dampers are designed to provide a predictable and uniform slip resistance over the anticipated range of deformations, dissipate input seismic energy, and limit lateral seismic forces imposed on the truss and column members. Because a TMF with friction dampers only (F-TMF) would exhibit no post-slip lateral positive stiffness, and thus, would be vulnerable to progressive drifting due to P-Δ effect. Adding tendons, which act in parallel with the dampers, provides positive lateral stiffness in the post-slip (nonlinear) range. The tendon cross-sections are selected and adjusted such that the sum of the positive stiffness of the tendons and the negative stiffness of the system, induced by P-Δ effect, remains positive and sufficiently large to enhance the system's seismic response. The tensile forces in the tendons generate self-centering capacity in the frame, reducing lateral deformations during an earthquake and minimizing residual drifts afterward. To function effectively, tendon strain must stay within the material's elastic range (Tremblay & Faraji, 2019).

The use of friction dampers as a means of adding energy dissipation capacity to a structural system has been investigated in a number of previous analytical and experimental studies (Christopoulos et al., 2008; Kim & Christopoulos, 2008) and the concept of using post-tensioned tendons, designed to re-center a structure and enhance its seismic performance has been studied in previous applications to frames with post-tensioned connections, self-centering steel plate shear walls and

rocking cores (Ricles et al., 2001; Garlock et al., 2007; Eatherton, 2010; Deierlein et al., 2011; Clayton et al., 2016; Grigorian & Grigorian, 2018; Martin et al., 2019).

In this study, the application of friction dampers and elastic tendons to a truss moment frame to form a novel lateral load resisting system, called FT-TMF, is described and a detailed design procedure is presented.

To verify the proposed design procedure and examine the seismic behaviour of the new system, three archetypal 4-, 7- and 12- storey buildings are designed and subjected to response spectrum, nonlinear pushover, and nonlinear time history analyses. The analytical results are compared in terms of base shear, displacement time history, and residual drift to investigate the seismic performance and resilience of the proposed FT-TMF structural system.

4.2 Archetypal buildings

The proposed FT-TMF system is used as the lateral load resisting system (LLRS) for a 4-, 7- and 12-storey steel commercial buildings, with heights of 18.5 m, 32 m, and 54.5 m, respectively, and are designed for a site on a firm ground (site class C) in Vancouver, British Columbia.

In all of the buildings the height of first storey is 5 m and all other stories have a constant height of 4.5 m.

Figure 4-1 shows a plan view of the studied buildings, which consists of 4 bays in the E-W direction with a constant span length of 14 m and 3 bays in the N-S direction with span lengths of 13 m, 10 m, and 13 m, respectively.

Two similar double span FT-TMFs, which are located symmetrically along the parallel perimeter walls are employed to resist lateral loads applied to the buildings in E-W direction and four similar single span FT-TMFs which are located symmetrically along perimeter walls (two by two in parallel) form the LLRS of the studied buildings in N-S direction.

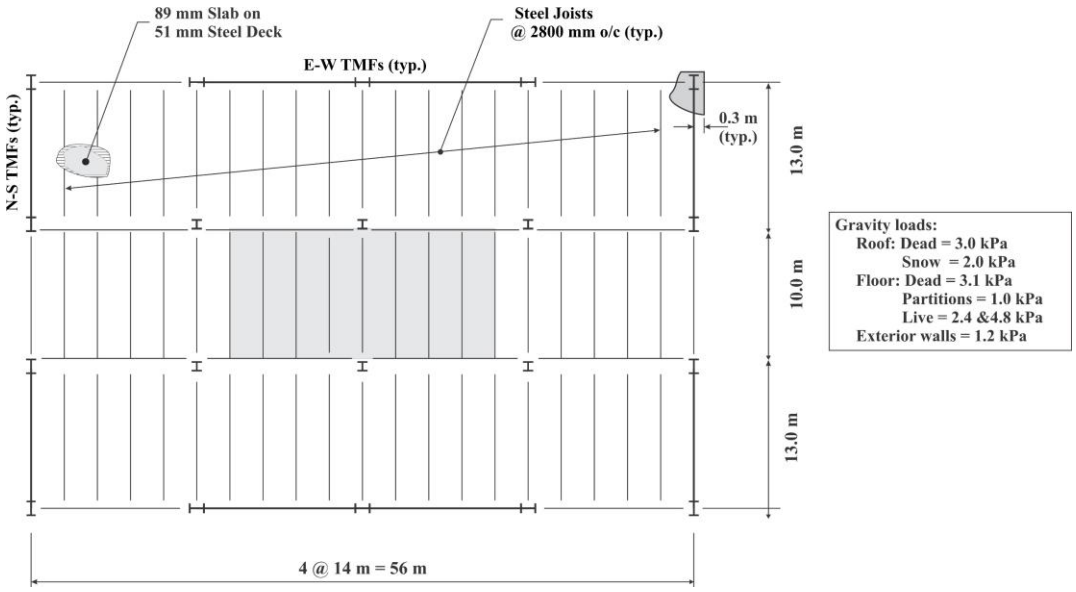

Figure 4-1 : Plan view of the studied buildings

Figure 4-1 also summarizes the gravity loads, including dead, live, and snow loads applied to the archetypal buildings, which are calculated based on the weight of building's elements, the use and occupancy of the building (commercial office space) and the location of the building, respectively, in accordance with NBCC 2015 (National Research Council of Canada, 2015).

4.3 Modeling, Analyses, and Design Procedure:

To study the seismic response of the archetypal buildings, the 4- ,7- and 12- storey truss moment frames are modeled in OpenSees (Mckenna, 2020) and SAP2000 (Computers&Structures Inc., 2023) finite element software. The two software are used to compare results and ensure the accuracy and reliability of the analytical results. The schematic of the 7-storey FT-TMF model is illustrated in Figure 4-2. Because the archetypal buildings' plans are symmetrical (Figure 4-1), only one of the FT-TMFs in E-W direction for each building is modelled and studied. In the studied models, the length of the spans (L) between columns is 14 m, the overall truss depth (d) and the length of special panels (Ls) are 1.4 m and 2.8 m, respectively.

In the archetypal buildings, the trusses are made of steel channel sections, which compared to angle sections, can provide higher capacity for the TMFs, which is required in high-seismic zones (Jiansinlapadamrong, 2018; Jiansinlapadamrong et al., 2019; Chao et al., 2020). The columns are wide flanged steel sections. Open web steel joists are utilized in the N-S direction to cover the span

length in the interior bays. Considering the length of panels and applied loads, composite steel decks which are made of roll formed corrugated steel plate with the thickness of 0.91 mm and 0.76 mm are selected for the floors and roofs of the buildings, respectively. The total thickness of the composite steel deck is 140 mm including 51 mm depth of the flutes and 89 mm thickness of light weight concrete slab over top of the flutes.

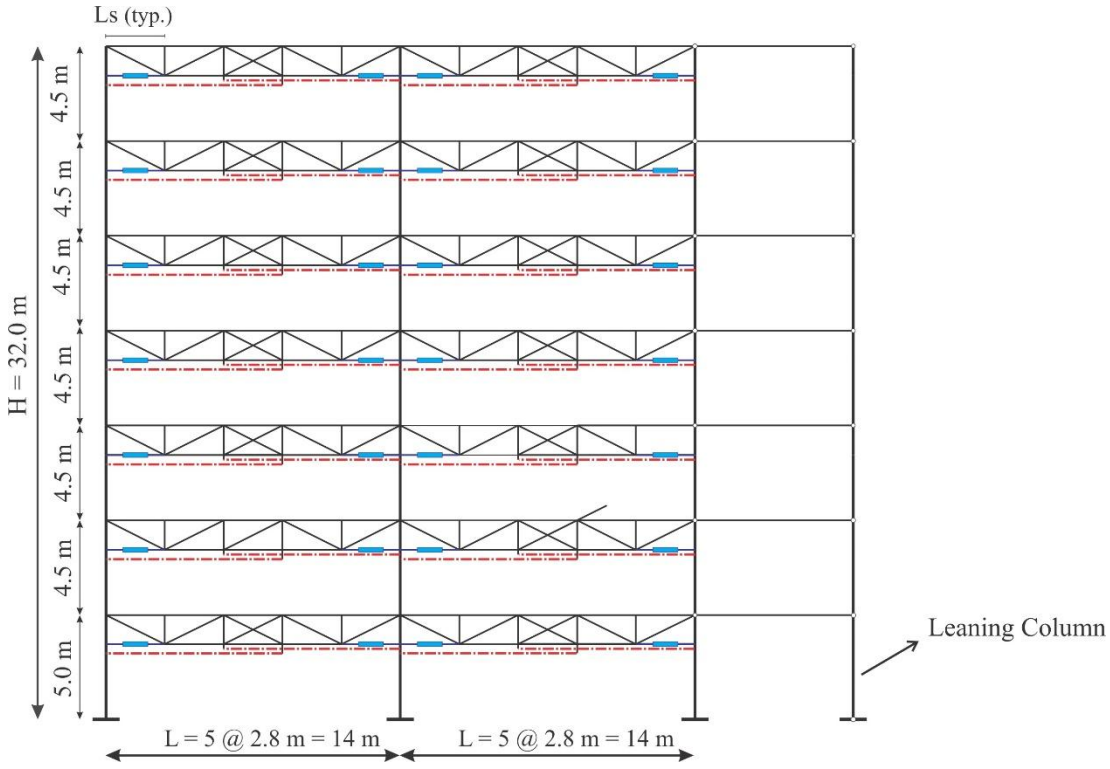

Figure 4-2: Schematic of the 7-storey FT-TMF model and the leaning column

To simulate the non-moment resisting frames and account for the induced P-Δ effects, each model includes a leaning column that carries half of the total loads on the gravity columns. The leaning columns are modelled with elastic elements and linked to truss moment frames with rigid elements in both software programs.

In OpenSees, two node link elements with elastic perfectly plastic uniaxial material, are utilized to simulate the friction dampers. The steel tendons are also modelled with two node link elements, but are assigned a bi-linear material. To model the columns, nonlinear BeamColumn elements with nonlinear fiber section elements are utilized. The fiber sections are assigned the Steel02 uniaxial material model to simulate their non-linear behaviour. The rest of elements, including the chords,

diagonals, verticals and braces behave elastically; they are modelled with elasticBeamColumn elements.

In SAP2000, multi-linear plastic type link elements are used to simulate the friction dampers and tendon elements are used to model the steel tendons, which are tension only elements with ASTM A416 Grade 270 material. The remaining structural elements, including columns, chords, verticals, diagonals and braces, are modelled using frame elements. Nonlinear plastic hinges, defined per ASCE 41-17 (The American Society of Civil Engineers, 2017), are placed close to column bases where the maximum interaction between axial load and moment is expected under lateral earthquake loads.

To determine the maximum force in the FT-TMFs and ensure that when subjected to a design-level earthquake, they provide immediate occupancy level of performance with low or no structural damage, an analyses and design procedure, that includes six stages is proposed, which includes (1) design initialization, (2) strength and stability control for gravity loads, (3) sizing of the steel tendons, (4) pushover analysis with 30% larger damper capacity (5) final design and (6) nonlinear time history analysis and design verification. Stages of the seismic analysis and design are performed in accordance with NBCC 2015 (National Research Council of Canada, 2015) and CSA S16-19 (The Canadian Standards Association, 2019).

4.3.1 Stage 1 - Design Initialization

In the first design stage, the lateral load resisting truss moment frames of the archetypal buildings are considered as conventional TMFs, without any dampers or tendons. The focus of this design stage is on the seismic design of the frames and initial sizing of their structural members including the diagonals, verticals, braces, chords, and columns. The dampers and tendons will be added to the TMFs at the end of design Stages 1 and 3, respectively, to form the proposed FT-TMFs.

For seismic analysis, elastic response spectrum procedure is employed, in which the base shear force is scaled to equivalent static force and is used to consider the contribution from each mode of vibration to indicate the likely maximum seismic response of the buildings. The study used the uniform hazard spectrum for Vancouver, British Columbia according to NBCC (2015). To combine the effect of gravity and earthquake loads and determine the maximum design forces, the load combination D+0.5L+0.25S+E, composed of dead (D), live (L), snow (S) and earthquake (E) load components, is used. Because the proposed system is new, the values of ductility and

overstrength related force modification factors, R_d and R_o, are not specified for it in NBCC 2015, the values of 4.0 and 1.0, respectively, are adopted. The recommended values of R_d and R_o for this system will be investigated in future studies.

The maximum forces developed in the frames' elements, which are derived from the applied gravity load combinations and the elastic response spectrum procedure, are used in initial seismic design of the members in accordance with CSA-S16-19 standard. Furthermore, the maximum axial forces developed in the bottom chords of the trusses at the end panels, closest to the columns, are used to design the friction dampers. The dampers are installed in both ends of the bottom chords connecting them to the adjacent columns to form F-TMF system. These forces are used as the specified slip (design) forces for the friction dampers.

4.3.2 Stage 2 - Strength and Stability Control for Gravity Loads

The secound design stage focuses on the verification of member sizes obtained in Stage 1 for a scenario that the dampers are not installed, simulating the situation in which the repair or replacement may need to be done. The frame without dampers and bottom chords at the end panels are subjected to the load combination 1.25D+1.5L+0.5S to prove the adequacy of their members under gravity loads and ensure the frames will remain stable during potential damper replacement or maintenance operations.

4.3.3 Stage 3 - Sizing of the Steel Tendons

In the third design stage, the steel tendons, which are designed to remain elastic and act as the self-centering elements, are added to the F-TMFs to form the FT-TMF system. The tendons should be designed to mitigate the induced P-Δ effect, providing required lateral positive stiffness resulting in restoring capability to efficiently reduce the lateral seismic deformations during an earthquake and residual drift after an earthquake. In this study, the tendons are assumed to be low-relaxation 7-wire high-strength strands with a yield stress (F_y) of 1760 MPa.

To determine the size of the steel tendons in each storey, Equation (4.1), which is derived from static equilibrium of the FT-TMF system under the lateral and gravity forces, can be utilized (Figure 4-3).

In Figure 4-3, for simplicity in equations, the frame in the i^{th} storey is simulated by a single column.

$$V_i h_{s,i} + P_i \Delta_i = T_i \mathrm{d} \rightarrow V_i = T_i(\mathrm{d}/h_{s,i}) - (P_i/h_{s,i})\,\Delta_i \tag{4.1}$$

Where V_i is storey shear force, P_i is gravity load combination carried by all columns at ith storey , T_i is tendons' force at ith storey and C_i represent internal reaction force of the frames applied to columns at ith storey level . Furthermore, d is the truss depth, $h_{s,i}$ is the storey height and Δ_i is lateral displacement of the FT-TMF after the friction dampers slip at ith storey level.

The tensile force in tendon in the ith storey, T_i, is obtained using Equation (4.2):

$$T_i = K_{T,i}\,\delta_i \tag{4.2}$$

where δ_i is the elongation of the tendons after the friction dampers slip and $K_{T,i}$ is the axial stiffness of the tendon, which can be determined using Equation (4.3):

$$K_{T,i} = EA_i/L_i;\ \delta_i = \Delta_i(d/, h_{s,i}) \tag{4.3}$$

Where $K_{T,i}$ is tendons' axial stiffness at ith storey, E is modulus of elasticity, A_i is tendons' cross section at ith storey working in each direction, L_i is the length of tendons at ith storey and δi represent elongation of tendons at ith storey occurring after the friction dampers slip. Substituting Equations (4.2) and (4.3) into Equation (4.1) results in an equation for the term V_i/Δ_i, which represents the net lateral stiffness of the storey when sliding of dampers occurs, and can be determined using Equation (4.4):

$$V_i/\Delta_i = K_{T,i}\,(d/, h_{s,i})^2 - (P_i/, h_{s,i}) \tag{4.4}$$

Where the terms $K_{T,i}(d/h_{s,i}))^2$ and $(P_i/h_{s,i})$ represent minimum required positive lateral stiffness that should be provided by tendons, and the negative stiffness induced in each storey by P-Δ, respectively.

Ultimately, the minimum required cross section of the tendons in each storey, A_i , is derived from the Equation (4.4).

Since the tendons work in tension, the calculated A_i give the required tendon cross section, in the considered storey *i*, which should act in each direction. The A_i value is divided to the number of spans (number of tendons for each direction) to get the number of strands needed in each tendon.

The frames equipped with the minimum calculated tendons sizes (1.0T) from Equation (4.4) are denoted FT-TMF (1.0T).

A coefficient of $n \geq 1$, can be applied to the A_i value in the FT-TMFs to achieve the required post-slip positive stiffness (restoring force) in the system. The resulting lateral stiffness of the system, incorporating tendons designed with the coefficient n and denoted as FT-TMFs (nT), can be determined using Equation (4.5):

$$\mathrm{V}_i/\Delta_i \; = \; nK_{T,i}(d/h_{s,i}))^2 - \; (P_i/h_{s,i})) \, , n \geq 1 \tag{4.5}$$

The employed tendons are expected to provide the archetypal buildings with the adequate self-centering capacity which can efficiently control the lateral drift and mitigate residual drifts when subjected to a design level earthquake and potential aftershock events. This design approach ensures that the building will remain functionally operational following the seismic event, minimizing downtime and economic losses.

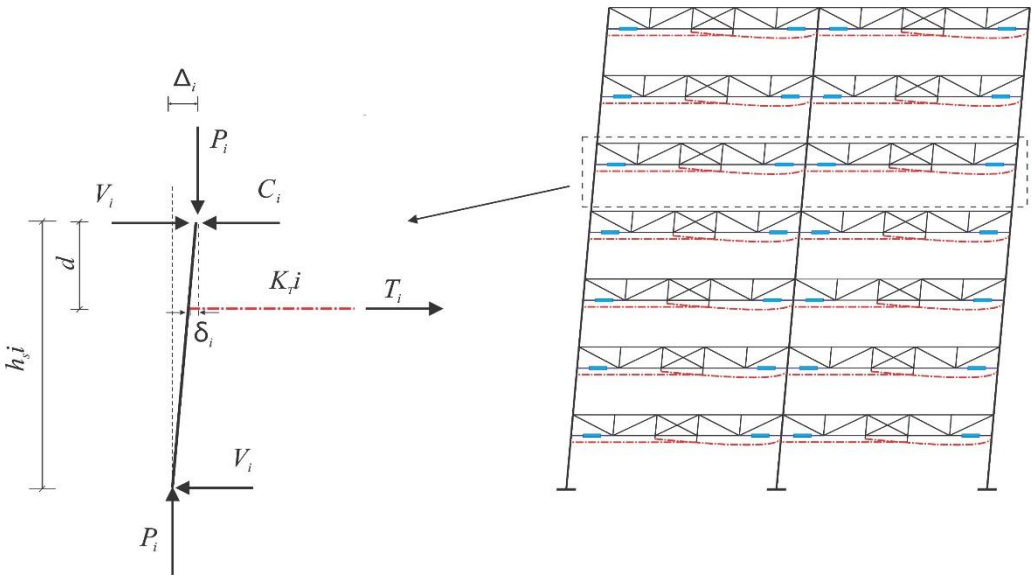

Figure 4-3: Equilibrium of the FT-TMF system upon activation of the dampers

4.3.4 Stage 4 - Pushover Analysis with 30% Larger Damper Capacity

In a realistic earthquake scenario, there could potentially be an increase in the damper slip force as a result of material properties change over time or human error during maintenance. Larger forces

in the friction dampers could lead to higher internal forces in other structural members, larger than those obtained from analyses in Stages 1 and 2, resulting in potential undesired performance or damage. Moreover, the tension force developed in tendons due to lateral seismic deformation, induces additional force in other structural elements of the frames such as columns which should be analyzed and considered in the design procedure.

Considering the above-mentioned factors and to ensure the structural members remain elastic under a design level earthquake, this fourth design stage artificially increases the damper slip forces by 30% and each building model is subjected to displacement controlled pushover analysis with the presence of gravity loads up to a lateral drift of 1.5% at the roof level. Two different lateral pushover force distributions are considered, including a triangular force pattern and a lateral load pattern normalized with spectral seismic forces. The maximum results obtained from using two patterns in the pushover analysis are almost similar.

The maximum force demands in the structural members from the pushover analysis are used in design stage 5. Furthermore, the maximum tendon forces and elongations are controlled to ensure the tendons remain in elastic range and function as expected.

4.3.5 Stage 5 - Final Design

In this stage, the forces in the structural members obtained from analyses performed in stages 1, 2 and 4, are compared to determine the maximum demand, which is then utilized for the final design iteration in accordance with CSA-S16-19 guidelines. Minor adjustment in dampers capacity may be required due to increase in members' sizes that leads to minor reduction in the periods of the frames.

At the end of this stage the models are subjected to a secound push over analysis, with the target displacement corresponding to 2.5% drifting at the roof level, to ensure the dampers and tendons function as expected and check the potential damage in the frame.

4.3.6 Stage 6 - Nonlinear Time History Analysis and Design Verification:

In this final stage, the TMF models are subjected to ground motion records to simulate the behaviour of the TMFs under seismic events and verify the design. Nonlinear time history analyses (NLTHA) are performed in accordance with NBCC 2015 guidelines.

The system-level response parameters of interest include the maximum inter-storey drift, base shear, tendon elongation, and residual drift.

At the component-level, the maximum force demands in the structural members such as columns, obtained from NLTHA, are compared with the force demands used in the design in stage 5 to verify that the members have sufficient capacity. Design stages 1-6 are summarized and visualized in the flowchart represented in Figure 4-4.

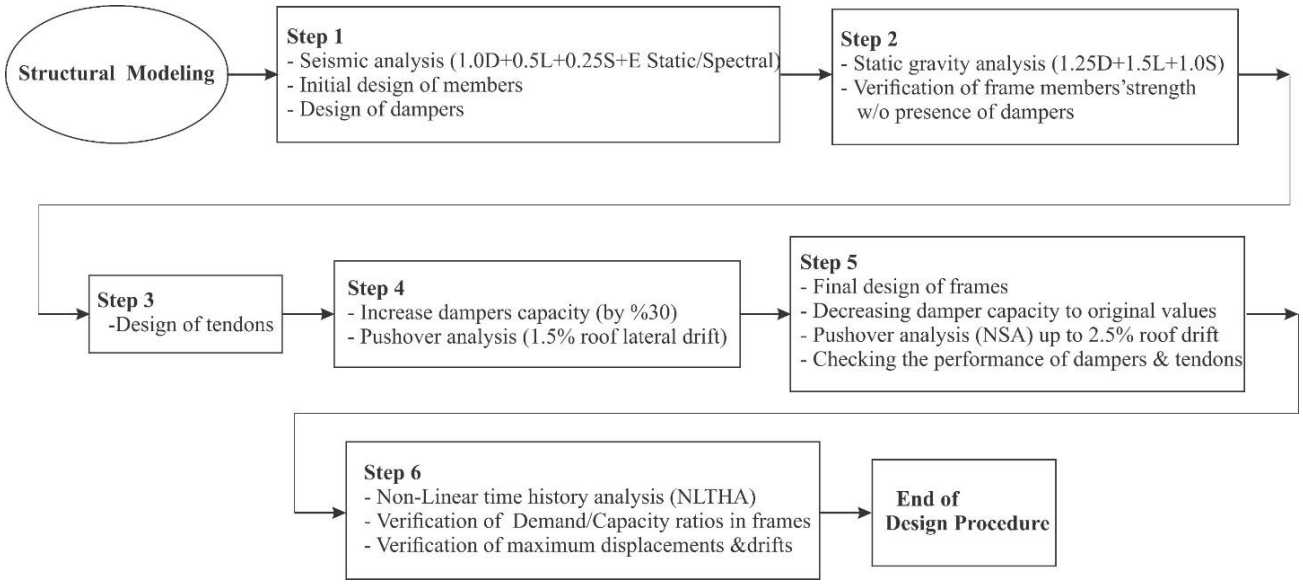

Figure 4-4: Flowchart of the design procedure from modelling to final design verification

The structural elements including diagonals, braces, top and bottom chords, vertical and column members as well as the calculated minimum tendons from Equations (4.4) for the 4-, 7- and 12-storey FT-TMFs (1.0 T), which are determined through the analyses and design procedure through the stages 1 to 6, are represented in Table 4-1 at Appendix I. The capacities (slip forces) of the employed dampers are also summarized in Table 4-2 (Appendix I). As discussed, the dampers are designed in accordance with the axial force obtained from the spectral analyses with the presence of gravity loads.

4.4 Non-Linear Static Analysis (NSA) and Anticipation of Seismic Response

To investigate the behaviour of the three prototype frames, a nonlinear static pushover analysis is employed. This analytical method offers a comprehensive overview of the system's global response to lateral loads, demonstrating the dampers' effectiveness in limiting base shear force, the

self-centering capability afforded by the elastic tendons, and variations in the system's lateral stiffness across both linear and nonlinear (post-slip) ranges.

The results of the pushover analysis for the archetypal buildings with F-TMF and FT-TMF (n =1.0 and 1.3) lateral load-resisting systems up to a lateral roof displacement corresponding to 2.5% drift are shown in Figure 4-5. The results show that in all of the models with F-TMF and FT-TMF systems, the damper slip occurs when the base shear forces reach to about 0.85, 0.90, and 0.95 of the base shear values calculated from spectral analyses in accordance with NBCC 2015 (V_{NBCC}), in the 4-, 7- and 12-storey frames, respectively. The calculated V_{NBCC} for 4-storey is 1365 (kN) , for 7-storey is 1810 (kN) and for the 12-storey is 2560 (kN).

The force corresponding to the point in which all of the dampers have reached their slip load, denoted $V_{Pushover}$, is approximately $1.35V_{NBCC}$, $1.20V_{NBCC}$ and $1.15\ V_{NBCC}$ in the 4-, 7- and 12-storey models at 2.5% roof drift, respectively (Figure 4-5) . The overstrength in $V_{Pushover}$ is the result of overstrength in the dampers caused by the presence of gravity loads considered in their design and the resisting moments in the rigid supports of the columns.

The comparative pushover curves, illustrate that the buildings with F-TMFs ,which have no tendons, experience negative lateral stiffness in post-slip range, which is intensified by the increase in the height of the building due to larger P-Δ effects. This negative stiffness can lead to large deformations and residual drifts under earthquake loads and make the buildings vulnerable to significant damage and potential stability issues. Alternatively, in the FT-TMF models the function of the tensons, neutralize the P-Δ effect providing the system with a self-centering capability (positive lateral stiffness) which is expected to limit seismic deformation and residual drifts.

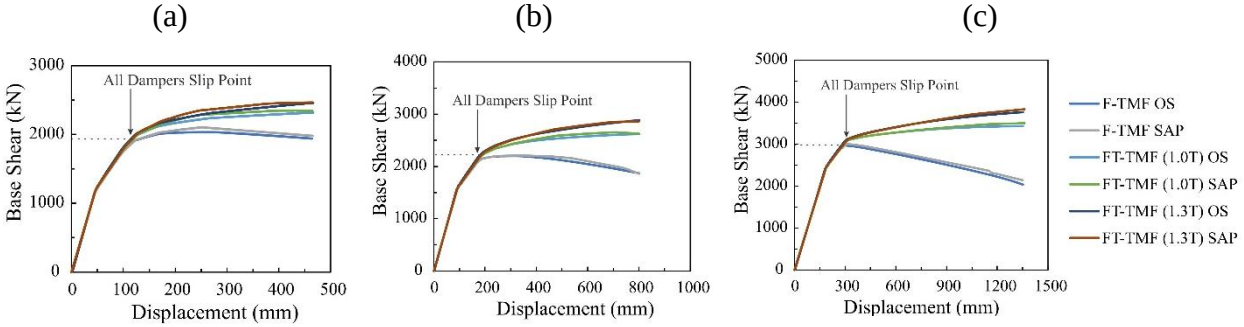

Figure 4-5: Force -Displacement curves of a: 4, b: 7 and c: 12-storey models

To study the nonlinear hysteretic behaviour of the archetypal buildings under controlled cyclic loading, the TMF models are subjected to a cyclic pushover analysis. Similar to the previous pushover analysis, the target displacement for the cyclic pushover is a lateral roof displacement corresponding to 2.5 % drift. The hysteretic cyclic force-displacement response of the buildings, illustrated in Figure 4-6, show that the results of the cyclic pushover analyses are similar to those in Figure 4-5. The FT-TMFs show a post-slip positive stiffness with stable hysteretic behaviour. While the negative lateral stiffness in post-slip rang in F-TMFs, which grows with the increase in height of the buildings makes them vulnerable to drifting and instability issue. The energy dissipation in the frames is not significantly impacted by the tendon's stiffness.

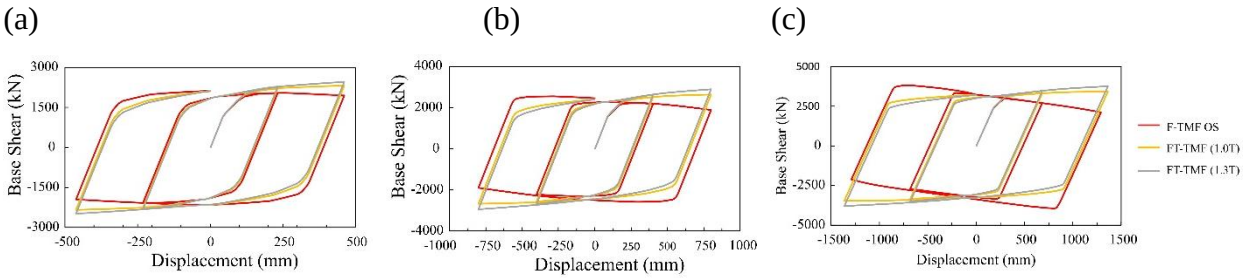

Figure 4-6: Cyclic Force -Displacement curves of a) 4-storey, b) 7-storey and c) 12- storey models

4.5 Non-linear Time History Analyses (NLTHA)

Nonlinear time history analysis is employed to simulate and study the seismic behaviour of the modelled FT-TMFs under potential earthquakes. Therefore, they are subjected to a suite of 15 ground motion records (GMs) considering three different earthquake sources, including crustal (VC-CR), deep in-slab subduction (VC-IS), and subduction interface (VC-SI) sources each of which contribute to the seismic hazard in southwest British Columbia, Vancouver, Canada (Figure 4-7).

The selected 15 events are scaled in accordance with the NBCC 2015, using a target spectrum for the design site with a probability of exceedance of 2% in 50 years. Figure 4-7 shows the scaled ground motion acceleration spectra (5% damping) for the earthquakes from the CR, IS and SI sources.

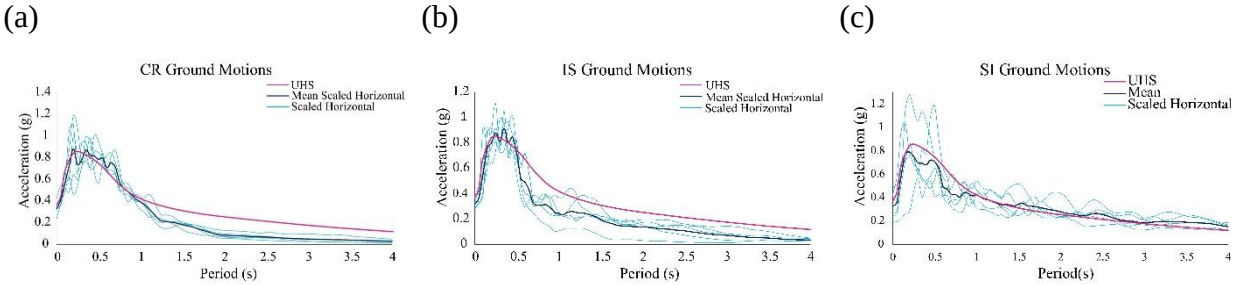

Figure 4-7: Ground motion acceleration spectra (with 5% damping) for the a) VC-CR, b)VC- IS and c) VC-SI sources

Key response parameters obtained from the NTHA include the inter-storey drift, maximum base and storey shear force, axial force, tendon strain and residual drift.

Due to space limitation, in this article, only the seismic response of the FT-TMFs (1.0T) are illustrated graphically. These results are then compared quantitatively using the key response parameters for FT-TMF (1.3T).

4.5.1 Inter-Storey Drift

Inter-storey drift is an important parameter in assessment of the behaviour in a structure during a seismic event because it can often be correlated to a level of expected damage and potential instability issues. As shown in Figure 4-8, the mean of the 5 maximum inter-storey drifts from the NTHA are approximately limited to 1.4%, 1.5%. and 1.8% for the 4-,7- and 12-storey buildings, respectively.

The analyses show that by increasing the tendon size to 1.3T, the largest values of the 5 maximum inter-storey drifts slightly reduce to approximately less than 1.3%, 1.4% and 1.6% for the 4-,7- and 12-storey FT-TMF (1.3T) buildings, respectively. Thus, it is expected that using more tendons can enhance the regulation and reduction of inter-storey drifts. The analyses indicate that the most significant drift ratios are attributed to the SI group of ground motions.

The peak inter-storey drifts in the 4-, 7-, and 12-storey FT-TMFs (1.0T) are approximately 1.8%, 1.9%, and 2.8%, respectively. These values are reduced to 1.7%, 1.9%, and 2.1% in the FT-TMFs (1.3T).

Due to the design of structural elements to remain elastic at 2.5% lateral drift, the resulting inter-storey drifts pose no concern. Furthermore, NLTHA results indicate that all structural models,

including FT-TMF (1.0T) and FT-TMF (1.3T), maintain stability, retain their operability and thus meet the design objectives under the applied earthquakes.

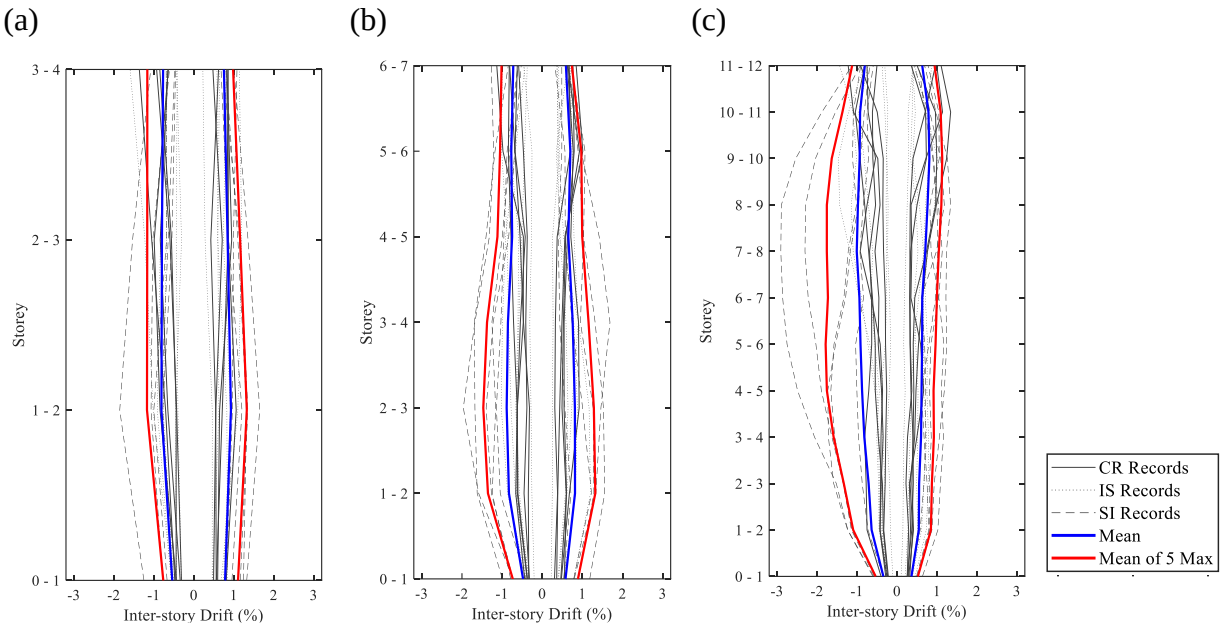

Figure 4-8: Lateral inter-storey drifts resulted from THA in the a) 4-storey b) 7-storey and c) 12-storey buildings with FT-TMF (1.0T)

4.5.2 Base Shear

Seismic base shear is an important factor for seismic analyses design and is a parameter that can be much more realistically estimated using NTHA compared to static and pseudo-dynamic analyses. Figure 4-9 shows the storey shears over the height of the buildings with FT-TMF (1.0T). The graphs in Figure 4-9, show that the mean of 5 maximum base shear force (V_{NTHA}) is close to the highest base shear value in the three FT-TMF (1.0) models.

The maximum base shear forces are about 2588 kN, 2988 kN, and 4095 kN in the 4-, 7- and 12-storey buildings that well match the base shear values resulted from pushover analysis at 2.5% target drift. Based on the results, V_{NTHA} for the FT-TMFs (1.3T) are very similar to those for the FT-TMF (1.0T) models.

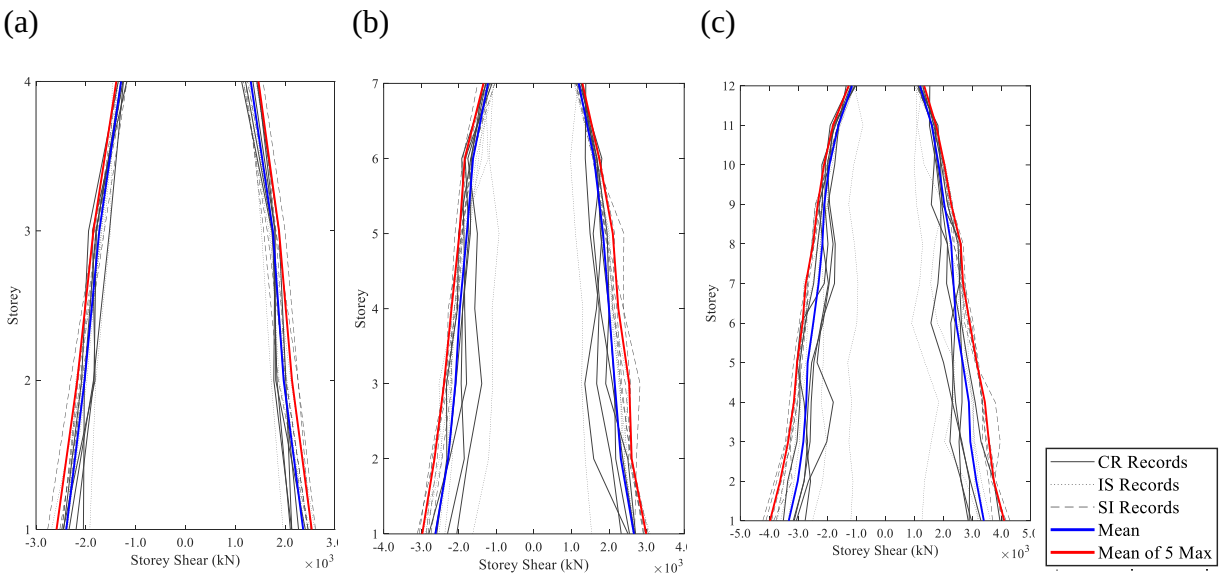

Figure 4-9: Base and Storey shears resulted from NTHA in a) 4-storey b) 7-storey and c) 12-storey FT-TMF (1.0T) models

4.5.3 Axial Force and Moment in Exterior Columns

It is also important to verify that the structural elements of the TMF, which were designed to remain elastic during a large earthquake, can resist the seismic loads obtained from the NTHA and confirm the design procedure (from design stage 5). Figure 4-10 and Figure 4-11 compare the maximum axial forces in exterior columns and corresponding moments with the design axial forces and moments in the archetypal buildings with FT-TMF (1.0T). The results demonstrate that the force and moment values utilized in design of the columns are very close or slightly higher than the average of the 5 maximum force and moment values from the NTHA.

It should be noted that the interaction of the maximum axial force and the corresponding moment dominates the interaction of the maximum moment plus corresponding axial force. Similar results are derived for the buildings with FT-TMF (1.3T). Therefore, the design of the columns is deemed to be acceptable. The analysis for the resistance of the other structural elements, including the interior columns and truss elements were also verified and showed they remain in elastic range.

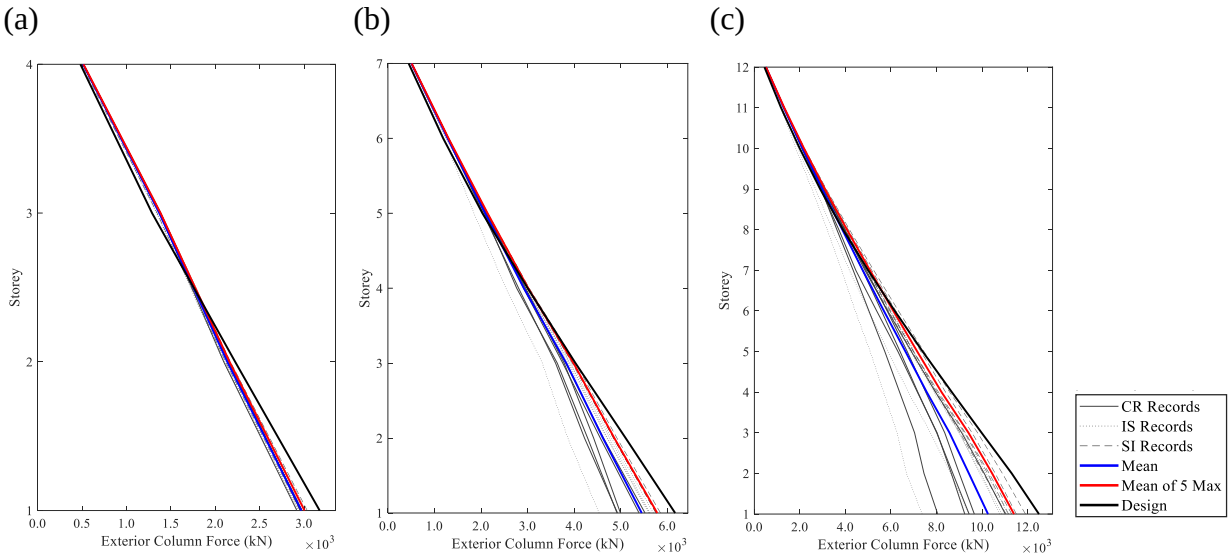

Figure 4-10:Exterior columns axial forces resulted from NTHA in a) 4-storey b) 7-storey and c) 12-storey FT-TMF models (1.0T)

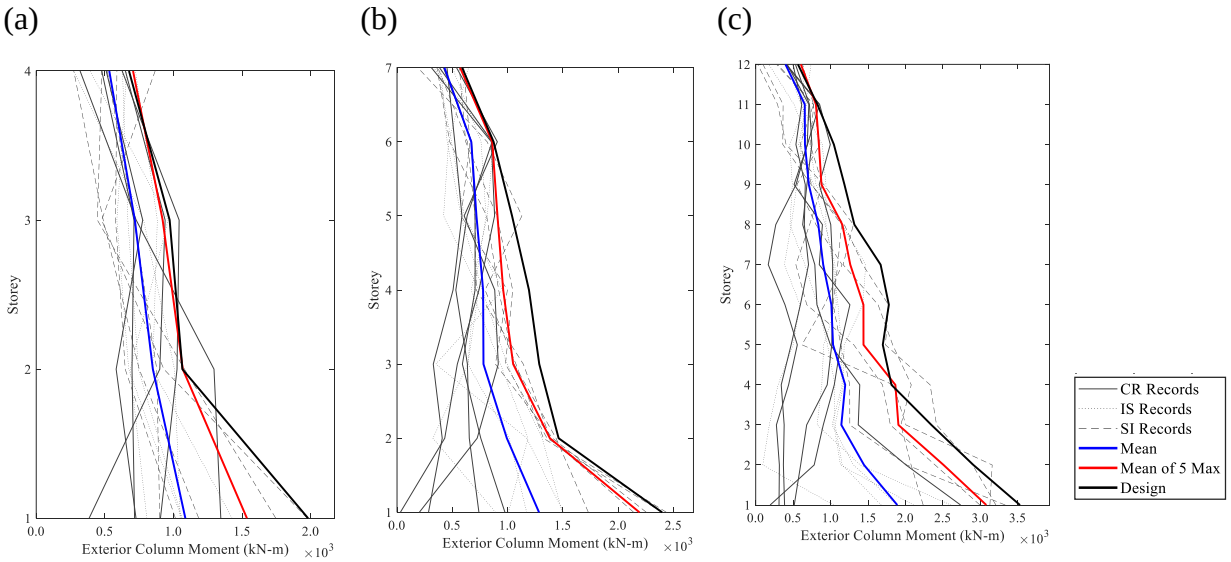

Figure 4-11: Exterior columns' moments resulted from NTHA in a) 4-storey b) 7-storey and c) 12-storey FT-TMF models (1.0T)

4.5.4 Tendon Strain

The tendons have a unique role in providing the proposed system with lateral stiffness in nonlinear range and controlling the lateral drifts. In the proposed system, any damage to the tendons would critically affect the performance of the structure and safety of the system during a large earthquake.

For the high strength tendons considered in this study, the yield strain is approximately 1%, and the tendons should be designed with a substantial safety margin, to ensure that they remain within the elastic range. Figure 4-12 shows the strain in the tendons at each storey level for the 15 ground motions records in the three archetypal buildings. The results show that the mean of the 5 maximum strain values from NTHA are 0.20% 0.23% and 0.25% for the 4-,7- and 12-storey buildings with FT-TMF (1.0T). The largest observed strains in the tendons are caused by subduction earthquakes SI4, SI2, and SI1 and are 0.28%, 0.31% and 0.44%, for the 4-, 7-, and 12 storey frames, respectively. The results indicate that the tendons remain elastic for the earthquake records considered in this study. The mean maximum 5 strain values in all of the buildings with increased tendon sizes of 1.3T decrease to approximately 0.20% and the largest tendon strain values are limited to 0.27%, 0.29% and 0.31% for the 4-,7- and 12-storey models, respectively. Once again, the results show that the selected tendon sizes are adequate and confirm the suitability of Equation (4-4).

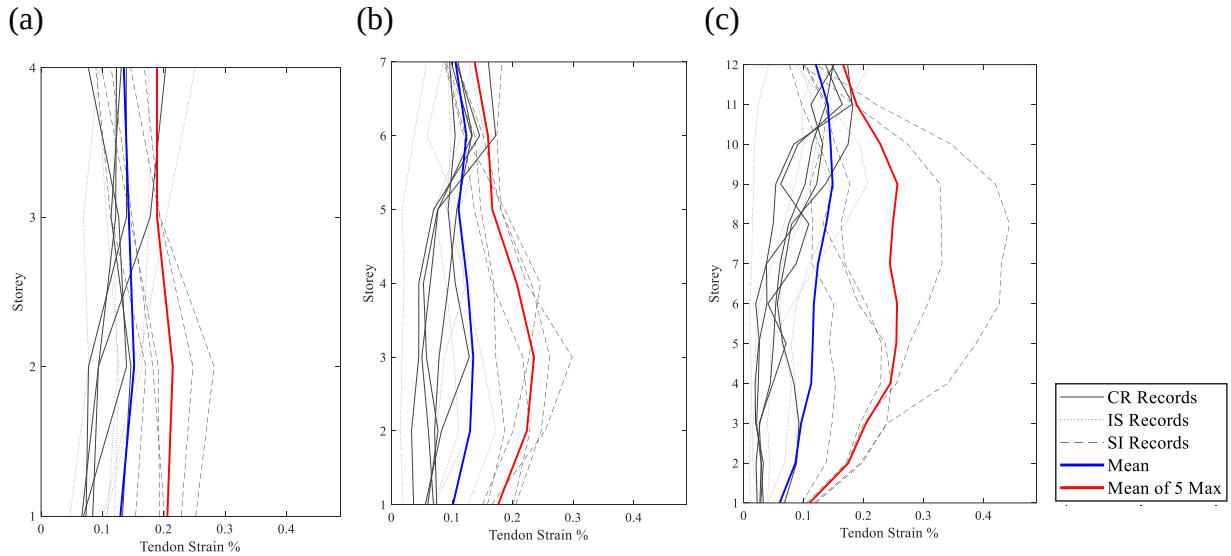

Figure 4-12: : Strain in tendons resulted from NTHA in in a) 4-storey b) 7-storey and c) 12-storey FT-TMF models (1.0T)

4.5.5 Residual Drifts

Residual drift is one of the most significant indicators in assessing the resilience of a structure and its ability to return to service following an earthquake, minimizing economic losses. To study the effect of the tendons in mitigating the residual drifts in the proposed system, the residual drifts for the archetypal buildings with FT-TMFs (1.0T and 1.3T) from NTHA are summarized in the bar charts represented at Figure 4-13. The findings reveal that, across 15 seismic events, the maximum residual drifts at the top storey levels are constrained to 0.45%, 0.32%, and 0.8% in the 4-, 7-, and 12-storey FT-TMF (1.0) buildings, respectively. These values are reduced to 0.35%, 0.30%, and 0.5% in the corresponding FT-TMF (1.3T) buildings. Consequently, these structures maintain post-event functionality. Analysis of the bar charts indicates that the addition of 30% more tendons can further reduce residual drifts. Furthermore, the sample displacement time-histories subjected to SI records, shown in Figure 4-14, show the effectiveness of the tendons at mitigating P-Δ effects and limiting residual drifts.

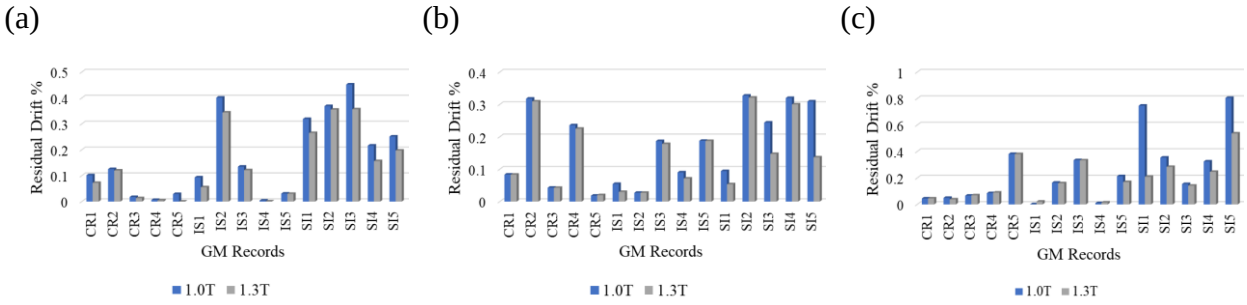

Figure 4-13: Comparative bar chart of residual drifts for a) 4-storey, b) 7-storey c) and 12-storey models subjected to CR, IS and SI ground motion records

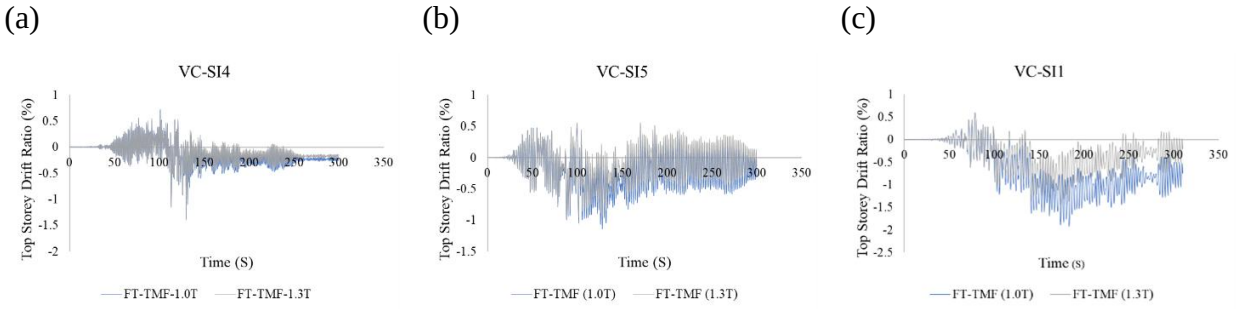

Figure 4-14: Time history response of the models a) 4-storey (SI3 GM), b) 7-storey (SI5 GM) and c)12-storey (SI1 GM)

4.5.6 Friction Damper's Behaviour

The satisfactory behaviour of the dampers is critical to limit the induced seismic forces and protecting structural elements in the proposed system. Figure 4-15 shows the force-displacement hysteretic behaviour of three selected dampers, as typical samples, including the response of the exterior and interior dampers in the 4-,7- and 12-storey FT-TMFs (1.0T). The results show that the slip force in the selected dampers were 1262 kN, 1360 kN and 1936 kN for the 4-,7- and 12-storey FT-TMFs (1.0T), respectively. These numbers are in agreement with the design slip forces shown in Table 4-2 at Appendix I, indicating suitability of the modelling approach.

(a) (b) (c)

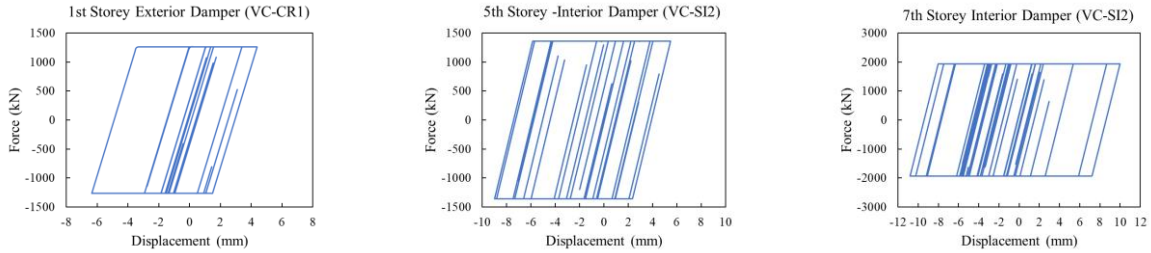

Figure 4-15: Force-Displacement hysteresis curves of a set of selected exterior and interior dampers in a) 4- storey b) 7- storey and c) 12- storey FT-TMF(1.0T) models Subjected to the GM records

4.6 Conclusion:

This study proposed a practical design procedure for an innovative FT-TMF system with friction dampers for energy dissipation and tendons to provide self-centering capacity, which was validated through a set of nonlinear static and nonlinear dynamic analysis. The validity of the seismic response and the proposed design method for the new system was evaluated through the study of 4-,7- and 12-storey archetypal buildings designed for a site with high seismicity in British Columbia, Canada.

The key conclusions of this work are summarized as follows:

1- Nonlinear static analysis including pushover and cyclic pushover analyses for the three 4-,7- and 12-storey FT-TMFs showed that the base shears in which the friction dampers start to slip were 0.85, 0.90 and 0.95 V_{NBCC}, respectively. These values were in average close to the base shear values calculated from spectral analysis. The cyclic pushover analysis results

showed stable hysteric behaviour and stable energy dissipation capacity provided by the friction dampers. Moreover, the results also showed the positive post-slip stiffness provided by the tendons, which notably mitigated the P-Δ effects.

2- The buildings with FT-TMFs illustrated satisfactory global stability under applied ground motions in the nonlinear time history analysis as none of the archetypal structures reached a collapse state under the design ground motions.

3- The nonlinear time history analysis showed that the tendons controlled the inter-storey drift values to within acceptable limits. The mean of 5 maximum inter-storey drifts for the 4-, 7- and 12- storey FT-TMF models with (1.0T) were limited to 1.4%, 1.5 and 1.8%, respectively. These values were marginally reduced to 1.3%, 1.4%, and 1.6%, with the incorporation of 30% additional tendons in the frames. Similarly, the peak inter-storey drifts in the 4-,7- and 12-storey FT-TMFs (1.0T) were approximately 1.8%, 1.9%, and 2.8%, which were subsequently reduced to 1.7%, 1.9%, and 2.1% in the FT-TMFs (1.3T).

4- In the buildings with FT-TMF (1.0T) and FT-TMF (1.3T), the maximum base shear values from nonlinear time history analysis approximately matched the largest base shear forces from pushover analysis in 2.5% target drift at roof. The seismic demands in principle structural members, as selectively illustrated for the exterior columns, remained close to their capacities and within the elastic range avoiding structural damage.

5- The axial strains in the tendons remained below the design threshold (1%) for all earthquake ground motion records. The peak strain values in the tendons, derived from the nonlinear time history analyses, were approximately 0.28%, 0.31%, and 0.44% in the 4- to 12-storey buildings with FT-TMF (1.0T), and slightly lower in the FT-TMF (1.3T). Hence, the tendons remained elastic and provided dependable self-centering forces.

6- The maximum residual drifts at the top storey of the 4-, 7- and 12-storey FT-TMFs(1.0T) were limited to 0.45%, 0.32% and 0.8%, respectively. These values slightly reduced to 0.35%, 0.30% and 0.5% respectively, in the buildings with FT-TMF (1.3T). Such low residual drifts ensured the post-event operability of the studied structures.

7- The maximum force in the friction dampers were limited to their design capacity across all models, thereby validating the proposed design procedure.

8- The analysis indicated overall marginal variations in the key response parameters of interest between FT-TMFs (1.0T) and FT-TMFs (1.3T). Given the comparable post-slip stiffness in both models, as demonstrated in the pushover analyses, the similarity in results was anticipated. However, the displacement time histories and residual drifts resulting from the application of subduction interface (SI) ground motions to the models well confirmed that the incorporation of additional tendons enhanced the seismic performance of the system.

Further improvements, including adding damage absorbing grade beams to prevent the formation of potential plastic hinges at the columns bases could lead to advances in the resilience of the proposed system and provide an opportunity to repair the system in the case of a very large earthquake. Complementary experimental tests on prototype models should also be performed to verify these theoretical results presented in this study and confirm the efficiency and reliability of this new system.

4.7 Acknowledgement

The support of the Natural Sciences and Engineering Research Council of Canada (NSERC) is gratefully acknowledged.

4.8 Appendix I

Table 4-1: Sections and tendons used in structural elements of the FT-TMFs (1.0T)

Design Table -Structural Elements							
4-Storey							
Storey ID	Diagonal	Brace	Chord	Vertical	Interior Column	Exterior Column	Number of Tendons *A_p=190mm^2
4	2MC150X22.5	2C100X10.8	2MC150X22.5	2C100X8	W610X155	W610X155	1
3	2MC150X24.3	2C150X12.2	2MC200X29.8	2C100X8	W610X155	W610X155	3
2	2MC150X26.8	2C150X15.6	2MC250X33	2C100X8	W610X262	W610X241	4
1	2MC150X26.8	2C150X19.3	2MC250X33	2C100X8	W610X262	W610X241	6
7-Storey							
	Diagonal	Brace	Chord	Vertical	Interior Column	Exterior Column	Number of Tendons *A_p=190mm^2
7	2MC150X17.9	2C100X8	2MC150X22.5	2C100X8	W610X155	W610X155	1
6	2MC150X24.3	2C130X13	2MC200X27.8	2C100X8	W610X155	W610X155	3
5	2MC200X29.8	2C150X15.6	2MC200X31.8	2C100X8	W610X307	W610X241	4
4	2MC200X31.8	2C150X19.3	2MC200X31.8	2C100X8	W610X307	W610X241	5
5	2MC200X31.8	2C200X20.5	2MC250X37	2C100X8	W610X307	W610X241	7
2	2MC250X33	2C200X20.5	2MC250X42.4	2C100X8	W610X372	W610X341	8
1	2MC250X33	2C200X20.5	2MC250X37	2C100X8	W610X372	W610X341	10
12-Storey							
	Diagonal	Brace	Chord	Vertical	Interior Column	Exterior Column	Number of Tendons *A_p=190mm^2
12	2MC150X17.9	2C100X10.8	2MC150X22.5	2C100X8	W610X155	W610X155	1
11	2MC150X22.5	2C100X10.8	2MC200X29.8	2C100X8	W610X155	W610X155	3
10	2MC200X27.8	2C130X13	2MC200X31.8	2C100X8	W610X307	W610X241	4
9	2MC200X31.8	2C200X17.1	2MC250X37	2C100X8	W610X307	W610X241	5
8	2MC250X33	2C200X17.1	2MC250X42.4	2C100X8	W610X307	W610X241	7
7	2MC250X37	2C200X20.5	2MC250X42.4	2C100X8	W610X372	W610X341	8
6	2MC250X37	2C250X22.8	2MC250X50	2C100X8	W610X372	W610X341	9
5	2MC250X42.4	2C250X22.8	2MC250X50	2C100X8	W610X455	W610X415	11
4	2MC250X42.4	2C250X30	2MC250X50	2C100X8	W610X455	W610X415	12
3	2MC250X42.4	2C250X30	2MC250X50	2C100X8	W760X582	W760X531	13
2	2MC250X42.4	2C250X30	2MC250X61.2	2C100X8	W760X582	W760X531	15
1	2MC250X42.4	2C250X22.8	2MC250X42.4	2C100X8	W760X582	W760X531	18

* Ap = cross section of the high strength tendons made of 7 wire low relaxation strands

Table 4-2: Capacity (slip force) of the dampers

Design Table -Friction Dampers						
Storey ID	4-Storey		7-Storey		12-Storey	
	*F_{ext} (kN)	*F_{int} (kN)	F_{ext} (kN)	F_{int} (kN)	F_{ext} (kN)	F_{int} (kN)
12	-	-	-	-	537	700
11	-	-	-	-	990	1093
10	-	-	-	-	1297	1420
9	-	-	-	-	1517	1590
8	-	-	-	-	1700	1750
7	-	-	542	706	1968	1936
6	-	-	935	1058	2118	2022
5	-	-	1212	1360	2285	2201
4	550	719	1389	1500	2366	2258
3	972	1094	1517	1597	2546	2430
2	1258	1327	1742	1702	2679	2470
1	1262	1277	1573	1519	1993	1866

* F_{ext} and F_{int} represent the exterior and interior dampers slip force, respectively.

4.9 References:

Basha, H. S., & Goel, S. C. (1994). *Seismic Resistant Truss Moment Frames with Ductile Vierendeel Segment*: Department of Civil Engineering, University of Michigan.

Basha, H. S., & Goel, S. C. (1995). Special truss moment frames with Vierendeel middle panel. *Engineering structures, 17*(5), 352-358.

Chao, S.-H., & Goel, S. C. (2008). Performance-based plastic design of special truss moment frames. *Engineering journal, 45*(2), 127.

Chao, S.-H., Jiansinlapadamrong, C., Simasathien, S., & Okazaki, T. (2020). Full-scale testing and design of special truss moment frames for high-seismic areas. *Journal of Structural Engineering, 146*(3), 04019229.

Christopoulos, C., Tremblay, R., Kim, H.-J., & Lacerte, M. (2008). Self-centering energy dissipative bracing system for the seismic resistance of structures: development and validation. *Journal of Structural Engineering, 134*(1), 96-107.

Clayton, P. M., Dowden, D. M., Li, C.-H., Berman, J. W., Bruneau, M., Lowes, L. N., & Tsai, K.-C. (2016). Self-centering steel plate shear walls for improving seismic resilience. *Frontiers of Structural, 10*(3), 283-290.

Computers&Structures Inc. (2023). SAP2000 (Version 21): CSI. Retrieved from https://www.csiamerica.com/

Deierlein, G., Krawinkler, H., Ma, X., Eatherton, M., Hajjar, J., Takeuchi, T., Kasai, K., & Midorikawa, M. (2011). Earthquake resilient steel braced frames with controlled rocking and energy dissipating fuses. *Journal of Steel Construction, 4*(3), 171-175.

Eatherton, M. R. (2010). *Large-scale cyclic and hybrid simulation testing and development of a controlled-rocking steel building system with replaceable fuses*: University of Illinois at Urbana-Champaign.

Faraji, K., & Tremblay, R. (2019). *Multi-story truss moment frames equipped with friction dampers and self-centering system for enhanced seismic performance*. Paper presented at the The Evolving Metropolis-IABSE Congress, New York, New York-USA.

Garlock, M. M., Sause, R., & Ricles, J. M. (2007). Behavior and design of posttensioned steel frame systems. *Journal of Structural Engineering, 133*(3), 389-399.

Goel, S. C., & Itani, A. M. (1994). Seismic-resistant special truss-moment frames. *Journal of Structural Engineering, 120*(6), 1781-1797.

Grigorian, M., & Grigorian, C. E. (2018). Sustainable earthquake-resisting system. *Journal of Structural Engineering, 144*(2), 04017199.

Hanson, R., Martin, H., & Martinez-Romero, E. (1986). *Performance of steel structures in the September 19 and 20, 1985 Mexico City earthquakes.* Paper presented at the The National Engineering Conf., AISC.

Ireland, R. C. (1997). *Special truss moment frames in low to moderate seismic regions with wind*: University of Michigan.

Jiansinlapadamrong, C. (2018). *Seismic performance of double-channel and double-HSS sections, special truss moment frame with buckling restrained braces, and long span Special Truss Moment Frame.*

Jiansinlapadamrong, C., Park, K., Hooper, J., & Chao, S.-H. (2019). Seismic design and performance evaluation of long-span special truss moment frames. *Journal of Structural Engineering, 145*(7), 04019053.

Kim, H.-J., & Christopoulos, C. (2008). Friction damped posttensioned self-centering steel moment-resisting frames. *Journal of Structural Engineering, 134*(11), 1768-1779.

Martin, A., Deierlein, G. G., & Ma, X. (2019). Capacity design procedure for rocking braced frames using modified modal superposition method. *Journal of Structural Engineering, 145*(6), 04019041.

Mckenna, F., Fenves, G. L., Scott, M. H., and Jeremic, B. . (2020). Open system for earthquake engineering simulation (OpenSees) (Version 3.2.1). Berkeley (CA). Retrieved from https://opensees.berkeley.edu/

Momeni, S., Aoudia, A., Tatar, M., Twardzik, C., & Madariaga, R. (2019). Kinematics of the 2012 Ahar–Varzaghan complex earthquake doublet (M w6. 5 and M w6. 3). *Geophysical Journal International, 217*(3), 2097-2124.

National Research Council of Canada. (2015). National Building Code of Canada (NBCC 2015),. In. Canada: National Research Council of Canada.

Pekcan, G., Linke, C., & Itani, A. (2009). Damage avoidance design of special truss moment frames with energy dissipating devices. *Journal of Constructional Steel Research, 65*(6), 1374-1384.

Potter, S. H., Becker, J. S., Johnston, D. M., & Rossiter, K. P. (2015). An overview of the impacts of the 2010-2011 Canterbury earthquakes. *International Journal of Disaster Risk Reduction, 14*, 6-14.

Ricles, J. M., Sause, R., Garlock, M. M., & Zhao, C. (2001). Posttensioned seismic-resistant connections for steel frames. *Journal of Structural Engineering, 127*(2), 113-121.

The American Society of Civil Engineers. (2017). Seismic Evaluation and Retrofit of Existing Buildings ASCE/SEI 41-17. In: ASCE.

The Canadian Standards Association. (2019). Design of steel structures CSA S16:19. In: CSA Group.

Tremblay, R., & Faraji, K. (2019). *Steel truss moment frames with self-centring energy dissipation mechanisms for enhanced seismic performance*. Paper presented at the 12th Canadian Conference on Earthquake Engineering, Quebec City, June 17-20, 2019, Quebec City- QC-Canada.

Wongpakdee, N., Leelataviwat, S., Goel, S. C., & Liao, W.-C. (2014). Performance-based design and collapse evaluation of buckling restrained knee braced truss moment frames. *Engineering structures, 60*, 23-31.

Yang, T., Li, Y., & Goel, S. C. (2015). Seismic performance evaluation of long-span conventional moment frames and buckling-restrained knee-braced truss moment frames. *Journal of Structural Engineering, 142*(1), 04015081.

CHAPTER 5 ARTICLE 2: SEISMIC COLLAPSE ASSESSMENT OF TRUSS MOMENT FRAME WITH FRICTION DAMPERS AND STEEL TENDONS

This article is submitted to: Journal of Structures on 27th October 2024 Manuscript Number:S-24-09096

Keyhan Faraji [a], Joshua Woods[b] and Robert Tremblay [a]

a Department of Civil, Geological and Mining Engineering, Polytechnique Montréal, Montréal, QC, Canada

b Department of Civil Engineering, Queen's University, Kingston, ON, Canada

Corresponding author: Keyhan Faraji, Email address: keyhan.faraji@polymtl.ca

Abstract:

Truss moment frame integrated with friction dampers and steel tendons (FT-TMF) is a novel and seismic resilient system, capable of maintaining sustained operability during and post seismic events. This paper addresses the seismic collapse risk assessment of the FT-TMF system, providing an in-depth analysis of its performance and resilience under seismic conditions. The procedure outlined in FEMA P-695 was used to investigate seismic behaviour and collapse capacity of FT-TMF system which was employed as the lateral load resisting frames in a set of 4-,7- and 12-story archetypal buildings. Incremental dynamic analysis (IDA) and statistical fragility assessment were conducted to explore the system's seismic performance and verify the suggested R factor (equal to 7) applied in the design procedure. The structural models of FT-TMFs, which were simulated in OpenSees, were analyzed and designed in compliance with ASCE 7-22, AISC 360-16 and AISC 341-16 requirements. The collapse risk assessment was performed under a suite of 44 far-field ground motion records and the fragility curves were generated for the estimated collapse points. Median collapse capacities, representing 50% of the records cause collapse, were derived to quantify the collapse margin ratios (CMRs) of the archetypes. The results revealed that the adjusted collapse margin ratios (ACMRs) satisfied FEMA P-695 acceptance criteria. Consequently, the archetypal buildings provided a desirable seismic response with a low probability of collapse.

Keywords: Truss moment frame, Tendons, Friction dampers, Incremental dynamic analysis, Collapse risk assessment, Fragility curves

5.1 Introduction:

Earthquakes are critical natural phenomena which have the potential to damage structures and lead to the loss of life, injury, and displacement of people from their homes. In seismically active regions, buildings can experience several earthquakes with different intensities over their life span. The experiences from past significant seismic events have revealed that buildings designed by contemporary design codes and seismic provisions could achieve the life safety level of performance. However, after intense ground motions, they often are left with severe damage and permanent deformations in their structural and non-structural elements, which make them cost-prohibitive or unfeasible to be repaired and realigned (Steele & Wiebe, 2016; Grigorian & Grigorian, 2018). In recent years, the concept of seismic sustainability has been developed in structural and earthquake engineering. In this context, the term seismic sustainability refers to earthquake-resilient structures which are expected to experience little-to-no damage after a strong earthquake and remain in service (Grigorian, 2021). The goal of seismic sustainability is to upgrade conventional and develop new structural systems such that they can competently resist earthquakes, requiring minimal repair and remain operational following a design-level earthquake. The greatest concerns in such mentioned systems are that they should be technically practical and economically viable in fabrication as well as post-event repair and realignment.

Over the past three decades, several low-damage and repairable structural systems have been proposed and studied. Two pivotal themes that have been considered in the advancement of earthquake-resilient and sustainable structural systems are the incorporation of energy dissipation devices and self-centering mechanisms. Friction dampers, recognized as effective and economical energy dissipation devices, have been tested in numerous numerical and experimental studies. These devices, which can be easily integrated to steel frames and suitable for both new constructions and retrofits, are increasingly used worldwide to mitigate seismic impacts on buildings (Tremblay, 1993; Latour et al., 2018; Gilbert & Erochko, 2019). Steel tendons have been incorporated in some advanced structural systems like self-centering braces, self-centering steel plate shear walls and post-tensioned rocking frames and their benefits such as stabilization and drift control in structures to enhance their seismic behaviour have been validated through numerous theoretical investigations and supported by experimental tests (Deierlein et al., 2011; Eatherton, Ma, Krawinkler, Deierlein, et al., 2014; Dowden & Bruneau, 2016). In some integrated cases, the combination of friction dampers and self-centering tendons have been used to create innovative

systems such as advanced braces or connections that can improve the seismic performance of the structure (Erochko et al., 2015; Zhang et al., 2016).

Truss moment frame is an economical structural system that can be designed in different shapes for long spans and can be constructed in a timely manner. Consequently, it has been a conventional and favorable structural system used in construction of single and multi-level structures such as arenas, hangars, malls, warehouses, and industrial buildings. Ease of fabrication and detailing for moment connection to columns, availability in different shapes, accessibility of elements for repair, simple and efficient installation are the main advantages of this system. Moreover, in this system, duct works can be accommodated through the open web space in the girders, resulting in story height reductions (Goel & Itani, 1994). A comprehensive study on the enhancement of the truss frame system began after the Mexico City earthquake in 1985, which revealed a number of noticeable seismic damage to these systems, including web member instabilities and local buckling in truss frames (Hanson et al., 1986; Goel & Itani, 1994; Ireland, 1997). The output of this investigation was the introduction of the special truss moment frames (STMF) with a substantial ductility and sustainable inelastic reserved strength provided by the X-diagonal or open Vierendeel ductile segments in their mid-panels (Basha & Goel, 1994; Goel & Itani, 1994; Basha & Goel, 1995; Goel et al., 1997; Goel et al., 1998; Chao & Goel, 2008). In this system, a considerable portion of the seismic energy can be dissipated through controlled inelastic deformation in the ductile segments which results a stable seismic response in the frame and prevents premature failures in the surrounding structural elements. Further studies led to the introduction of another type of seismically resilient TMF, referred to as the Restrained Knee Braced Truss Moment Frame (BRKB-TMF). In this system, the special segments were replaced by buckling-resisting knee braces (BRBs) installed between bottom chords and adjacent columns in the end panels (Wongpakdee et al., 2014; Yang et al., 2014; Wongpakdee & Leelataviwat, 2017). The buildings constructed with STMF systems are normally designed to satisfy life-safety performance and are expected to adequately resist against progressive collapse. However, it is not possible to repair and replace the special segments or BRBs immediately after the seismic event and the potential strong aftershocks. Hence, it could put the damaged buildings at the risk of the propagation of the damage in their structural and non-structural elements which could result in considerable repair and realignment cost plus disruption in serviceability during the downtime period (Momeni et al., 2019).

To upgrade the conventional STMF to an earthquake-resisting system with higher level of seismic performance and sustainability, the conventional configuration of the truss moment frame could be integrated with friction dampers and high-strength tendons denoted FT-TMF (Faraji & Tremblay, 2019; Tremblay & Faraji, 2019).

The FT-TMF system is a steel truss moment frame equipped with friction dampers linking bottom chords to the adjacent columns at the end panels and a pair of tendons in each span that connect the bottom chords to the columns. In this system, the friction dampers are designed to dissipate the seismic energy without experiencing any damage while the high-strength steel tendons are employed to provide the system with positive stiffness (self-centering capacity) in the post-slip range. For further resilience, replaceable support-level grade beams which are designed to act as fuses, could be attached to the columns to absorb the potential seismic damage preventing the formation of plastic hinges at the bases of the columns. The FT-TMF system is expected to experience no or low damage in its structural elements during potential earthquakes and keep its operability.

The key attributes of the novel FT-TMF system are as follows:

1- Controlled lateral stiffness and strength: The ability to control the stiffness and strength by adjusting the friction dampers capacity and sizing the tendons.
2- Stable hysteretic behaviour: The capability to represent stable hysteretic behaviour under cyclic and seismic loading conditions added to the system by the function of the friction dampers.
3- Seismic drifts reduction: As a result of the self-centering capacity added to the system due to the presence of the tendons.
4- High energy dissipation: The high capacity of the friction dampers in dissipation of seismic energy and reducing strength degradation in the structural elements.
5- No damages in columns: The capability to implement the strong-column weak-beam principle and avoid or delay premature damage to the columns' feet at the expense of support-level grade beams.
6- Post event repairability and realignment : Post-event replacement of the grade beams, as well as the repair of friction dampers and tendons, are feasible. The building can be realigned statically due to its simple pin supports.

The overarching aim of this paper is to study the seismic performance and collapse risk level of the new FT-TMF system through simulation of a series of archetypal buildings. In the following sections, the description of the studied archetypal buildings, utilized design procedure, and employed collapse evaluation process are described. Accordingly, a seismic response modification factor (R) is first proposed. A methodology proposed in FEMA P-695 is followed and implemented to investigate the seismic behaviour and collapse resistance capacity of the proposed system . The seismic performance of the designed archetypal buildings is evaluated using incremental dynamic analysis (IDA), a well-accepted method, to quantify their seismic behaviour over a range of intensity levels and classify their performance at different hazard levels (Vamvatsikos & Cornell, 2002; Vamvatsikos & Cornell, 2004; Steele et al., 2017).

The outcomes of the IDAs are used to verify the employed design method and the adopted R factor and assess the collapse resistance capacity of the selected archetypal buildings. In this regard, a set of 4-, 7- and 12-story archetypal steel office buildings are modeled, and their collapse capacity is evaluated.

The structural FT-TMF models are fitted with the minimum tendons, required to mitigate the P-Δ influence, and are analyzed under 44 far-field ground motions recommended in FEMA P-695, to evaluate their collapse risk capacities.

To examine the effects of tendons on enhancing the system's response and collapse capacity, the installed tendons' sizes (i.e., number of strands per tendon) of the 12-story building are increased by almost 30% and the analyses are repeated.

The estimated collapse risk level of the archetypal buildings is illustrated by a set of fragility curves obtained from statistical methods and assuming a lognormal distribution function. The quantified results, representing seismic performance and collapse probability of the studied buildings, are eventually compared with FEMA P-695 acceptance criteria to examine the efficiency of the proposed system.

5.2 Design of the Archetypal Buildings

The FT-TMF system is used as the lateral load resisting system (LLRS) in a set of 4-, 7- and 12-story commercial office buildings with total heights of 15.5 m, 32.0 m and 54.5 m, respectively.

The plan view of the archetypal buildings, represented in Figure 5-1, comprises of 4 bays in the E-W direction with a constant span length of 14.0 m and 3 bays in the N-S direction with the span lengths of 13.0 m, 10.0 m, and 13.0 m, respectively.

In all the buildings, the height of the first story is 5.0 m and the rest of the stories have a similar heights of 4.5 m. The buildings are considered to be located on an area with stiff soil characteristics in an active high seismic hazard zone within Los Angeles area (Lancaster) in the western US.

To resist lateral loads, a pair of identical two span FT-TMFs are located parallelly along the perimeter walls of the building in E-W direction, and four similar single span FT-TMFs, placed along perimeter walls in N-S direction, forming the lateral load resisting system (LLRS) of the buildings.

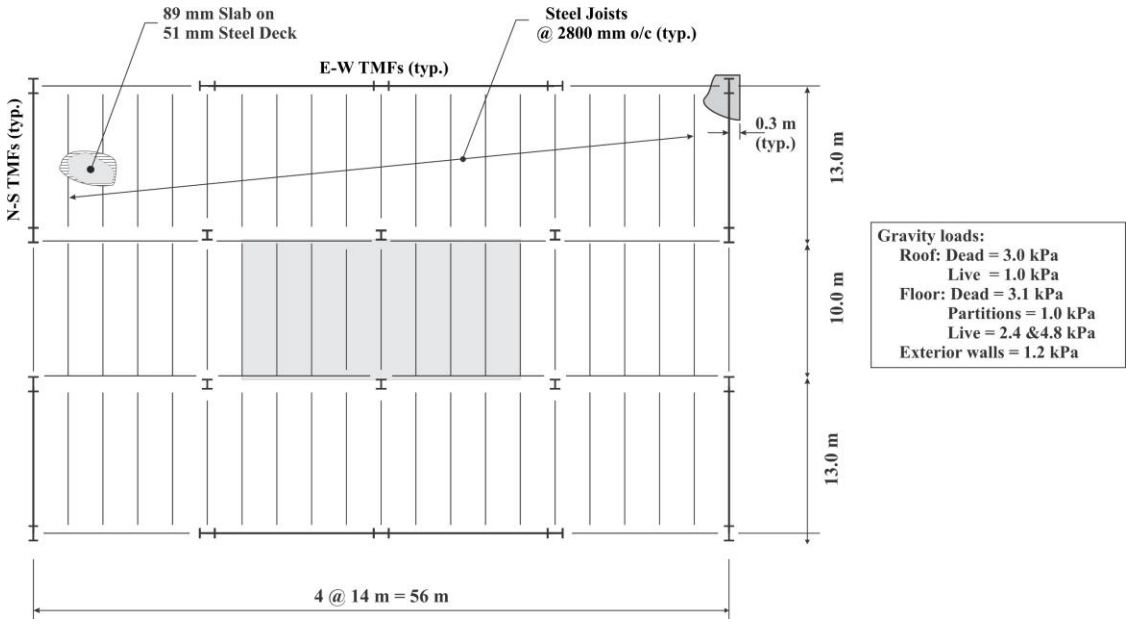

Figure 5-1 : The plan view of the archetypal buildings

This research examines the seismic response of archetypal structures when subjected to E-W oriented ground motions. In the two span FT-TMFs, in the E-W direction, the length of the spans (L), the overall truss depth (d) and the length of special panels (Ls) are 14.0 m, 1.4 m and 2.8 m, respectively (Figure 5-2). The trusses in the studied buildings are made of back-to-back steel channel sections that can better offer the required capacity for the TMFs located in high seismic areas compared to double channel sections (Jiansinlapadamrong et al., 2019; Chao et al., 2020). Wide flange steel sections are used to fabricate the columns. A set of support-level grade beams,

measuring 4.0 meters in length with comparatively smaller size, are accommodated in the bases of the columns. These beams are rigidly connected to the columns' bases at one end and to pin supports at the other, functioning as energy-absorbing fuses.

This design aims to limit the potential seismic damage to the replaceable beams and prevent the formation of the plastic hinges in the columns' feet during a strong seismic event. Conventional composite steel decks resting on open web steel joists which are installed in the interior bays in the N-S direction, are forming the floor and roof system in the studied buildings. The steel decks are fabricated from roll-formed galvanized corrugated steel plates, with thicknesses of 0.91 mm for floors and 0.76 mm for roofs. Accounting for the lightweight concrete slabs, which are 89 mm thick for floors and 74 mm thick for roofs, over the flutes with a depth of 51 mm, the total composite thicknesses of the steel decks are 140 mm for floors and 125 mm for roofs.

The straight friction dampers are installed between the tip of bottom chords and adjacent columns at the end panel of the FT-TMFs. In each span, a pair of 7-wire low relaxation high strength steel strands with a length of 8.4 m link the bottom chords to the columns.

5.3 Finite Element models

To study the seismic performance of the FT-TMFs and evaluate their collapse resistance, a set of 4-, 7- and 12-story computational models are built in OpenSees software (Mckenna, 2020). Three supplementary and comparative models are also built in SAP2000 (Computers&Structures Inc., 2023).

The second group of models are used in spectral analysis and also to verify of the outputs resulted from the analyses in OpenSees. Figure 5-2 depicts a schematic of the FT-TMF model, illustrating the location of the dampers, tendon, grade beams, and the modelled concentrated plastic hinges.

The numerical model includes the lateral resisting truss moment frames (FT-TMFs) and a leaning column, which supports the loads over the gravity columns of the parent building to simulates the dynamic P-Δ effect induced on the system during a seismic event.

In the OpenSees model, the truss elements, columns, and the support-level grade beams are simulated with elasticBeamColumn elements.

A set of lumped plastic (LP) hinges, simulated with non-linear rotational springs, is included at both ends of the support-level grade beams as well as the top and bottom of the columns. This ensures that the non-linear behaviour of the frames is accounted for.

The rotational spring elements are modeled based on a modified version of a Ibarra–Medina–Krawinkler model which represents a hysteresis behaviour by a multilinear force-displacement capacity curves and includes stiffness and strength degradation parameters (Lignos & Krawinkler, 2011). A web base tool developed by Al-Shawwa and Lignos (Al-Shawwa & Lignos, 2023) is used to verify the specifications assigned to the rotational springs (plastic hinges). All truss elements are expected to remain in the elastic range due to the existence of the dampers.

The friction dampers are simulated by two node link elements with elastic-perfectly plastic material. To model tendons, a combination of Bilinear and MinMax materials are assigned to two node link element. This approach enables the capture of strength degradation in the post-yielding range. The leaning column is modeled with segmental elastic elements with a negligible bending stiffness and linked to the FT-TMF with two node rigid elements. A schematic of a the 7-story FT-TMF archetype with its components is represented in Figure 5-2.

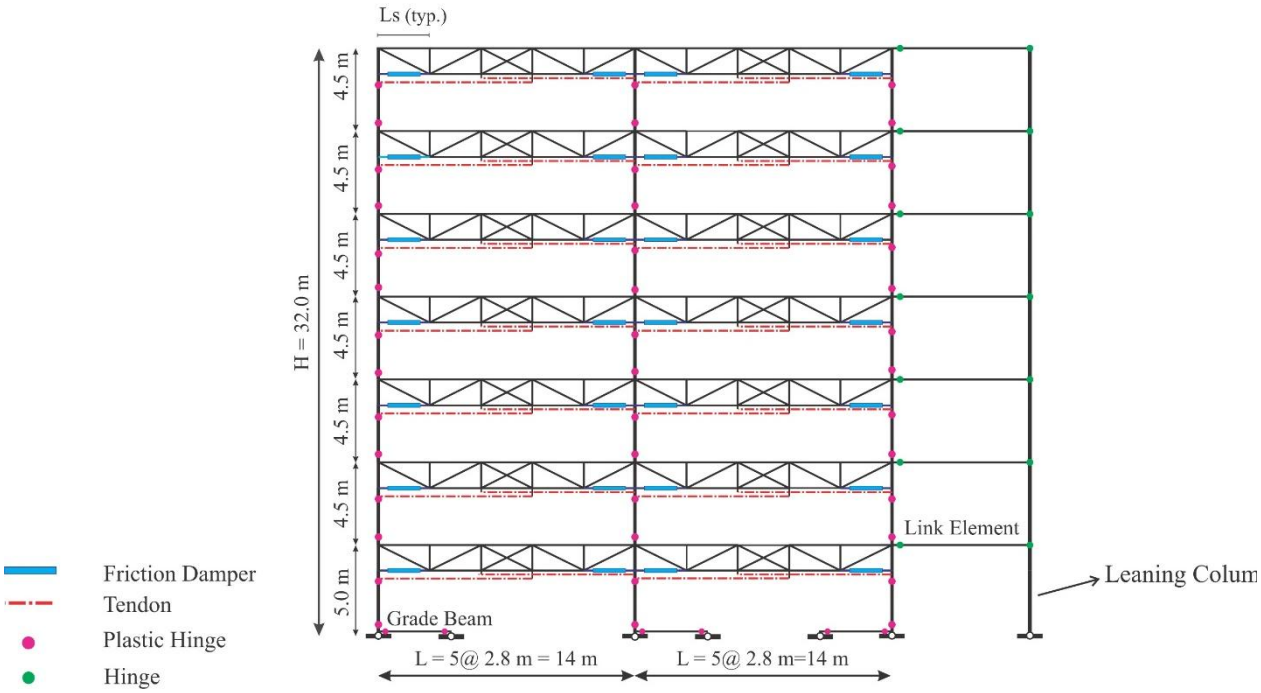

Figure 5-2: The schematic of the computational model simulated in OPENSEES software

5.4 Design Procedure:

The design procedure for the FT-TMFs is summarized in the following 4 stages.

5.4.1 Primary Seismic Analysis and Design:

At this stage the structural models are considered as conventional TMFs without any damper and tendon. A gravity load combination of 1.2 D+1.0 L, is applied to the models and they are subjected to a pseudo-dynamic modal spectrum analysis (RSA) to obtain the forces developed in their elements. The resulting maximum forces are used in the preliminary seismic design of the frames.

5.4.2 Design of the Friction Dampers

In this stage the friction dampers are included in the models and following the initial design stage, the largest axial forces in the bottom chords, resulted from the RSA, are utilized to quantify the slip forces in the dampers. Table 5-1 summarizes the utilized slip forces in the design of the dampers. In Table 5-1, F_{ext} and F_{int} refer to the slip forces in the dampers adjacent to exterior and interior columns, respectively.

Since the friction dampers are installed in series with the bottom chord, the equivalent axial stiffness of bottom chord-damper element in end panels ($K_{eqivalent}$), which is calculated from Eq. (5.1) is used in the numerical models.

$$\frac{1}{K_{equvalent}} = \frac{1}{K_{Damper}} + \frac{1}{K_{chord\ section}} \tag{5.1}$$

In Equation (5.1) the term K_D and K_C refer to the damper's initial stiffness and axial stiffness of the bottom chord section, respectively.

Table 5-1: Capacity (slip force) of the dampers

Story ID	4-Story		7-Story		12-Story	
	F_{ext} (kN)	F_{int} (kN)	F_{ext} (kN)	F_{int} (kN)	F_{ext} (kN)	F_{int} (kN)
12	-	-	-	-	585	498
11	-	-	-	-	964	991
10	-	-	-	-	1142	1112
9	-	-	-	-	1342	1256
8	-	-	-	-	1574	1474
7	-	-	512	632	1737	1560
6	-	-	1004	1203	1891	1700
5	-	-	1178	1323	1988	1729
4	607	745	1352	1466	2188	1912
3	1127	1310	1462	1530	2245	1990
2	1403	1519	1624	1695	2438	2182
1	1337	1458	1680	1671	2423	2167

A schematic of the utilized dampers and their theoretical hysteretic behaviour under cyclic loading are illustrated in Figure 5-3. In the represented hysteretic loop, the terms K_0 and K_1 denote the initial and post-slip stiffness, respectively.

(a) (b)

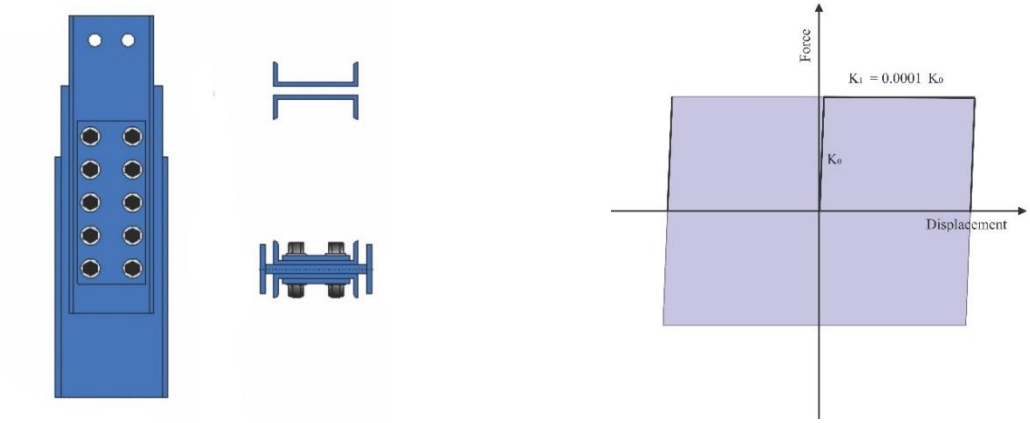

Figure 5-3: a) Friction dampers- b) Damper's hysteresis Loop (right)

5.4.3 Design of the Self-centering Tendons

The static equilibrium in the FT-TMF system resulted from the application of gravity and seismic forces is used to compute the size of the tendons (i.e. number of strands per tendon) required to suppress the seismic P-Δ effects and mitigate residual drifts (Tremblay & Faraji, 2019).

Figure 5-4 shows the free-body diagram of the applied lateral forces in the frames and the internal reactions which are used to generate the static equilibrium. Accordingly, the static equilibrium is

formulated in the form of Equation (5.2). As shown in Figure 5-4, the frame in the ith story is considered as a single column to simplify the calculations.

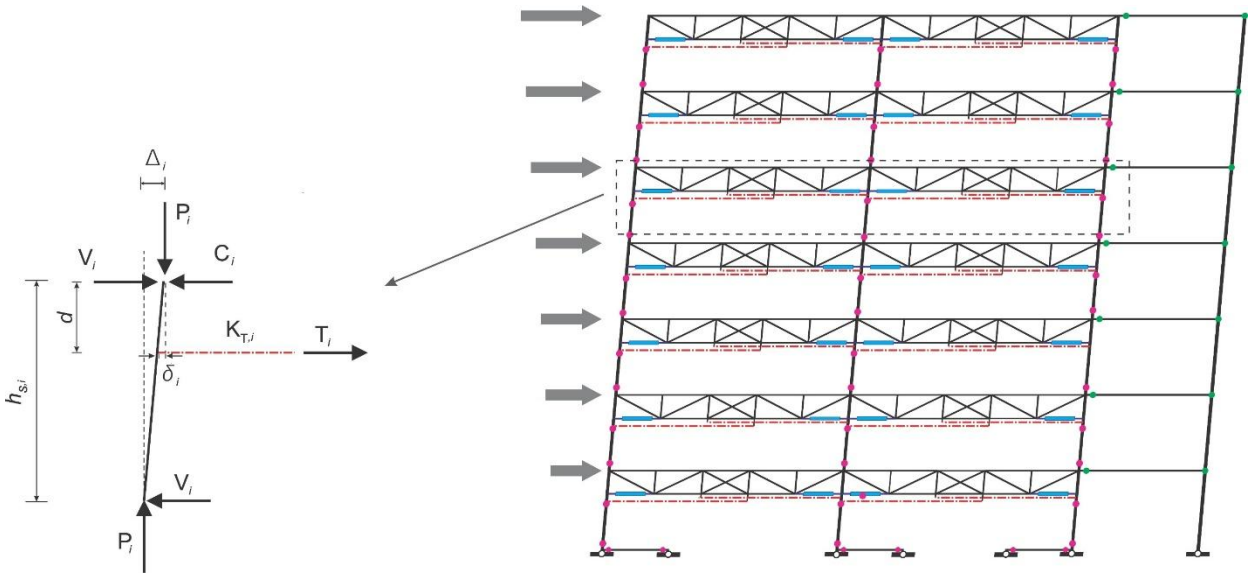

Figure 5-4: Equilibrium of force vectors applied to ith story

$$V_i h_{s,i} + P_i\,\Delta_i = T_i \mathrm{d} \;\rightarrow V_i = T_i(\mathrm{d}/h_{s,i}) \;-(P_i/h_{s,i})\,\Delta_i \tag{5.2}$$

where V_i is the story shear force, P_i is total gravity load supported by all columns at ith story , T_i is the tendons' force at ith story and C_i represents internal reactions of the frames applied to columns at ith story. Moreover, the terms, d, $h_{s,i}$ and Δ_i refer to the truss depth, ith story height and lateral displacement of the FT-TMF after the slip of friction dampers at ith story level, respectively. The tendon force in the ith story, T_i, is calculated from Equation (5.3).

$$T_i = K_{T,i}\,\delta_i \tag{5.3}$$

where δ_i is the elongations of the tendons that occur subsequent to the slip of the dampers and $K_{T,i}$ represents the axial stiffness of the tendon, which is calculated using Equation (5.4):

$$K_{T,i} = EA_i/L_i;\; \delta_i = \Delta_i(d/, h_{s,i}) \tag{5.4}$$

In Equation (5.4), E is the modulus of elasticity for the steel tendons, A_i represents tendons' cross section at ith story acting in each direction, L_i is the length of the tendons at ith story.

The length of the tendon is evaluated that the largest stain in tendons to be less than 1%. Substituting Equations (5.3) and (5.4) into Equation (5.2) gives equation (5.5), which represents the net lateral stiffness of the story when the dampers slip (V_i/Δ_i).

$$V_i/\Delta_i = K_{T,i}\,(d/,h_{s,i})^2 - (P_i/,h_{s,i}) \tag{5.5}$$

In Equation (5.5), $K_{T,i}(d/h_{s,i}))^2$ and $(P_i/h_{s,i})$ refer to the positive lateral stiffness provided by tendons and the negative stiffness induced in each story by P-Δ, respectively. In each story the lateral stiffness provided by the elastic tendons should not be less than the value of $(P_i/,h_{s,i})$, to ensure that the P-Δ effects are neutralized.

In Equation (5.5) by considering the term $K_{T,i}\,(d/,h_{s,i})^2$ equal to $(P_i/,h_{s,i})$, the resulted net lateral stiffness of the story i, V_i/Δ_i , in post-slip range becomes zero. In this case the resulting tendons' cross section for the ith story becomes the minimum required size. However, previous studies showed that if the selected tendons are larger than the minimum size (e.g. 25-30%), the net lateral stiffness become positive, and the TMFs' seismic response will be more satisfactory due to the larger self-centering capability added to the system (Tremblay & Faraji, 2019).

Based on this design approach, the required minimum tenson size to neutralized P-Δ effects are summarized in Table 5-2.

Table 5-2: Tendons installed in FT-TMF archetypes

4-Story Archetype			7-Story Archetype			12 Story Archetype		
	Story ID	Number of Tendons *A_p=190mm^2		Story ID	Number of Tendons *A_p=190mm^2		12-Story	Number of Tendons *A_p=190mm^2
	-	-		-			12	1
	-	-		-	-		11	3
	-	-		-	-		10	6
	-	-		-	-		9	8
	-	-		--	-		8	10
	-	-		7	1		7	12
	-	-		6	3		6	14
	-			5	6		5	16
	4	1		4	8		4	18
	3	3		3	10		3	20
	2	6		2	12		2	22
	1	8		1	15		1	26

* Ap = cross section of the high strength tendons made of 7-wire low-relaxation strands

A schematic of a tendons and the theoretical stress-strain curve representing the behaviour of a steel wire in elastic and plastic range are shown in Figure 5-5.

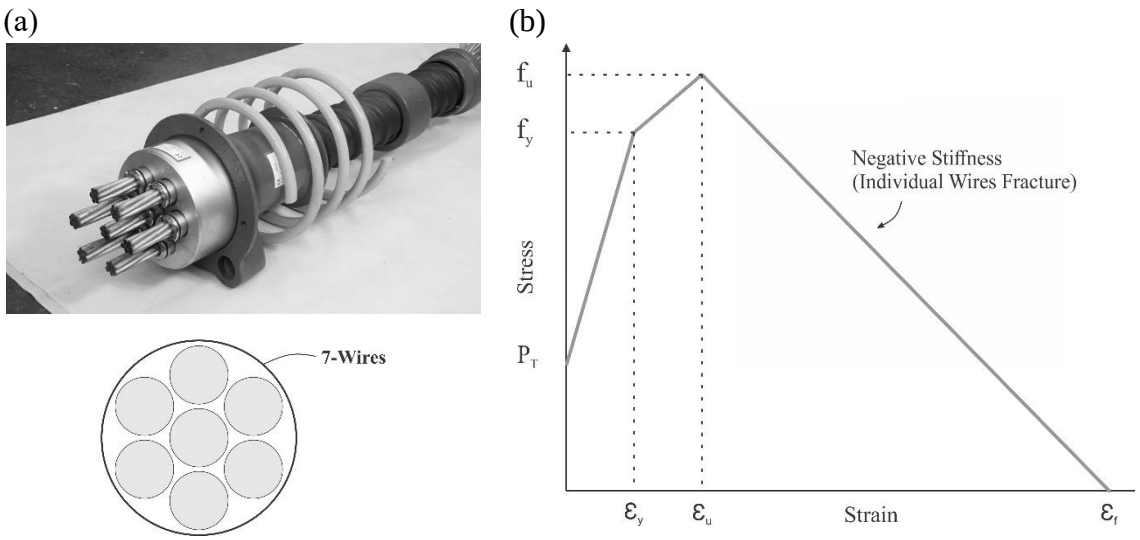

Figure 5-5: a) A tendon built of 7-wire strands- b) Stress-strain curve for an individual wire

5.4.4 Design Verification using Nonlinear Static Analysis (NSA)

After the preliminary design of the FT-TMF system, the design of the structural members is validated by NSA. This is required to ensure the columns as well as the truss members will remain in the elastic range of the material behaviour during a seismic events (Tremblay & Faraji, 2019).

As part of this procedure, the slip force of the dampers are increased by 30% and then the archetypes were subjected to a nonlinear static analysis (lateral pushover) with the presence of the gravity loads. Pushover analysis of the archetypal buildings is conducted until they experience the 1.5% drift at the roof level. At the last step of the pushover process, the forces developed in the structural elements are compared with the demands obtained from the initial spectral analysis. The maximum demands from this analysis were used in the final design iteration for the structural members.

Since the support-level grade beams are intended to act as energy dissipation and damage absorbing elements, and therefore they are engineered to undergo the plastic behaviour during the final steps of the lateral pushover to prevent the propagation of the damage (plastic hinge) at base of the columns.

Finally, the dampers were once again set back to their original capacity and the structural models are subjected to a final spectral analysis to verify the analytical outputs, including the buildings' natural period and base shears values with those derived from the initial spectral analysis. Fine-tuning of the damper specifications could be conducted. The utilized analysis and design method was theoretically examined in a previous study (Faraji & Tremblay, 2019; Tremblay & Faraji, 2019).

The sections assigned to the frames' components are included in Table 5-6 in Appendix I.

5.5 Collapse Risk Assessment:

Incremental dynamic analysis (IDA) provides a comprehensive approach to defining the seismic demand and capacity prediction for buildings that can be utilized in collapse assessment procedures (Vamvatsikos & Cornell, 2002).

In this study the collapse resistance of the archetypal buildings is evaluated using a set of IDAs performed under a suite of far-field ground motion records which are normalized and scaled in accordance with FEMA P-695 methodology (Federal Emergency Management Agency 2009). The results obtained from the IDAs are utilized to generate the fragility curves of the archetypal buildings, representing their collapse probability. Furthermore, the outputs of the collapse assessment analyses are interpreted in accordance with FEMA P-695 requirements.

5.5.1 Earthquake records - Normalization and scaling:

A set of 44 far-field earthquake records, represented in FEMA P-695, are utilized to perform IDA and collapse evaluation of the archetypal buildings. These records are composed of 22 component pairs of ground motions taken from 14 strong events. The selected records, downloaded from the Pacific Earthquake Engineering Research Center (PEER) database, which are normalized and scaled in compliance with FEMA P-695 guidelines.

The normalization of the records is performed by using their peak ground velocity to mitigate unnecessary inherent variability between records which are coming from the differences in event magnitudes, distance to earthquake source, source type, and site conditions. However, in this method the record-to-record variability needs to be taken into the consideration to ensure that the collapse assessment process is done precisely. In this regard, the normalization factor calculated from the median of the peak ground velocity values of the records set that is divided by the peak ground velocity of each record and is applied to the individual records.

The normalized record set is then collectively scaled to anchor the median spectrum of the record set to MCE intensity level (S_{MT}) of the selected site (Lancaster, California, USA) at the first-mode period of each archetypal building.

The scaling factors for the 4-,7- and 12-story models are 2.30 (T_1 = 1.12 s), 2.77 (T_1 = 2.03 s) and 3.54 (T_1 = 3.0 s), respectively.

Figure 5-6, which is represented in logarithmic scales, shows the median spectrum of the 44 far-field ground motions scaled to the MCE level spectrum at the first natural period (anchored point) for the 7-story model.

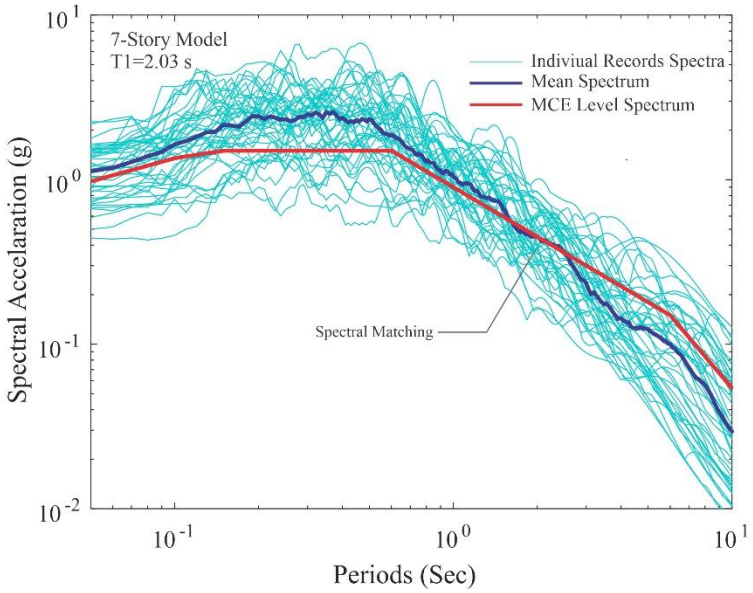

Figure 5-6: Spectral accelerations of individual records matched to design spectrum at first-mode period of 7-story model.

5.5.2 Incremental Dynamic Analysis (IDA)

To investigate the seismic performance and evaluate collapse probability, the structural models are subjected to incremental dynamic analysis (IDA) comprising a set of nonlinear time history analysis under the 44 FEMA P-695 far-field records. In these analyses, the intensity of each earthquake is increased from small to large, in 10% increments relative to MCE level intensity (S_{MT}), until the buildings experience collapse. Then the IDA curves are generated by the damage measure of peak inter-story drift versus the ground motion intensity measured by the 5% damped spectral acceleration at the first natural period of each model (SaT_1; 5%). To capture collapse points, the collapse stage of the archetypal buildings is considered the maximum values of the peak inter-story drift ratio of about 10 % and the ultimate limit at which the gravity frames lose their stability under gravity loads whichever occurs first (Steele et al., 2017).

5.5.3 Collapse Risk Evaluation of Archetypes

The IDA curves cover the seismic behaviour of each model from elastic range to inelastic range until collapse, and are utilized to generate fragility curves for the collapse data points by means of a cumulative distribution function (CDF). In this regard, a lognormal distribution function, defined

by the two parameters: the median collapse intensity ($\hat{S}_{CT}$) corresponding to the 50% probability of collapse, and the record-to-record variability (β_{RTR}), is first fitted to the collapse data points.

In this study, a probability curve fit software developed by Baker (Baker, 2015) is employed to plot the fitted fragility curve (initial fragility curve) which relates the earthquakes' intensity (i.e., spectral acceleration) to the probability of collapse. Subsequently a collapse margin ratio (CMR) is determined by using the generated fragility curve using Equation (5.6). The CMR is the main factor showing the collapse probability of a building in its fundamental period.

$$CMR=\hat{S}_{CT} /S_{MT} \quad (5.6)$$

In Equation (5.6), the term S_{MT} denotes the MCE-Level spectral intensity at the fundamental period of the building.

As per FEMA P-695, previous studies have proved that, based on variability in the response of archetypes to different ground motion, records record to record variability (β_{RTR}) falls within a range of 0.35 and 0.45 for many types of conventional structural systems.

In this study, to be more precise, the β_{RTR} values, are directly captured from IDA results and used to derive the fragility curves.

Beyond record-to-record uncertainty (β_{RTR}) which refers to variable response of the archetypal buildings to different earthquake records, an additional system-level uncertainty needs to be considered in generating the collapse fragility curves to achieve more precise results (Federal Emergency Management Agency, 2009).

The system level-uncertainty arises from the robustness and completeness of design requirement (β_{DR}), accuracy and reliability of the test data (β_{TD}), and the quality of the computational model (β_{MDL}). Therefore, the total collapse uncertainty (β_{TOT}) is quantified by Equation (5.7):

$$\beta_{TOT} = \sqrt{\beta_{RTR}^2 + \beta_{DR}^2 + \beta_{TD}^2 + \beta_{MDL}^2} \quad (5.7)$$

The system-level uncertainties (i.e., β_{DR}, β_{TD}, and β_{MDL}) can be qualitatively ranked as "superior", "good", "fair", or "poor" , as per FEMA P-695, corresponding to quantitative values of 0.1, 0.2,

0.35 and 0.5, respectively. Since in a number of the selected ground motions, their spectral shapes are different from the shape of design spectrum provided by ASCE 7-22, the median collapse intensity $\hat{S}_{CT}$ is amplified by a spectral shapes factor (SSF) which is defined based on FEMA P-695 recommendations to take into account the effect of the spectral shape in the estimation of the collapse probability and alter the plotted fragility curves. Consequently, the resulted collapse margin ratio (CMR), derived from the IDA, is modified as shown in Equation (5.8):

$$ACMR = SSF \times \hat{S}_{CT} / S_{MT} \quad (5.8)$$

As per FEMA P-695, to acknowledge the seismic behavior of the novel structural system theoretically, the evaluated ACMR for the individual archetypes and their average value ($ACMR_m$), with considering the total uncertainties, should satisfy the two following conditions represented in Equation (5.9).

$$ACMR_m \geq ACMR_{10\%}(\beta_{TOT}) \text{ and } ACMR \geq ACMR_{20\%}(\beta_{TOT}) \quad (5.9)$$

These conditions mean that the probability of collapse for a set of archetypical buildings should not exceed 10% while it needs to be less than 20% in the individual buildings. However, it should be noted that in this study only one model for each of the 4-, 7- and 12-story buildings is examined. Therefore, the probability of collapse in the S_{MT} for each model needed to be less than 10% to be accepted (first criteria) and the other criteria is not applicable.

The IDA and collapse fragility curves for the good rated 4-, 7-, and 12- story FT-TMF archetypes are represented in Figure 5-7. For the studied archetypes, the record-to-record uncertainty (β_{RTR}), obtained from IDA results, are equal to 0.277, 0.461 and 0.373 for the 4-,7- and 12-story models, respectively. The robustness of design requirements is rated good (i.e., β_{DR} =0.2) because the applied design procedure is considered proficient to protect the system against collapse mechanisms due to the presence of the tendons, elastic design of the structural elements in the specified drift, and the expectation that there would be no damage to the friction devices or tendons.

The computational models are prepared in two commonly used finite element software (OpenSees and SAP2000) and the output analytical results from both software match well. Therefore, the model quality (β_{MDL}) is rated as good. Although there is no test data available, the test data reliability (β_{TD}) is assumed good to generate the benchmark fragility curves. However, in section

5.6.2 the other scenarios including superior to poor ranks are considered for β_{MDL} and $\beta_{TD,}$ which are dependent to test validation, to evaluate the system response.

Then after, by using Equation (5.7) the resulted total collapse uncertainties (β_{TOTs}) are subsequently determined 0.443, 0.576 and 0.509 for the 4-, 7- and 12-story models, respectively.

Figure 5-7 shows the IDA and fragility curves for the models rated good. In Figure 5-7 (a) the IDA curves of the studied models, under the 44 ground motion records are shown which represent the increase in maximum inter-story drifts resulted from the rise in the seismic acceleration until the collapse. Mean of the IDA curves are also plotted, to visualize the resulted median collapse intensity $\hat{S}_{CT}$ (g). Figure 5-7 (b) represents the fitted function (CDF) to the collapse points obtained from IDAs.

In the blue curve the impact of β_{RTR} uncertainty is taken into consideration. Then the SSF factor is applied to the fitted function to derive the fragility curve demonstrated as the black curve. And finally, in the red curve, the β_{RTR} is replaced with β_{tot} to demonstrate the effect of total uncertainty in the system's fragility. The collapse assessment parameters from IDAs for FT-TMFs are summarized in Table 5-3.

As shown in Figure 5-7, and Table 5-3, the resulted ACMRs for the archetypes ranked good, determined using Equation (5.8), are 3.52, 6.44 and 6.53 for the 4-,7- and 12-story models. In this table the ACMRs are compared with the values of $ACMR_{10\%}$ derived from FEMA P-695.

The comparison shows that the related ACMRs for all of the archetypal buildings are well beyond the $ACMR_{10\%}$ which means the probability of collapse for each archetype at MCE intensity level is less than 10% and therefore satisfies the acceptance measures of FEMA P-695.

Furthermore, it proves that the R factor of 7, which is used in the analysis to tune the friction dampers, and shows it can involve in offering the appropriate safety margin to the system under MCE-level ground motions.

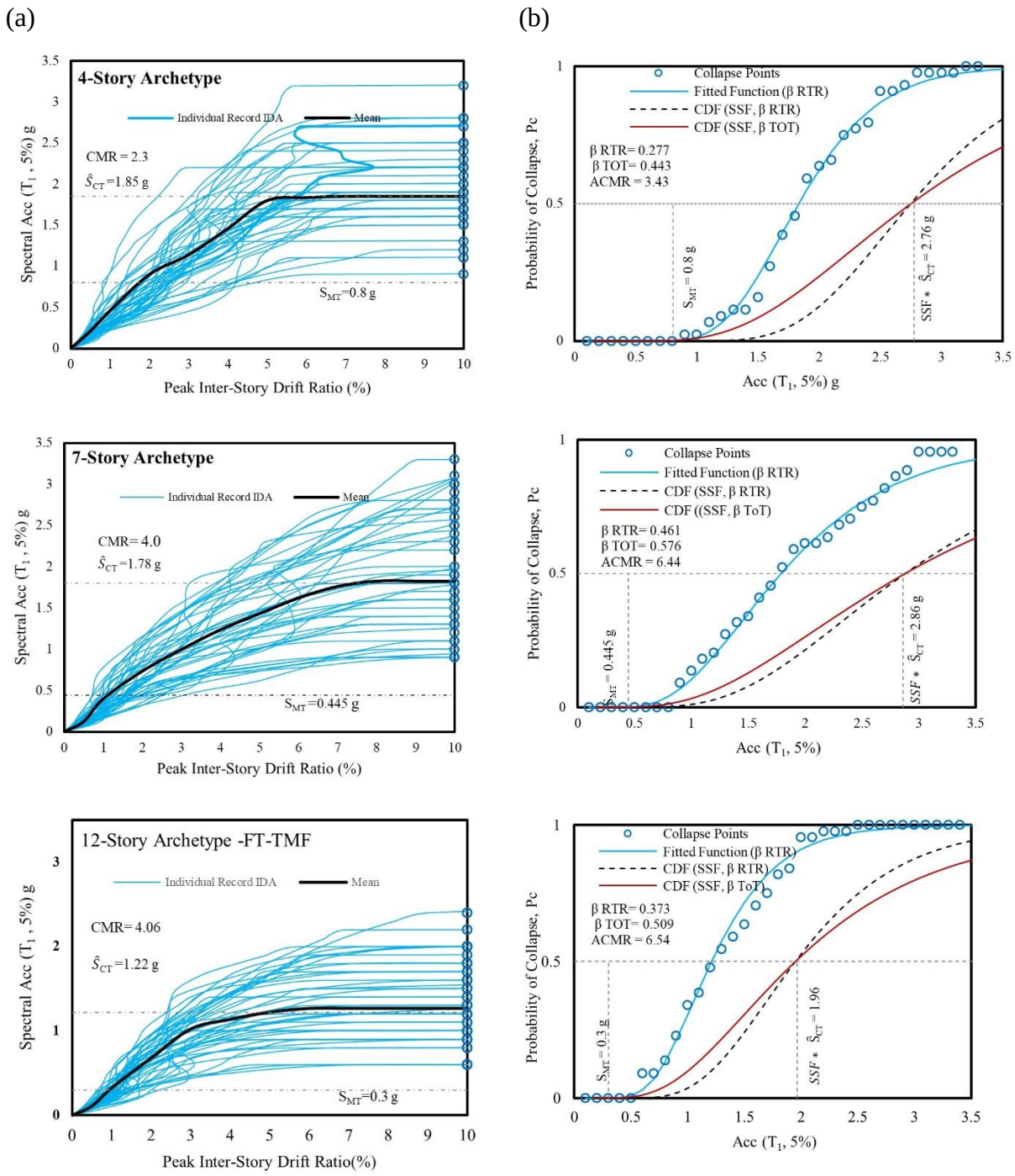

Figure 5-7: a) IDA and b) Collapse fragility curves for the 4-, 7-, and 12-story FT-TMF archetypes

Table 5-3: Collapse risk evaluation results for FT-TMF archetypes

Archetypes	A1: 4 story (1.0T)	A2: 7-story (1.0T)	A3: 12-story (1.0T)
First mode period (T_1)	1.12 s	2.03 s	3.0 s
Median collapse intensity $\hat{S}_{CT}$ (g)	1.85 g	1.78 g	1.22 g
MCE-level spectral acceleration S_{MT} (g)	0.78 g	0.443 g	0.3 g
Record-to-record uncertainty, βRTR	0.277	0.461	0.373
Total collapse uncertainty, βTOT	0.443	0.576	0.509
Collapse margin ratio, CMR	2.35	4.0	4.06
Spectral shape factors, SSF	1.5	1.61	1.61
ACMR (adjusted CMR)	3.52	6.44	6.53
$ACMR_{10\%}$	1.76	2.09	1.96
System acceptance check, Pass/Fail	Pass	Pass	Pass

5.6 Parametric Analysis

To better investigate variations in factors such as tendon size and system-level uncertainties, this study considers these aspects as follows:

5.6.1 Effect of Tendon Size

The tendons play an important role in the seismic resistance of FT-TMF system. Consequently, one key parameter examined through a parametric study is the effect of an increase in tendons' size in the 12-story model. This is accomplished by increasing the number of strands in the tendons in 12-story FT-TMF model, by approximately 30%, to study its effect in seismic behavior and collapse probability.

Figure 5-8, illustrates the Incremental Dynamic Analysis (IDA) and fragility curves for the 12-story model with enhanced tendon sizes (i.e., 30% more strands per tendon), subjected to a suite of the 44 ground motion records.

The analysis indicates that the median collapse intensity of the system ($\hat{S}_{CT}$), increases by 27%, while the adjusted collapse margin ratio rises by 28%. These improvements, driven by the use of larger tendon sizes, contribute to a more robust system response. As a result, the larger tendons, provide better stability and resilience, enhancing the system's overall seismic behavior.

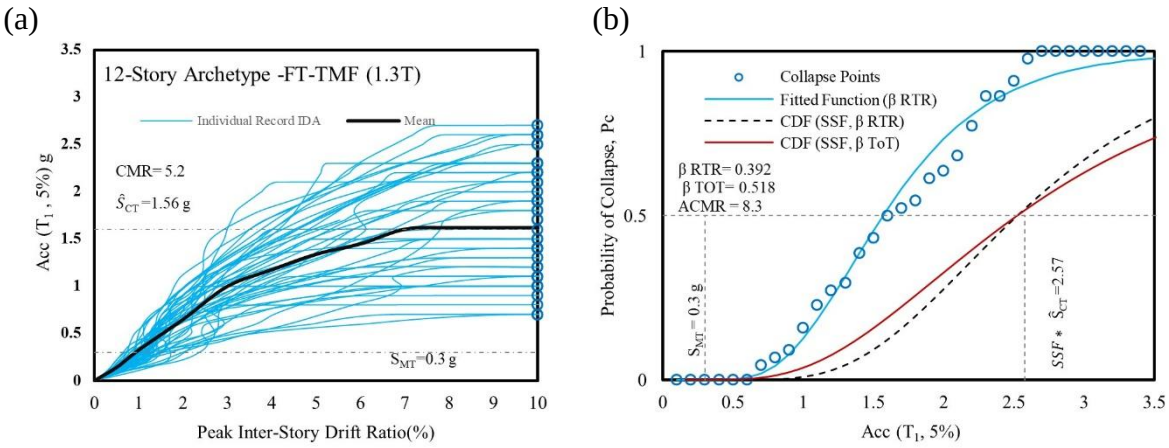

Figure 5-8: a) IDA and b) Collapse fragility curves for 12-story FT-TMF archetype with tendon sizes 30% larger than minimum required

5.6.2 Effect of the Variation in System -level Uncertainties

It is essential to examine the variation in total system-level uncertainty due to the lack of test data and experimental results and to investigate its impact on the system's response in collapse risk analysis. In this regard, computational model quality (β_{MDL}) and test data reliability (β_{TD}) are ranked as superior, fair, and poor, in addition to good rank, to generate comparative collapse fragility curves for each model.

It should be noted that the record-to-record variability (β_{RTR}) and the robustness of design requirement (β_{DR}) remain unchanged, as they were considered in the earlier analysis and are incorporated into the collapse fragility curves shown in Figure 5-7.

The resulted comparative fragility curves, representing the collapse probability of the archetypes under the applied seismic events, are shown in Figure 5-9.

The quantified probability of collapse in the models, with and without SSF effect, are summarized and compared with the acceptance criteria from FEMA P-695 in Table 5-4, and Table 5-5.

The results in Table 5-4 (with SSF), illustrate that for all of the considered scenarios, regarding the system-level uncertainty ranks, the archetypes meet the FEMA P-695 acceptance criteria. However, as it is shown in Table 5-5, the collapse risk analysis without consideration of the SSF, reveals that the probability of collapse considerably increases such that the 4-story archetype, with system-level uncertainty ranked as poor with the probability of collapse 14%, does not meet the FEMA P-695 acceptance criteria.

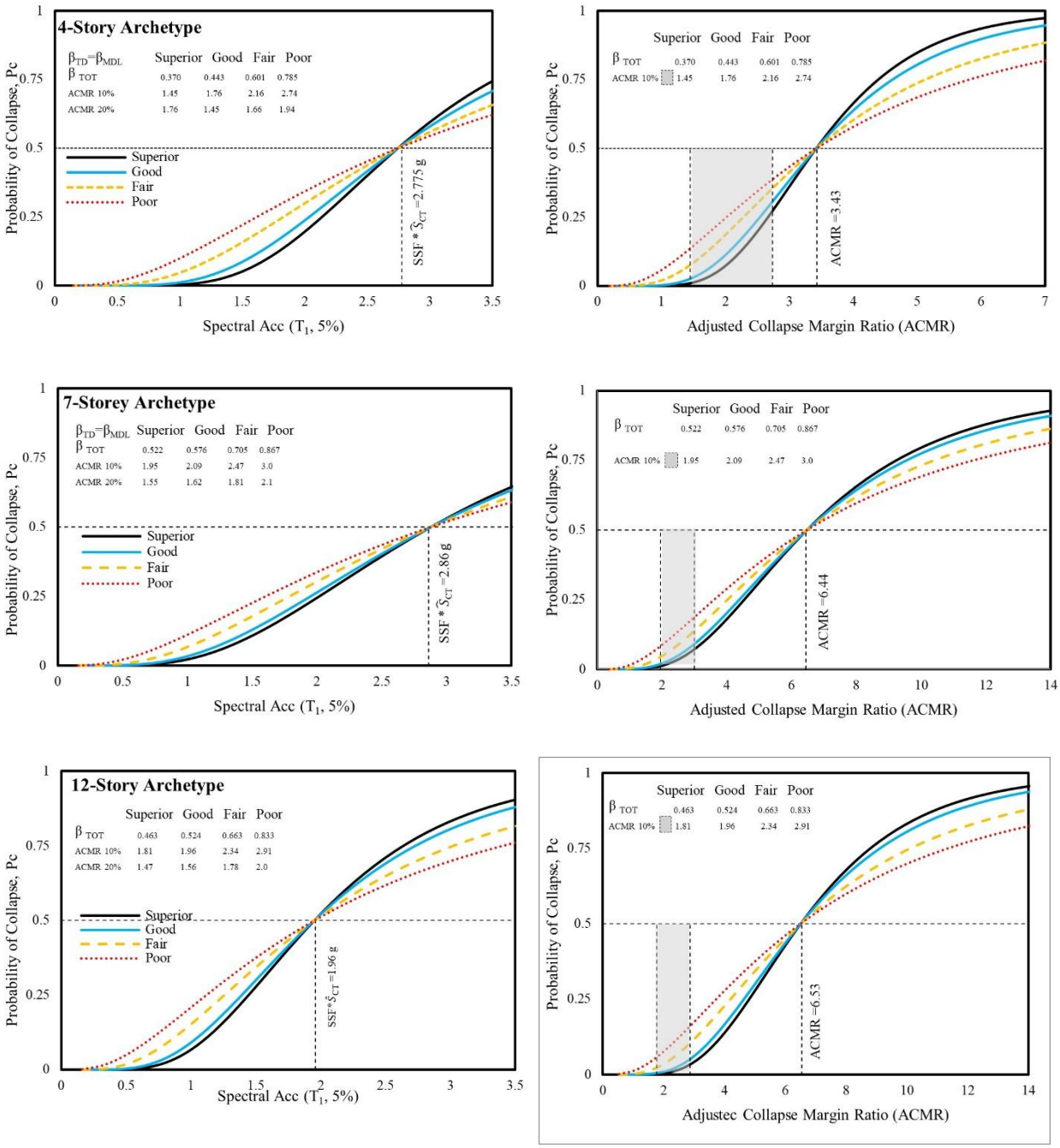

Figure 5-9: Comparative fragility curve and ACMR values for 4-,7- and 12-story archetypes with different levels of system-level uncertainty ranks

Table 5-4: Probability of collapse in the archetypes (with SSF)

	Probability of collapse (with SSF) (Pass if ≤ 10%)			
Frame	Superior	Good	Fair	Poor
4-Story (FT-TMF)	0.05	0.3	2.1	5.9
7-Story (FT-TMF)	0.03	0.09	0.5	1.9
12-Story (FT-TMF)	0.02	0.015	0.2	1.4

Table 5-5: Probability of collapse in the archetypes (without SSF)

	Probability of collapse (without SSF) (Pass if ≤ 10%)			
Frame	Superior	Good	Fair	Poor
4-Story (FT-TMF)	1.2	3.0	8.4	14 (Fail)
7-Story (FT-TMF)	0.5	0.9	2.6	5.6
12-Story (FT-TMF)	0.08	0.26	1.6	4.5

5.7 Conclusions:

This paper investigated the seismic performance and collapse risk level of a new special truss moment frame system (FT-TMF), employed as the lateral load resisting system in a set of 4-, 7- and 12-story archetypal steel buildings, which were designed for an active high-seismic zone in the western United States. FEMA P-695 methodology was applied to evaluate the system's seismic performance, assess its collapse probability, and prove the suitability of the applied design method. The key conclusions from the seismic collapse risk assessment of the FT-TMF system are summarized as follows:

1- The peak inter-story drifts versus earthquake intensity levels obtained from the incremental dynamic analysis (IDA) illustrated that the 4-, 7- and 12-story archetypes experienced the median collapse intensity ($\widehat{S}_{CT}$) levels of 1.85g, 1.78g, and 1.22 g, respectively. These results show that there was an increasing trend in the collapse risk level related to the increase in the number of stories (i.e., building height).

2- In the 12-study archetype with 30% larger tendon size had a median value of collapse intensity level ($\widehat{S}_{CT}$) that was about 27% higher (from 1.22g to 1.56 g) than the original

model due to additional self-centering capability added to the system resulting in higher seismic resilience in the system.

3- The ACMR values were 3.52, 6.44 and 6.53 for the 4-,7- and 12-story archetypes, respectively, which satisfied the corresponding acceptance criteria of ACMR10% provided in FEMA P-695. In other words, the collapse risk in all the studied buildings was less than 10% at the MCE hazard level.

4- The effects of system-level ratings (i.e., "superior", "good", "fair", and "poor") on the collapse risk of the archetypes were examined and it was observed that the probability of collapse, represented by ACMR values, increased as the system-level uncertainties increased. However, the archetypes satisfied the acceptance benchmarks. Only the 4- story archetype, without considering SSF and ranked poor, failed.

5- Ultimately, IDA results showed that the R-factor of 7 used to design the dampers in the proposed design method , was acceptable for an MCE level seismic hazard.

5.8 Appendix I:

Table 5-6: Sections assigned to the structural elements of the archetypal buildings

4-Story					
Story ID	Diagonal	Brace	Chord	Vertical	Column
4	2MC150x17.9	2C130x10.4	2MC150x22.5	2C100x9.3	W610x241
3	2MC150x22.5	2C130x13	2MC 200x31.8	2C100x9.3	W610x241
2	2MC150x26.8	2C150x15.6	2MC 230x35.6	2C100x9.3	W610x341
1	2MC150x26.8	2C150x19.3	2MC 230x35.6	2C100x9.3	W610x341
7-Story					
	Diagonal	Brace	Chord	Vertical	Column
7	2MC150x17.9	2MC150x10.4	2MC150x22.5	2C100x9.3	W610x217
6	2MC200x29.8	2MC150x10.4	2MC200x31.8	2C100x9.3	W610x217
5	2MC200x31.8	2MC150x17.9	2MC200x33.9	2C100x9.3	W610x217
4	2MC200x31.8	2MC150x17.9	2MC200x33.9	2C100x9.3	W610X307
5	2MC200x33.9	2MC150x17.9	2MC 250x42.4	2C100x9.3	W610x307
2	2MC200x33.9	2MC150x17.9	2MC 250x42.4	2C100x9.3	W610x415
1	2MC200x33.9	2MC150x17.9	2MC 250x42.4	2C100x9.3	W610x415
12-Story					
	Diagonal	Brace	Chord	Vertical	Column
12	2MC150x17.9	2MC150x10.4	2MC200x27.8	2MC150x10.4	W610x217
11	2MC150x22.5	2MC150x10.4	2MC200x31.8	2MC150x10.4	W610x217
10	2MC200x31.8	2MC150x17.9	2MC200x31.8	2MC150x10.4	W610x241
9	2MC200x31.8	2MC150x17.9	2MC230x35.6	2MC150x10.4	W610x241
8	2MC230x37.8	2MC150x17.9	2MC230x35.6	2MC150x10.4	W610x341
7	2MC230x37.8	2MC150x17.9	2MC 250x42.4	2MC150x10.4	W610x341
6	2MC230x37.8	2MC150x17.9	2MC 250x42.4	2MC150x10.4	W610x415
5	2MC250x42.4	2MC150x22.5	2MC 250x50	2MC150x10.4	W610x415
4	2MC250x42.4	2MC150x22.5	2MC 250x50	2MC150x10.4	W610x551
3	2MC250x42.4	2MC150x22.5	2MC 250x50	2MC150x10.4	W610x551
2	2MC250x42.4	2MC150x22.5	2MC 250x50	2MC150x10.4	W920x656
1	2MC250x42.4	2MC150x22.5	2MC 250x50	2MC150x10.4	W920x656

5.9 References:

Al-Shawwa, N., & Lignos, D. (2023). Web-Based Interactive Tools for Performance-Based Earthquake Engineering. Retrieved from https://resslabtools.epfl.ch/index.php

Basha, H. S., & Goel, S. C. (1994). *Seismic Resistant Truss Moment Frames with Ductile Vierendeel Segment*: Department of Civil Engineering, University of Michigan.

Basha, H. S., & Goel, S. C. (1995). Special truss moment frames with Vierendeel middle panel. *Engineering structures, 17*(5), 352-358.

Chao, S.-H., & Goel, S. C. (2008). Performance-based plastic design of special truss moment frames. *Engineering journal, 45*(2), 127.

Chao, S.-H., Jiansinlapadamrong, C., Simasathien, S., & Okazaki, T. (2020). Full-scale testing and design of special truss moment frames for high-seismic areas. *Journal of Structural Engineering, 146*(3), 04019229.

Computers&Structures Inc. (2023). SAP2000 (Version 21): CSI. Retrieved from https://www.csiamerica.com/

Deierlein, G., Krawinkler, H., Ma, X., Eatherton, M., Hajjar, J., Takeuchi, T., Kasai, K., & Midorikawa, M. (2011). Earthquake resilient steel braced frames with controlled rocking and energy dissipating fuses. *Journal of Steel Construction, 4*(3), 171-175.

Dowden, D. M., & Bruneau, M. (2016). Dynamic shake-table testing and analytical investigation of self-centering steel plate shear walls. *Journal of Structural Engineering 142*(10), 04016082.

Eatherton, M. R. (2010). *Large-scale cyclic and hybrid simulation testing and development of a controlled-rocking steel building system with replaceable fuses*: University of Illinois at Urbana-Champaign.

Eatherton, M. R., Ma, X., Krawinkler, H., Mar, D., Billington, S., Hajjar, J. F., & Deierlein, G. G. (2014). Design concepts for controlled rocking of self-centering steel-braced frames. *Journal of Structural Engineering, 140*(11), 04014082.

Erochko, J., Christopoulos, C., & Tremblay, R. (2015). Design and testing of an enhanced-elongation telescoping self-centering energy-dissipative brace. *Journal of Structural Engineering*

141(6), 04014163.

Faraji, K., & Tremblay, R. (2019). *Multi-story truss moment frames equipped with friction dampers and self-centering system for enhanced seismic performance*. Paper presented at the The Evolving Metropolis-IABSE Congress, New York, New York-USA.

Federal Emergency Management Agency. (2009). Quantification of Building Seismic Performance Factors (FEMA P695). In. USA: Federal Emergency Management Agency

Gilbert, C. F., & Erochko, J. (2019). Development and testing of hybrid timber-steel braced frames. *Journal of Engineering Structures, 198*, 109495.

Goel, S., Leelataviwat, S., & Stojadinovic, B. (1997). Steel moment frames with ductile girder web opening. *ENGINEERING JOURNAL-AMERICAN INSTITUTE OF STEEL CONSTRUCTION INC, 34*(4), 115-125.

Goel, S., Rai, d. C., & Basha, S. (1998). *Special Truss Moment Frame*. Retrieved from

Goel, S. C., & Itani, A. M. (1994). Seismic-resistant special truss-moment frames. *Journal of Structural Engineering, 120*(6), 1781-1797.

Grigorian, M. (2021). Resiliency and post-earthquake realignment. *30*(5), e1836. doi:https://doi.org/10.1002/tal.1836

Grigorian, M., & Grigorian, C. E. (2018). Sustainable earthquake-resisting system. *Journal of Structural Engineering, 144*(2), 04017199.

Hanson, R., Martin, H., & Martinez-Romero, E. (1986). *Performance of steel structures in the September 19 and 20, 1985 Mexico City earthquakes.* Paper presented at the The National Engineering Conf., AISC.

Ireland, R. C. (1997). *Special truss moment frames in low to moderate seismic regions with wind*: University of Michigan.

Jiansinlapadamrong, C., Park, K., Hooper, J., & Chao, S.-H. (2019). Seismic design and performance evaluation of long-span special truss moment frames. *Journal of Structural Engineering, 145*(7), 04019053.

Latour, M., D'Aniello, M., Zimbru, M., Rizzano, G., Piluso, V., & Landolfo, R. (2018). Removable friction dampers for low-damage steel beam-to-column joints. *Journal of Soil Dynamics & Earthquake Engineering, 115*, 66-81.

Lignos, D. G., & Krawinkler, H. (2011). Deterioration modeling of steel components in support of collapse prediction of steel moment frames under earthquake loading. *Journal of Structural Engineering, 137*(11), 1291-1302.

Mckenna, F., Fenves, G. L., Scott, M. H., and Jeremic, B. . (2020). Open system for earthquake engineering simulation (OpenSees) (Version 3.2.1). Berkeley (CA). Retrieved from https://opensees.berkeley.edu/

Momeni, S., Aoudia, A., Tatar, M., Twardzik, C., & Madariaga, R. (2019). Kinematics of the 2012 Ahar–Varzaghan complex earthquake doublet (M w6. 5 and M w6. 3). *Geophysical Journal International, 217*(3), 2097-2124.

Steele, T. C., & Wiebe, L. D. (2016). Dynamic and equivalent static procedures for capacity design of controlled rocking steel braced frames. *Earthquake Engineering &Structural Dynamics, 45*(14), 2349-2369.

Steele, T. C., Wiebe, L. D., & Dynamics, S. (2017). Collapse risk of controlled rocking steel braced frames with different post-tensioning and energy dissipation designs. *46*(13), 2063-2082.

The American Institute of Steel Construction. (2016a). Seismic Provisions for Structural Steel Buildings, ANSI/AISC 341-16. In: American Institute of Steel Construction, Chicago, IL.

The American Institute of Steel Construction. (2016b). Specification for Structural Steel Buildings-ANSI/AISC 360-16. In. American Institute of Steel Construction, Chicago, IL: AISC.

The American Society of Civil Engineers. (2022). Minimum Design Loads and Associated Criteria for Buildings and Other Structures (ASCE 7-2022). In. USA: The American Society of Civil Engineers,.

Tremblay, R. (1993). *Seismic behavior and design of friction concentrically braced frames for steel buildings.* University of British Columbia,

Tremblay, R., & Faraji, K. (2019). *Steel truss moment frames with self-centring energy dissipation mechanisms for enhanced seismic performance*. Paper presented at the 12th Canadian Conference on Earthquake Engineering, Quebec City, June 17-20, 2019, Quebec City- QC-Canada.

Vamvatsikos, D., & Cornell, C. A. (2002). *The incremental dynamic analysis and its application to performance-based earthquake engineering.* Paper presented at the 12th European Conference on Earthquake Engineering.

Vamvatsikos, D., & Cornell, C. A. (2004). Applied incremental dynamic analysis. *Earthquake Spectra, 20*(2), 523-553.

Wongpakdee, N., & Leelataviwat, S. (2017). Performance-based design of mid-rise buckling-restrained knee braced truss moment frames. *SURANAREE JOURNAL OF SCIENCE TECHNOLOGY, 24*(4), 445-454.

Wongpakdee, N., Leelataviwat, S., Goel, S. C., & Liao, W.-C. (2014). Performance-based design and collapse evaluation of buckling restrained knee braced truss moment frames. *Engineering structures, 60*, 23-31.

Yang, T., Li, Y., & Leelataviwat, S. (2014). Performance-based design and optimization of buckling restrained knee braced truss moment frame. *Journal of Performance of Constructed Facilities, 28*(6), A4014007.

Zhang, A.-l., Zhang, Y.-x., Li, R., & Wang, Z.-y. (2016). Cyclic behavior of a prefabricated self-centering beam–column connection with a bolted web friction device. *Engineering structures, 111*, 185-198.

CHAPTER 6 ARTICLE 3: TRUSS MOMENT FRAME SYSTEM WITH FRICTION DAMPERS AND POST-TENSIONED ROCKING CORE

This article is submitted to: Journal of Structures on 27th October 2024 Manuscript Number: S-24-09097

Keyhan Faraji (1), Robert Tremblay (2)
(1) PhD student, Polytechnic-Montreal, keyhan.faraji@polymtl.ca
(2) Professor, Polytechnic-Montreal, robert.tremblay@polymtl.ca

Corresponding author: Keyhan Faraji, Email address: keyhan.faraji@polymtl.ca

Abstract

A new earthquake-resistant hybrid structural system is proposed that combines a truss moment frame with friction dampers (F-TMF) and a post-tensioned rocking core (R) acting as a strong back for the system. The hybrid system, named RF-TMF, is intended to create a resilient low damage and repairable structural system for applications in seismically active regions. The friction dampers, which are installed between the bottom chord of the trusses and the adjacent columns in the F-TMFs, are the principal elements that are designed to dissipate seismic energy and protect surrounding structural elements by limiting the lateral load on the rest of the structure. A set of fuse joints are also accommodated in the link beams connecting the two systems and support-level grade beams attached to the columns in the F-TMFs to participate in the seismic energy dissipation. The post-tensioned rocking core mitigates higher mode effect during an earthquake and controls lateral deformations of the entire system keeping them in a normalized linear pattern and provides the system with re-centering capacity that reduces drifts. To evaluate the seismic performance of the proposed hybrid system, it is examined in a set of 7-, 9- and 12- story archetypal buildings. Numerical models of the RT-TMFs are developed and a series of nonlinear time-history analyses are conducted to capture and examine their seismic response. The analyses are performed for a suite of ground motions at the maximum credible earthquake (MCE) hazard level with the probability of 2% in 50 years. The analytical results demonstrate the resilience of the proposed structural system and its capability to reduce seismic force demand and control lateral transient displacements during strong earthquakes mitigating permanent drifts afterwards.

Keywords: Truss moment frame, friction damper, post-tensioned rocking core, re-centering capacity

6.1 Introduction:

Earthquakes are natural phenomena that occur without warning. Historically, earthquakes have been a significant source of loss of life and property, injuries, economic falls, changes in geomorphic characteristics of earth and immediate damage to cities and civilization.

For example, a recent catastrophic seismic event and following aftershocks affected large areas of Turkey on February 6, 2023. This catastrophic earthquake caused at least 45,000 life losses, destroyed thousands of structures including buildings and infrastructure, rendered millions houseless people across numerous cities and triggered immediate damage estimated at $34 billion, which is approximately 4% of Turkey's annual economic output (The World Bank, 2023). However, the indirect costs and consequent economic falls and weight downs related to the post-disaster recovery, medical and psychological care, critical social impacts, as well as rehabilitation and reconstruction will be much higher and considered as a long term recovery situation.

Lessons from past strong earthquakes in different areas of the world revealed that in many cases, despite complying with design codes and standards, many buildings and infrastructure remain vulnerable to irreparable damage to their structural and non-structural members and components (Mahin, 1998; Steele & Wiebe, 2016). From a broader perspective, these damaged structures could impose considerable financial and environmental challenges to societies. The limitation of natural resources, excessive carbon footprint in the planet, irreversible environmental damage of disposable construction material to the natural world, expensive and complex process of disposable material recycling as well as high cost of demolition and reconstruction are factors that support and justify a new approach of sustainability in design of structures and buildings referring to earthquake resistance design and viable post-event repairability. One of the practical methods that could be used in developing sustainable buildings is to enhance and combine multiple earthquake resistant structural systems such that the advantages and capabilities of each system are applied in a hybrid system with a concern to energy dissipation, predictable lateral movements, controlled damage in pre-defined replaceable elements and post-event repairability and realignment (Grigorian & Grigorian, 2018).

The concept of employing energy dissipation devices and self-centering mechanisms in structural systems to enhance their earthquake resilience and limit seismic damage has been a subject of interest for researchers and engineers . In this regard, comprehensive studies and experimental tests

have been conducted over the past three decades. A considerable number of these studies have been focused on developing different types of dampers and base isolators, special connections, and frames with energy dissipation and re-centering capacity (Ricles et al., 2001; Pan et al., 2005; Garlock & Li, 2008; Wang et al., 2017; De Luca & Guidi, 2019; Grigorian et al., 2023). Rocking systems with a variety of configurations, which were inspired by the notable earthquake resilience of ancient pagodas constructed in China and Japan have also been in the focal points of engineers and researchers as a cutting edge structural system (Wu et al., 2018). Satisfactory seismic performances of structural systems enhanced with different types of energy dissipation devices such as friction dampers and competence of post-tensioned rocking frames have been proven in a number of conceptual and experimental studies performed in the past (Wiebe & Christopoulos, 2009; Deierlein et al., 2011; Eatherton, Ma, Krawinkler, Deierlein, et al., 2014; Grigorian et al., 2017; Martin et al., 2019). Therefore, the combination of a structural system with device-induced high energy dissipation capacity plus a self-centering rocking system is expected to demonstrate an enhanced, stable, and reliable seismic behaviour.

In this paper, a new hybrid structural system composed of two truss moment frames equipped with friction dampers (F-TMFs) with a post tensioned rocking core (R) installed in between, is proposed. In this hybrid system, the trusses and the rocking core are inter-connected via link beams at each story level. The friction dampers are the principal energy absorbers which are installed between the bottom chords and the adjacent columns in the truss frames. The key role of the rocking frame is to act as a strong back suppressing the impact of higher modes and provide the entire system with a regulated lateral movement with a predictable displacement pattern. A pair of post-tensioned high strength tendons are installed through the rocking frame which play the role of the stabilizers and provide the system with self-centering capacity that limits the seismic drifts. The link beams are connected to the rocking frame and the trusses with hinge and repairable connections (RBS-treated fuse joints), respectively. The fuse joints limit the local moments transferred from the rocking frame to the links during an earthquake and participate in energy dissipation. In this system a set of support-level grade beams are attached to the columns via similar fuse joints to protect the columns against seismic damage.

6.2 Research Objectives and Methodology:

The goal of this research is to combine the advantages of truss moment frames improved with energy dissipation devices including friction dampers and repairable fuse connections, with the re-centering capability of post-tensioned rocking system to propose a sustainable earthquake resistant system. The proposed hybrid system is intended to demonstrate reliable seismic behaviour subjected to design-level ground motions experiencing no or low damage and viably lend itself to post-event repair and realignment. This research proposes a design method for the new system including the technics used to design its supplemental elements consisting of the friction dampers, grade and link beams as well as the elastic tendons. Moreover, this study explores the interaction of the truss frames with the rocking core in the new system and examines their global seismic performance as well as the functionality of the supplemental elements under a set of non-linear time history analyses subjected to strong ground motions.

The main structural and dynamic attributes of the proposed system are summarized as follows:

6.3 Structural attributes:

1- High energy dissipation capacity: provided by the friction devices and the fuse joints (Christopoulos et al., 2008; Tremblay & Faraji, 2019; Grigorian et al., 2023).
2- Adjustable energy dissipation capacity: a range of slip force can be provided by the adjustable friction dampers (Faraji & Tremblay, 2019).
3- Adjustable self-centering capacity: provided by number/size of tendons and the post-tensioning force (Ma, 2010; Eatherton, Ma, Krawinkler, Mar, et al., 2014).
4- Static Analyses: qualifying of the system for non-linear quasi-static analyses (Eatherton, Ma, Krawinkler, Deierlein, et al., 2014).
5- Predicted seismic load distribution: due to the function of the rigid rocking core (Mohammadi et al., 2004).
6- Resilience and repairability: no damage is considered in friction dampers, fuse joints are repairable, tendons are replaceable, post-event static realignment process of the system is viable (Grigorian, 2021).
7- Controlled lateral movement and elimination of drift concentration: near linear angular displacement due to the presence of the rigid rocking core (MacRae et al., 2004; Lai & Mahin, 2015).

8- Minimized transient and residual drifts: due to re-centering capacity, provided by the post tensioned tendons (Eatherton, Ma, Krawinkler, Deierlein, et al., 2014; Eatherton, Ma, Krawinkler, Mar, et al., 2014).
9- Controlled base shear: achieved by adjusting the slip force in the friction dampers (Tremblay & Faraji, 2019).
10- Preventing soft-story formation: the rocking core functions as a strong back that prevents the formation of soft-story and premature seismic damage (Qu et al., 2012; Lai & Mahin, 2015; Simpson & Mahin, 2018).
11- Redundancy: the post-tensioned rocking core improves redundancy and stability level of the entire system.
12- Availability and reliability: the elements such as friction damper and high strength tendons, utilized in fabrication of this system, are available and have been used in some conventional structural systems.

6.4 Dynamic attributes:

1- Stable hysteretic response: the capability to demonstrate a stable hysteretic response due to the presence of the friction dampers.
2- First mode domination: the first mode dominates in both elastic and inelastic stages due to the presence of the rocking core (Eatherton, Ma, Krawinkler, Mar, et al., 2014).
3- Suppressing the effect of the higher modes: functionality of the rocking core as a strong back.
4- Longer first natural period: provided by energy dissipation elements and rocking frame.
5- Mitigation of dynamic P-Δ effect: a noticeable portion of P-Δ effect is neutralized by the post-tensioning tendons accommodated in the rocking core.
6- High energy damping ratio: provided by the inherent and device-applied energy dissipation that reduce strength degradation and results in less damages in structural and non-structural elements.
7- Compatible with time-history validation: the functionality of this system subjected to ground motions can be verified by using non-linear time history (Ajrab et al., 2004).
8- Controllable lateral stiffness: by adjusting the friction dampers slip force in the trusses and the number of post-tensioned tendons in the rocking frame.

To achieve the defined goals and explore the functionality of the proposed system, it is designed and employed as the lateral load resisting structural system (LLRS) in a set of 7-, 9- and 12-story archetypal buildings. The performance of the archetypes was examined under a set of non-linear static (pushover) and time history analyses subjected to 22 far-field strong ground motions, represented in FEMA P-695, which are scaled to the MCE level spectrum of the high-seismic zone in the western United States.

6.5 Description of Archetypal Buildings:

The archetypal models include a set of 7-, 9- and 12-story steel buildings with a similar plan but varying heights of 32 m, 41 m, and 54.5 m, respectively. The studied buildings are considered to be located at a high- seismic zone in Los Angeles, CA, USA.

The plan view of the studied buildings, which is illustrated in Figure 6-1, consists of 3 bays with the span lengths of 14 m, 11.2 m and 14 m in the E-W direction, respectively, and 3 bays with constant length of 10 m in N-S direction. RF-TMFs, which are accommodated along the perimeter of the plan, function as the LLRS of the buildings in E-W and N-S direction.

The RF-TMFs consist of two F-TMFs in the first and the last bay with a rocking core (R) in between which are connected via link beams with the length of 2.8 m. A set of grade beams with the length of 4.0 m, are attached to columns' feet. (Figure 6-2). The depth and panel lengths of the trusses are 1.4 m and 2.8 m respectively.

Since the LLRS are similar, only one of the RF-TMFs in E-W direction for each archetypal building is selected and analyzed.

The gravity loads including dead, live and snow loads, As per ASCE 7-22, are applied to the building models (Figure 6-1).

Since the archetypal buildings are located in a high-seismic zone, the trusses are made of steel channel sections that can provide higher capacity for the TMFs compared to angle sections (Jiansinlapadamrong et al., 2019; Chao et al., 2020). The columns and the rocking frame are designed with wide flange steel sections. A composite steel deck system is selected for the floors and roofs, supported by conventional open-web steel joists spanning in the N-S direction.

The design tables of the RF-TMFs are included in Appendix I (Table 6-3 & Table 6-4).

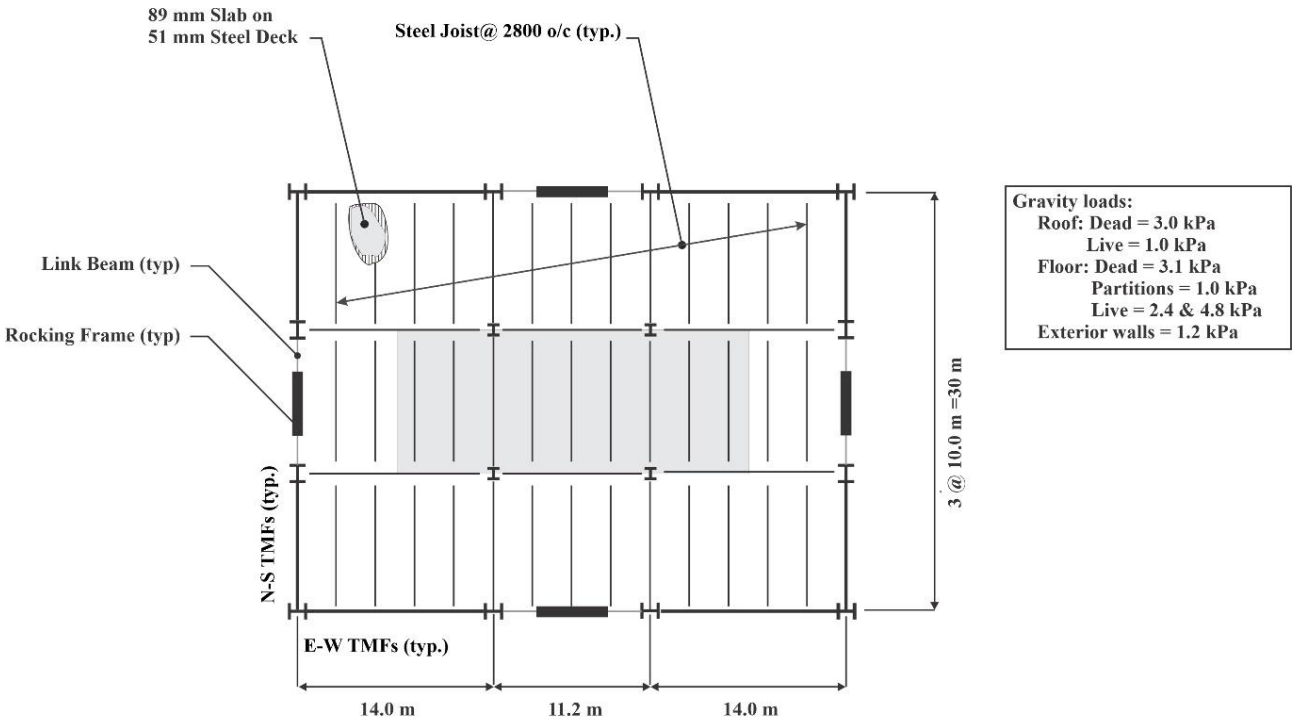

Figure 6-1: The plan view of the 7-, 9- and 12-story archetypal buildings

6.6 Structural Models:

Numerical models of the 7-, 9- and 12-story RF-TMFs are created in OpenSees (Mckenna, 2020). These models are used to simulate the behaviour of the system under a series of seismic events by means of non-linear time history analyses. A set of supplementary computational models of the RF-TMFs are also produced in SAP2000 software (Computers&Structures Inc., 2023) which are used for the relevant modal-spectrum analysis and verification of the OpenSees models. Figure 6-2 shows a schematic of the 7-story RF-TMF system (E-W direction).

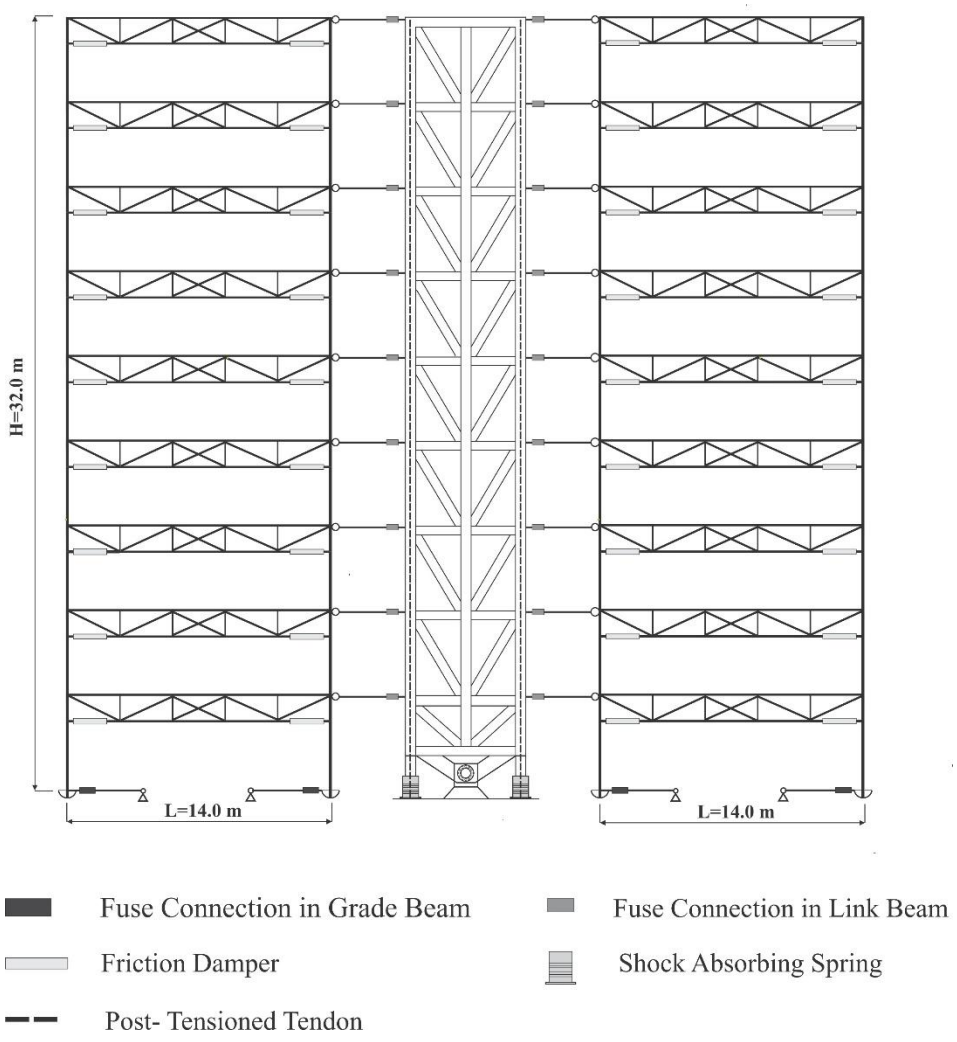

Figure 6-2: The schematic of the 7-story RF-TMF lateral resisting system

In the OpenSees models, the truss components including the chords, diagonals, verticals and braces are modeled with elasticBeamColumn elements. Due to the presence of friction dampers attached to the bottom chords, the truss components are considered to remain in elastic range of behaviour during earthquakes. The columns, grade and link beams, are modeled with elasticBeamColumn elements as well. A set of lumped plastic hinges (LP) are considered in the column's feet, both ends of the grade beams and in the connection between the link beams and the rocking core, to take into account the potential plasticity that develops in the system. The LPs are modeled by rotational spring elements which are defined based on a modified version of the Ibarra–Medina–Krawinkler

model. The utilized spring element can simulate the hysteresis behaviour of a plastic hinge by a multi-linear force-displacement capacity curves with the consideration of stiffness and strength degradation (Lignos & Krawinkler, 2011). In the OpenSees models, the friction dampers are modeled using two node link elements with uniaxial elastic-perfectly plastic material. A schematic of a friction damper and a force-displacement hysteretic curve, representing its behaviour under lateral loading, is illustrated in Figure 6-3.

(a) (b)

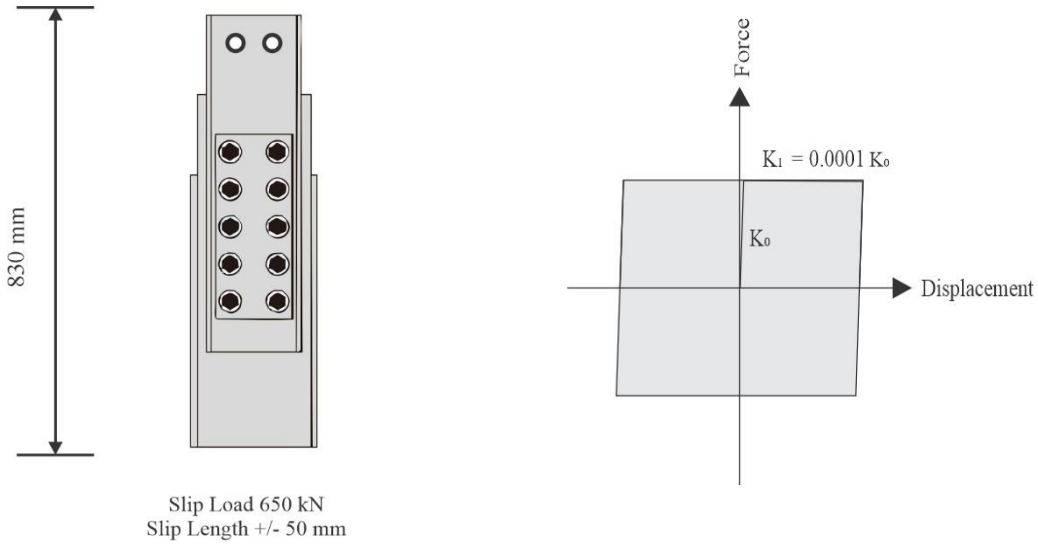

Figure 6-3: a) A sample friction damper, b) Force- displacement hysteretic curve for friction damper

The post-tensioned elastic tendons, installed on the rocking core are also modeled using three, two node link, elements combining in series, which include Bi-linear, MinMax and initial strain (initStrain) materials which simulate the elastic range of behaviour, post yielding degradation, and the post-tension force in the tendons, respectively.

A schematic of a 7-wire high-strength strand and an individual wire behaviour under tensile loading including elastic, yielding, strain hardening, and final rupture stages are shown in Figure 6-4.

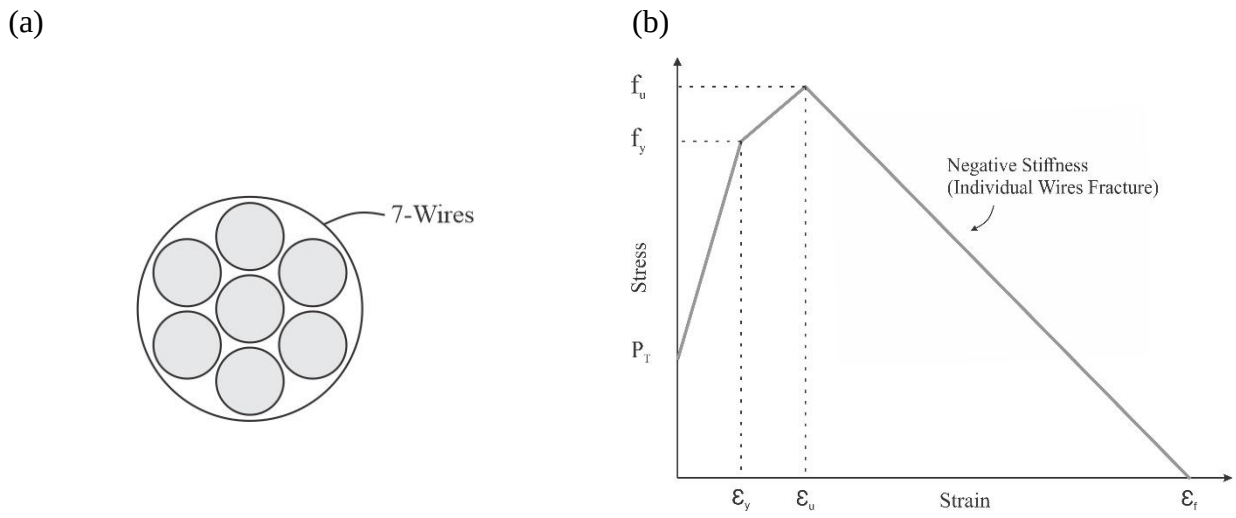

Figure 6-4: a) The schematic of a 7-wire strand, b) The force- displacement curve for a tendon

The independent and combined effects of the friction device and post-tensioned tendon in the system plus the negative stiffness induced by lateral loading in the presence of gravity loads (P-Δ) is demonstrated in Figure 6-5

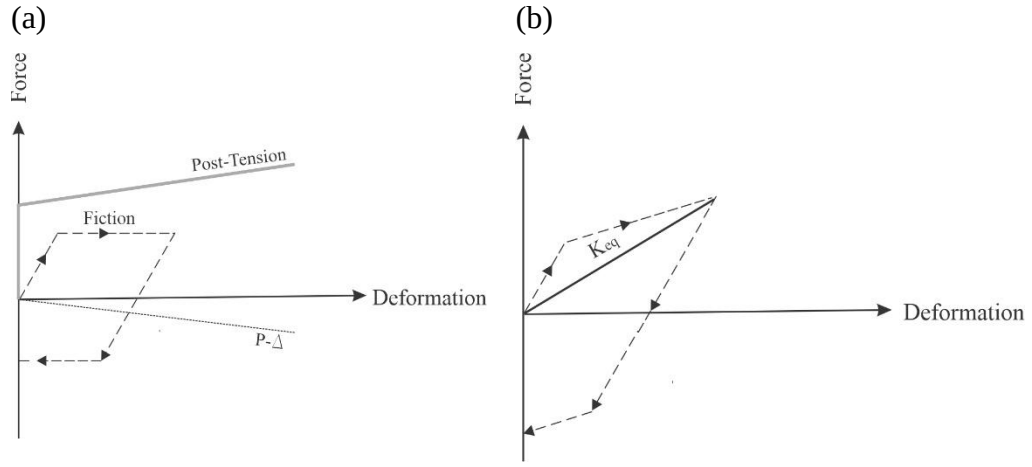

Figure 6-5: a) Independent response of post-tensioned tendon, friction device and P-Δ in the system, b) The combined response curve and equivalent stiffness of the system

In each RF-TMF model, two segmental leaning columns, which resist the total loads on the gravity columns of the parent building, are symmetrically tied to the RF-TMFs to simulate the induced dynamic P-Δ effect during the seismic analyses. The leaning columns are modeled with elastic elements and are linked to truss moment frames which modeled with elastic elements as well.

The models are subjected to a set of non-linear static (cyclic pushover) and dynamic (non-linear time history) analyses to investigate their response under displacement-controlled static loading as

well as simulated seismic events to determine their response, verify the functionality of friction dampers, fuse joints and post-tensioned tendons and prove the proposed design method.

6.7 Design Procedure:

The design procedure for the proposed RF-TMF system consists of six (6) steps as follows:

Step One- Initial Design of TMFs

To design the proposed RF-TMF, the preliminary model of the system, including truss frames and the rocking core without any dampers and tendons, is subjected to the MCE-level spectral analysis for Los Angeles area, in accordance with ASCE 7-22. The demands developed in the truss frames are used to size its structural elements including columns, chords, diagonals, verticals, bracing and support-level grade beams.

Step Two- Design of Dampers and Tendons

The maximum axial forces developed in the bottom chords obtained from the spectral analyses in step one, is considered as the design slip forces of the friction dampers.

To size the post-tensioned tendons, the seismic moment obtained from the spectral analyses plus the additional P-Δ moment produced by the gravity loads at 2.5% drift are considered as the seismic demand in the system, which should be neutralized by the resistance moment equal to the tensile force (T) in a tendon which is pulled by the rocking action, at 2.5% drift multiple by half of the rocking core span length, which is the lever arm (L_R), in Equation (6.1) as follows:

$$M_v + M_{P-\Delta} = \sum_{i=1}^{n} V_i\, h_i \; + \; \sum_{i=1}^{n} P_i\, \Delta_i \; = \; TL_R \tag{6.1}$$

where M_v and $M_{P-\Delta}$ refer to the seismic lateral and P-Δ moments, which are produced by the summation of story shears multiple by story heights ($V_i\ h_i$), and gravity loads multiple by lateral story displacements ($P_i\ \Delta_i$), at i^{th} story level, respectively.

Step Three- Design of Rocking Core

At this step, the system is subjected to a spectral analysis performed under the truncated MCE-level spectrum of the selected site, with R=1 to perform initial design of the rocking frame and the

link beams. The utilized spectrum is truncated in the first period to consider the higher modes effects in the design.

Step Four- Modification of the Structural Elements by Pushover Analysis

At this step the dampers' capacities (slip forces) are artificially increased by 30% and the models are subjected to a linear static analysis until 1.5% drift. The forces developed in the structural members are compared to the values obtained in previous steps (1&3) and the maximum demands are used to finalize the design of the trusses and verify the design of the rocking frame with applying required modifications in the sections' size.

Step Five- Tendons Capacity Validation by Pushover Analysis

At this step the dampers' slip forces are returned to their original values and the system is pushed laterally till 2.5% drift to validate the capacity and functionality of the tendons with the force-displacement pushover curve. Furthermore, the structural performance of the grade and link beams is evaluated to confirm the development of plastic hinges within these elements.

Step Six -Verification of the System Response by Non-linear Time History Analysis (NLTA)

Finally, the RF-TMF is subjected to a set of 22 ground motions, scaled to the MCE-level spectrum for the location of the building (Los Angeles area), to obtain the maximum internal forces in the structural elements and get the seismic drifts to compare with the structural capacity and the permitted range of drifts, respectively.

The design procedure is summarized in the flowchart represented as Figure 6-6

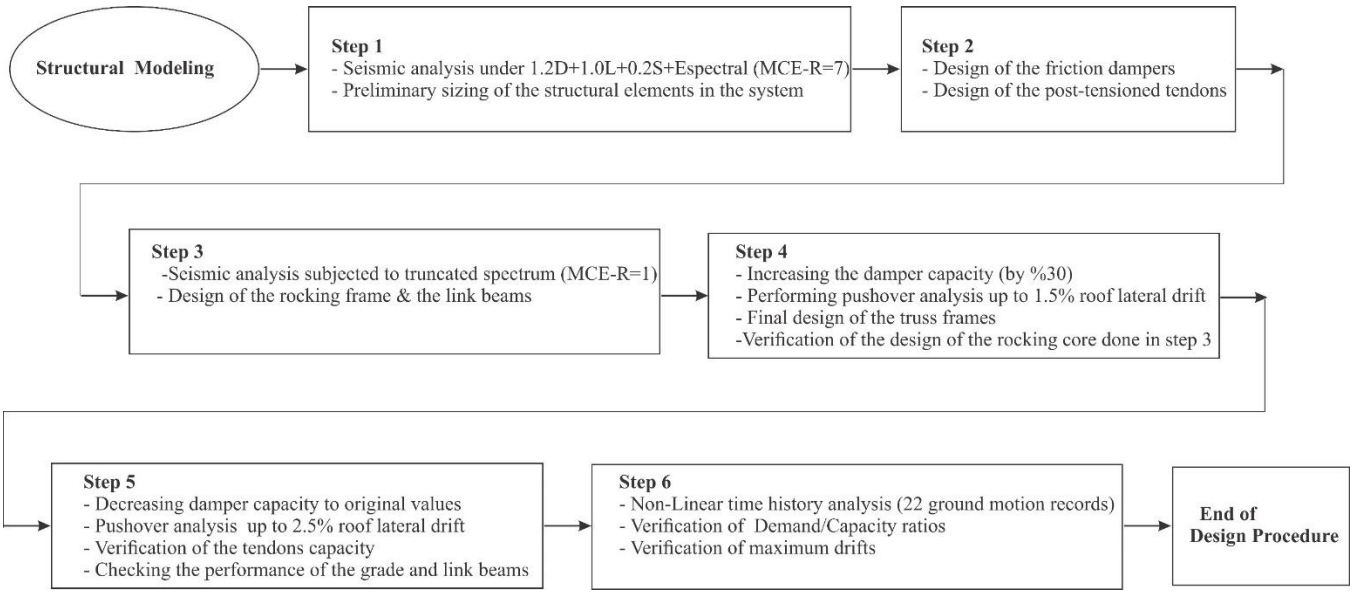

Figure 6-6 : Design procedure flowchart for RF-TMF

6.8 Non-linear Static Analysis (NSA):

Nonlinear static analysis, in the form cyclic displacement-controlled pushover, can provide an estimation of the structure's behavior and provide an initial evaluation of the performance of the dampers and tendons under seismic loads.

Figure 6-7, shows the force-displacement graphs, from the cyclic pushover of the buildings up to the target displacement of 1.5% drift. The results show that all archetype buildings exhibit stable hysteretic behavior with a significantly large energy dissipation capacity, primarily attributed to the friction dampers. Furthermore, the buildings exhibit robust stability, with the post-tensioned tendons delivering positive stiffness (re-centering capability) that effectively reduces the P-Δ effect in the post-slip range. However, given the significant P-Δ effect in the system from the parent building and the large number of friction dampers, which result in high energy dissipation capacity, achieving a fully self-centering response with a flag-shaped hysteresis that can entirely eliminate residual drifts requires much larger tendons (i.e., many more strands per tendon) and a significantly larger post-tensioning force.

The shape of the cyclic pushover curves shows that the combined response curve and equivalent stiffness of system correspond to the conceptual graphs represented in Figure 6-5.

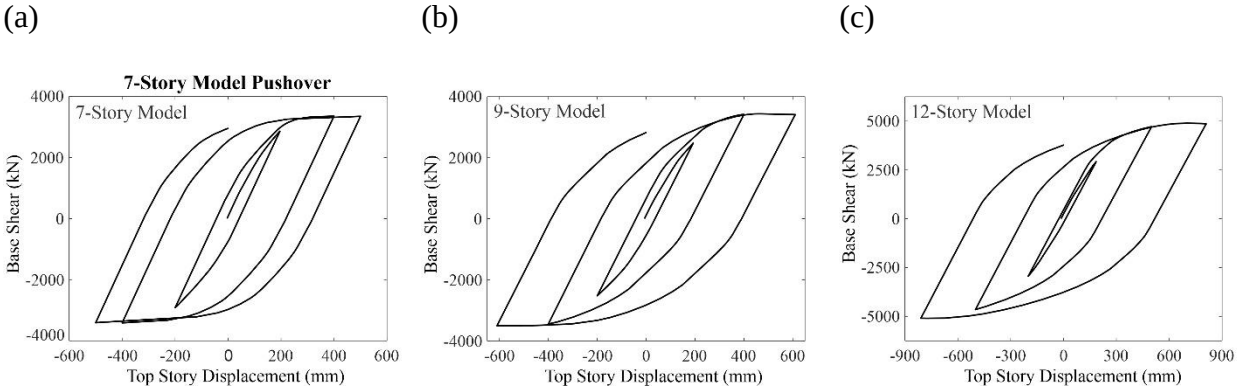

Figure 6-7: Force-displacement curve of pushover analysis up to the target drift for the a) 7-, b) 9- and c) 12-story buildings

6.9 Nonlinear Time History Analyses (NLTHA):

To simulate the behavior of the archetypes under target earthquakes and verify the design procedure, the numerical models are subjected to a set of non-linear time history analyses (NLTHA). The analyses are performed using 22 ground motion records from 14 intense seismic events which are suggested in FEMA P-695 (Federal Emergency Management Agency 2009).

The selected records are normalized and scaled to the MCE level spectrum of the selected site (Los Angeles area). The scaling is performed by factors obtained from anchoring the spectral acceleration of the records to the MCE level spectrum (Figure 6-8), at the first natural period for each archetype.

The modal analyses showed that the first natural period of the 7-, 9- and 12-story archetypal buildings are 1.4 s,1.8 s and 2.2 s, respectively. The anchor point of the selected records for the 7-story model is illustrated in Figure 6-9.

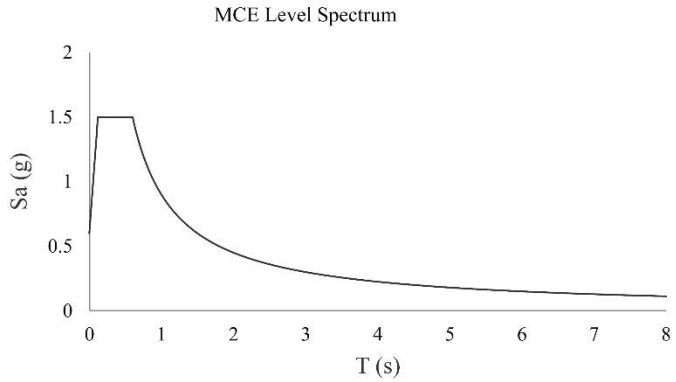

Figure 6-8: MCE spectra for Los Angeles Area- CA -USA

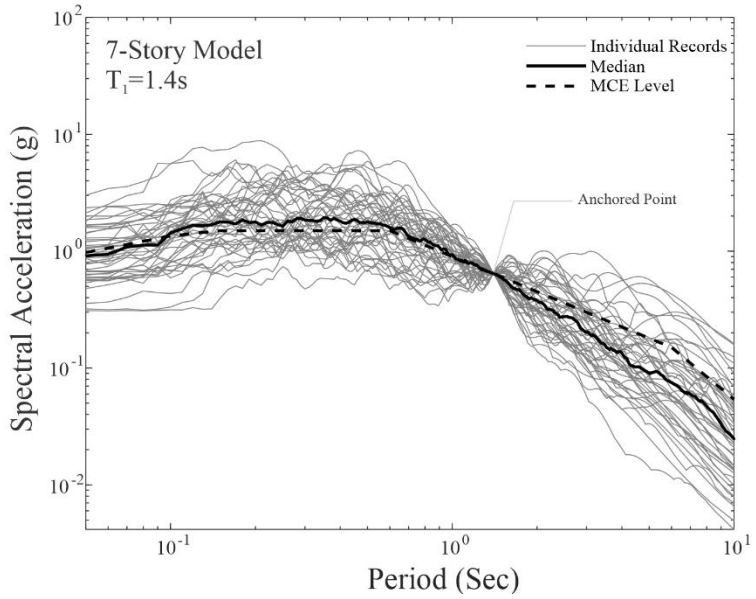

Figure 6-9: The spectral accelerations of the individual records matched to the design spectrum at first-mode periods of the 7-story RF-TMF model

6.9.1 Story Drifts:

Lateral drift is a key parameters to determine the possibility of the propagation and intensity of plastic deformations in the structural elements during an earthquake and identify its seismic performance level. Moreover, this factor is used to verify the efficiency of the utilized design procedure and validate the achievement to the intended performance level. The inter-story drifts vs

story height graphs, which are resulted from the application of the nonlinear time history analysis (NLTHA) to the archetypes, are illustrated in Figure 6-10.

The graphs show that under the 22 ground motions the seismic drifting through the story levels in all buildings are following an approximately normalized linear pattern overall. This confirms the satisfactory functionality of the rocking core in suppressing the higher mode effects, which forces the system to move in accordance with the first mode pattern, thereby mitigating the risk of soft-story formation and drift-induced damage. This is considered as an important advantage of the system over other conventional systems.

The mean of the transient drift ratios, under the applied records, is approximately 1.38%, 1.25% and 1.27% for the 7- ,9- and 12-story buildings, respectively. The resulted values correspond to damage control level in conventional moment frames according to FEMA 356 (Federal Emergency Management Agency, 2000); however, the system with the post-tensioned rocking core can withstand these drifts and remain operational. This is due to the system's elevated redundancy and stability level, and the fact that any potential damage is expected to be limited to repairable fuse joints.

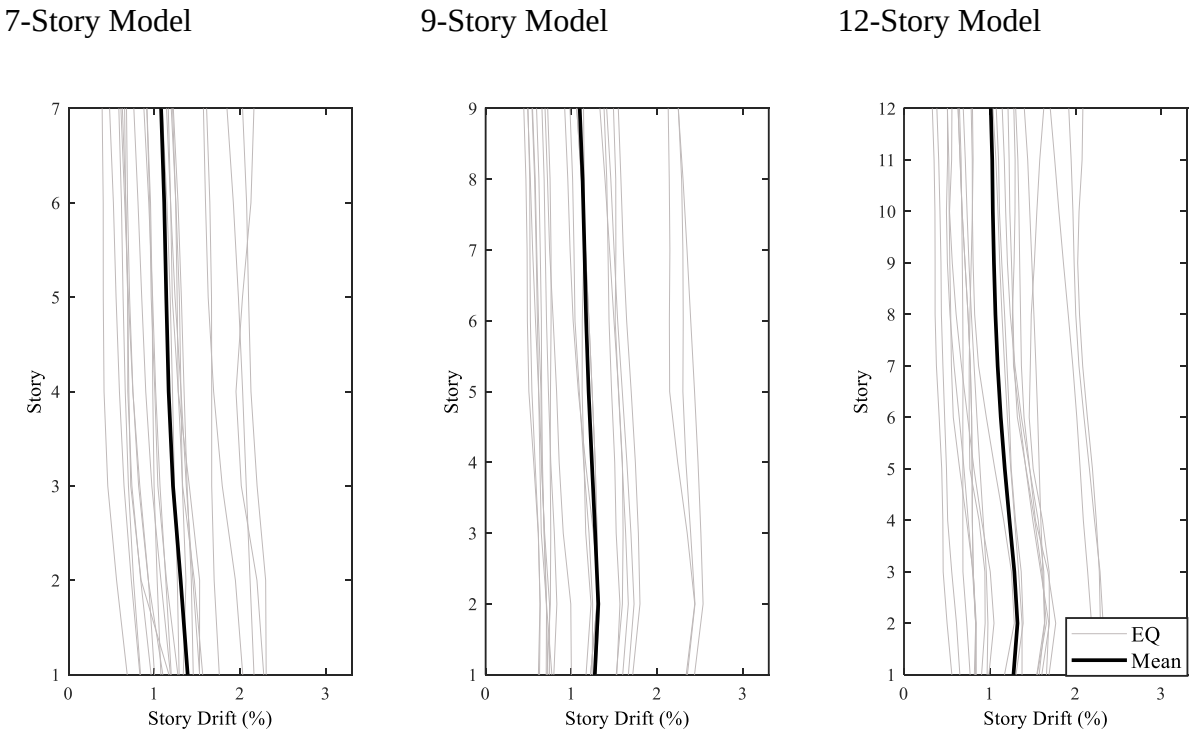

Figure 6-10 : story drift ratio in the 7-, 9- and 12-story archetypal buildings

6.9.2 Residual Drift Results:

Residual drifts ratio is considered as a scale parameter that represents serviceability and performance of a structure and is utilized to determine the post-event repairability capacity of a building as per FEMA P-58-1 (Federal Emergency Management Agency, 2018).

The results from application of NLTHA under 22 strong ground motion records in the studied buildings (Figure 6-11 to Figure 6-13) show that the mean of the experienced residual drift ratios, subjected to the MCE level ground motions, is limited to 0.48%, 0.43% and 0.47% in the 7- ,9- and 12-story models, respectively. Such values of the residual drift verify the repairability of the buildings (FEMA P-58-1, 2018). In this system, residual drifts are attributed to reversible movements confined within the friction dampers (no damage) and plastic deformations in the repairable joints, which are accommodated in the link and support-level grade beams (low damage). Achieving a more effective response to better reduce residual drifts requires balancing the energy dissipation capacity provided by the friction devices with the restoring force in the system, which depends on the size of the tendons and the value of the post-tensioned force. Additionally, optimizing the rocking frame size is necessary, as all factors must be adjusted to provide a good self-centering reaction. Based on these results, a practical and viable post-event repair and alignment scenario for these buildings is likely, following a major earthquake.

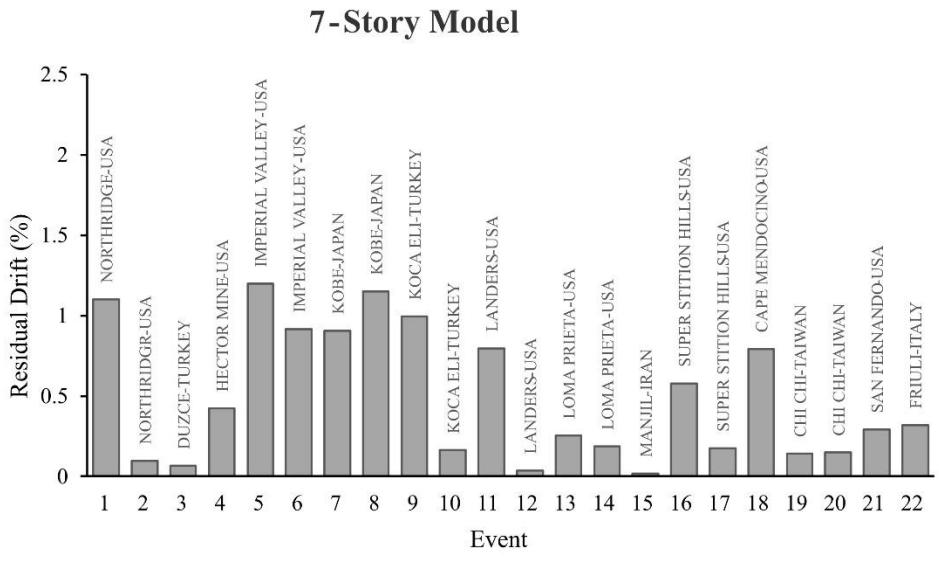

Figure 6-11: Residual drift ratio in the 7-Story building for 22 seismic events

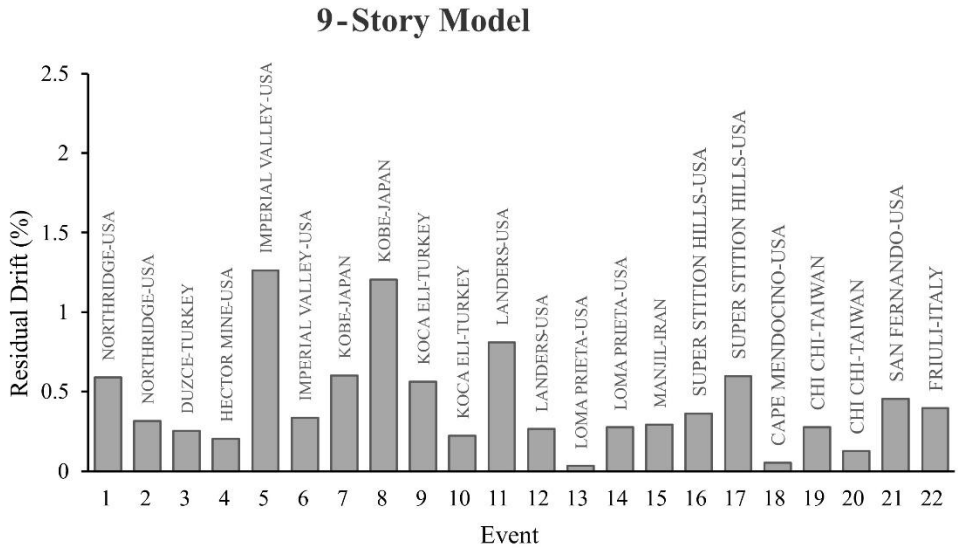

Figure 6-12: Residual drift ratio in the 9-Story building for 22 seismic events

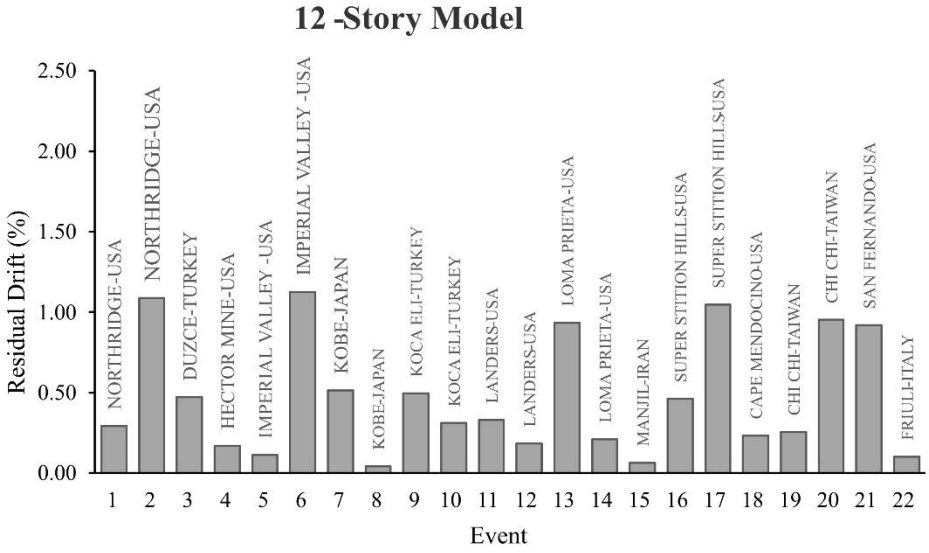

Figure 6-13: Residual drift ratio in the 12-Story building for 22 seismic events

6.9.3 Performance of the friction devices and post-tensioned tendons

Friction Dampers:

The friction devices play an important role in dissipating the seismic energy that results in limiting the induced seismic demand in the system and reducing the damage in the structural and non-structural elements.

Figure 6-14, illustrates the force-displacement graphs for a set of typical dampers installed in the studied RF-TMFs, that show their hysteretic response and energy dissipation capacity subjected to the applied ground motions. It is seen that the slip force in the dampers match the intended design values which are represented in Table 6-1.

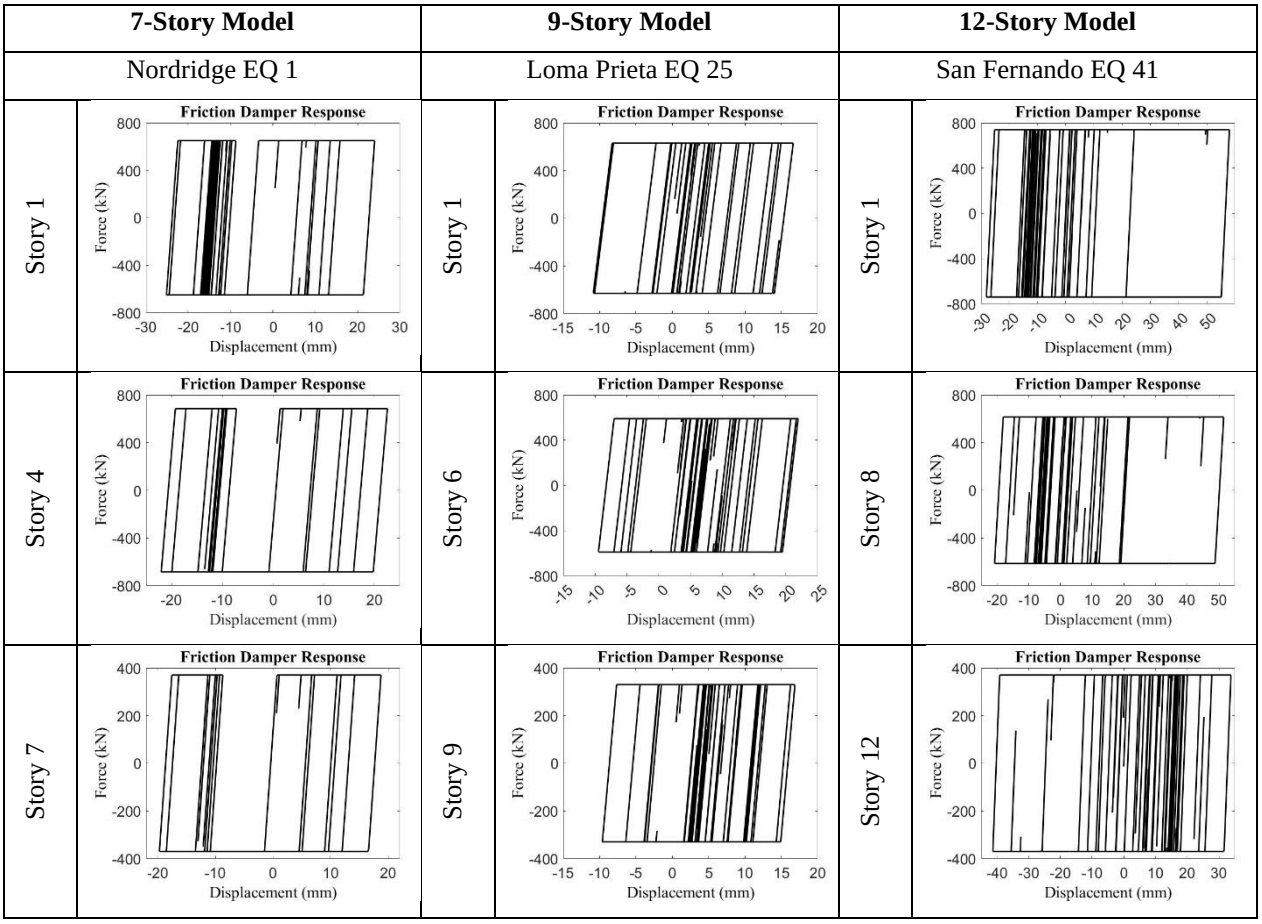

Figure 6-14: Typical force-displacement plots under three seismic events for the 7-, 9- and 12-story archetypal buildings

Table 6-1: Slip force of the dampers installed in the 7-, 9- and 12-story archetypal buildings

Story ID	7-Story	9-Story	12-Story
	$F_{friction}$ (kN)	$F_{friction}$ (kN)	$F_{friction}$ (kN)
12	-	-	370
11	-	-	560
10	-	-	575
9	-	330	615
8	-	525	635
7	370	545	640
6	655	590	690
5	670	620	715
4	685	635	730
3	715	690	800
2	785	725	835
1	650	630	740

Steel Tendons:

The post-tensioned tendons incorporated into the rocking frames serve as indispensable stabilizers, and are crucial for maintaining the integrity of the entire system. Additionally, they play a pivotal role in regulating and enhancing the lateral stiffness of the system. The tendons are made of 7-wire low relaxation high strength strands (grade 270) with an area of 190 mm^2 and maximum yield force of 318 kN at 1% strain. The results of the NLTHA verify that all the tendons well suit with the rocking core and remain operative under the applied ground motions. The post-tensioned force applied in the tendons is limited to about 15% of their yielding force with 1% strain.

Subjected to the applied earthquakes, the maximum strains in the tendons represented in Figure 6-15, are limited to 0.35%, 0.35% and 0.31% in the 7-,9- and 12-story RF-TMFs, respectively. The captured strain values which are about one third of the tendons strain at yielding stage (%1) guarantee the perfectly elastic behaviour of them during the target seismic events.

The size of the tendons (i.e., number of strands per tendon) and the applied post-tensioned forces are represented in Table 6-2.

To improve the tendons efficiency in the 9- and 12-story rocking frames, two pairs of tendons, each with half of the required strands, are placed between the 7^{th} and 9^{th} stories and the support,

respectively. Tendons with a similar number of strands are then installed between the highest level and the support.

Table 6-2: The size & post-tensioned force of the self-centering tendons in the rocking frame

Story ID	7	9	12
Tendon's size (number of strands)	36 A_p*	50 A_p	72A_p
Total Post-tensioned force	1700 kN	2300 kN	3400 kN

* A_p (Strand area) = 190 mm^2, Grade 270, F_y =318 kN

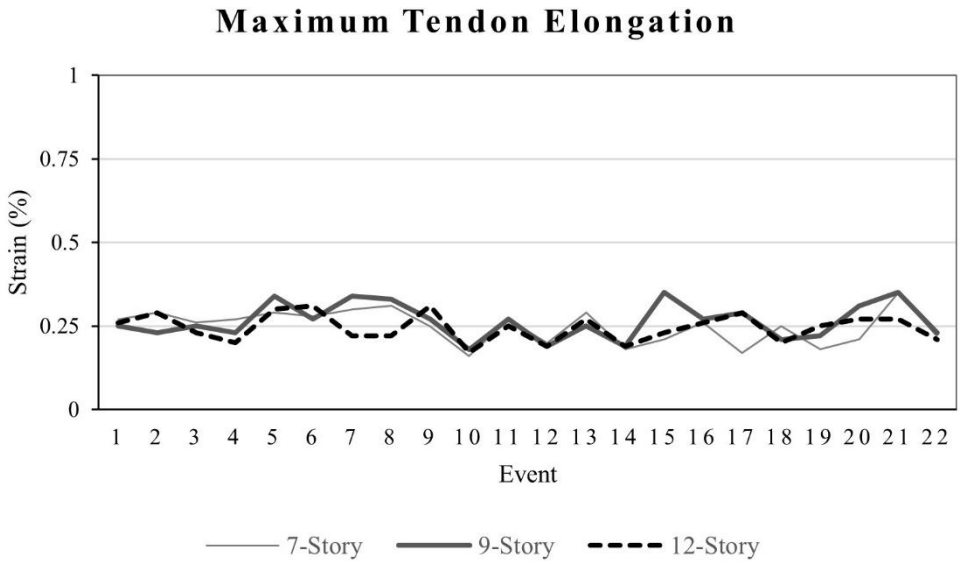

Figure 6-15: Maximum strain of the tendons in the 7-,9- and 12-story building subjected to 22 seismic events

6.9.4 Fuse Connections in Link and Grade Beam:

The link beams, inter-connecting the truss frames with the rocking core, transfer the forces between the two systems and participate in the regulation of the lateral movement through deflections.

The analyses show that under a seismic event the combination of the axial force and bending moment enforced to these elements, can lead to seismic damage and formation of plastic hinges in the connection zone where they are rigidly attached to the rocking core. To control seismic damage, repairable joints (fuse joints) with a damage control detailing are accommodated in the connection zones. The details of the proposed fuse connections used in the link and grade beams are

represented in Figure 6-16. In this type of fuse joints, the web of the link beam is joined to the web of a short stub beam, attached rigidly to the rocking frame with a long-slotted shear connection and a pair of replaceable moment transfer plates (RBS-treated) connecting the flanges. Similar fuse connections are accommodated between the grade beams and columns' feet where the columns are vulnerable to seismic damage. The fuse joint in the grade beams limits the seismic moment developed in the column and prevents the propagation of a plastic hinge. The first propagation of the plastic hinges in the fuse connection installed in link and grade beams for the 7-story RF-TMF during a typical ground motion (Northridge event) is represented at Figure 6-17.

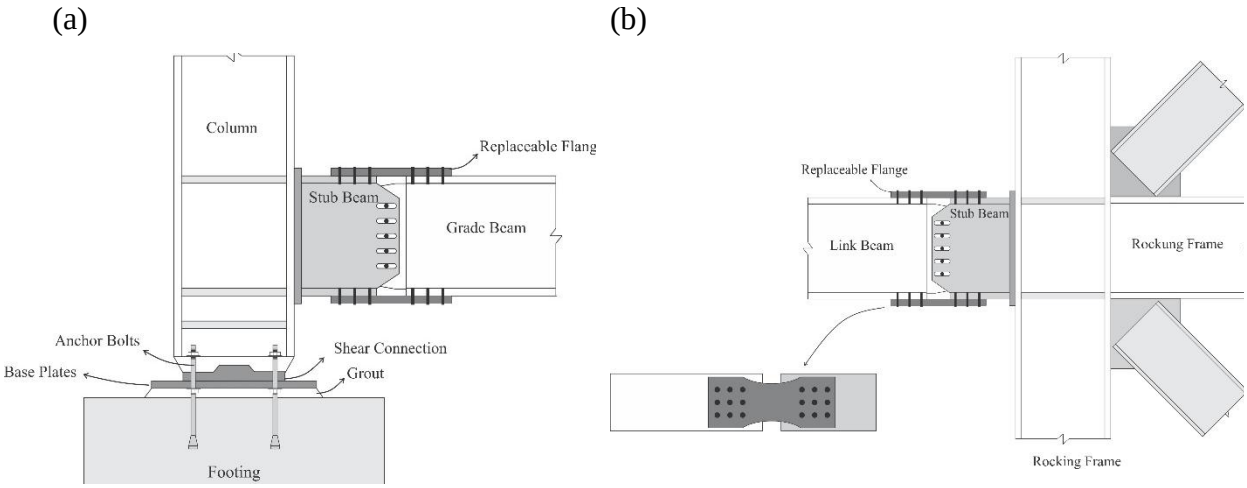

Figure 6-16: a) Fuse connection in Grade Beam – b) Fuse connecion in Link Beam

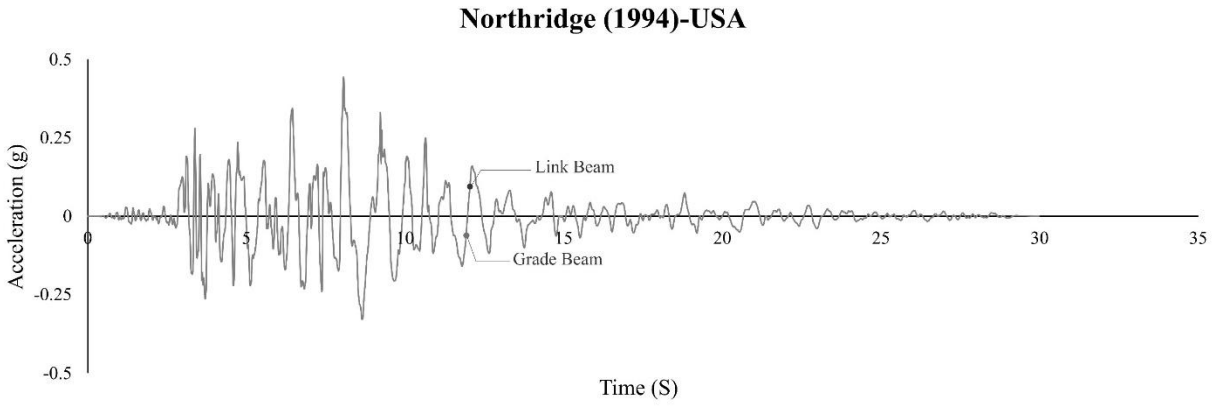

Figure 6-17: Propagation of first plastic hinge at the fuse joints of the link & grade beams in the 7-story model subjected to a selected ground motion (Northridge).

6.9.5 Demand in Columns:

In structural systems, the columns have the most important role in providing structural stability. In the proposed system, the interior columns resist larger seismic demands, including axial force and bending moment, compared to the exterior columns, due to the lateral load distribution resulting from the system configuration. The graphs shown in Figure 6-18, represent the demand per capacity ratio (D/C) for the interior columns calculated in accordance with AISC 360-16 guidelines. It is seen, the largest D/C ratio, happening in the first story columns' feet, are limited to approximately 0.85, 0.82 and 0.86 in the 7-, 9- and the 12- story RF-TMFs, respectively. These results represent that the columns are well protected against seismic damage.

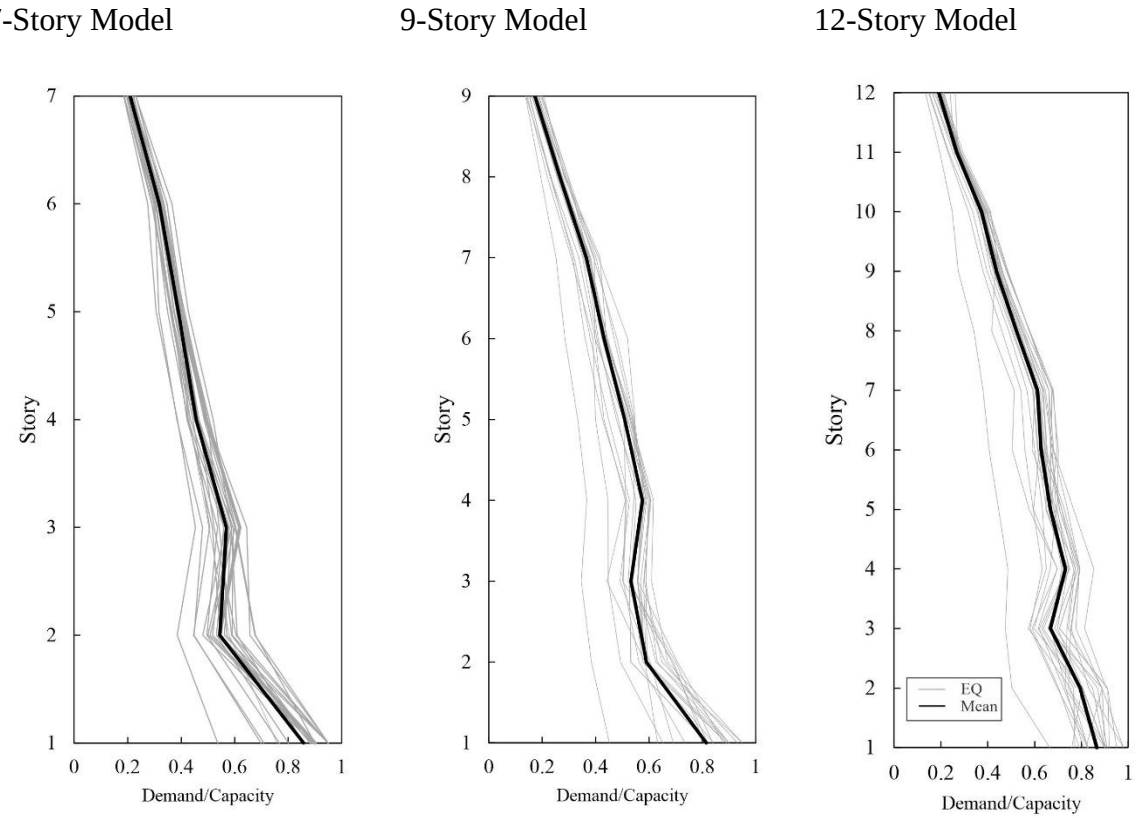

Figure 6-18: Demand /capacity ratio in the interior columns of the 7-,9- and 12-story building subjected to 22 seismic events

6.10 Conclusion:

This study represented a new hybrid earthquake resistant structural system with the goal of minimizing post-event repair. A set of analyses including non-linear static (NLSA) and non-linear time history (NLTHA) analyses were applied to the archetypal buildings to study the seismic response of this system. The simulation of the structural models under a set of 22 strong earthquakes showed that the system covered the target structural response under the applied ground motion records and remained stable without experiencing any structural damage in its main structural elements. In this system all the friction devices and post-tensioned tendons, which were employed to improve the performance, remained functional during seismic events. The two components of the hybrid system including the F-TMFs and the rocking core (R) well matched and worked as a united system such that RF-TMF benefited from the advantages of both contributed systems. The specific conclusions related to the system's performance under the 22 ground motions are summarized as follows:

1. The mean value of the residual and inter-story drifts in the archetypal buildings was limited to less than 0.5% and 1.4% overall.
2. The system sustained minimal damage, confined to the fuse joints, making it feasible for repair and realignment.
3. A considerable portion of the induced kinetic energy of the applied earthquakes was dissipated by the friction in the dampers.
4. The experienced slip force in the friction dampers was limited to the specified design values (design values).
5. In all RF-TMF models, the tendons remained elastic and the maximum strain in the post-tensioned tendons was limited to approximately 30% of their yield strain.
6. The dynamic P-Δ effect was efficiently neutralized by the post-slip stiffness provides by the tendons.
7. The columns remained elastic (no plastic hinge) during the earthquakes.
8. The D/C ratios in the interior first story columns in the 7- , 9- and 12-story RF-TMFs was limited to of 0.85, 0.82 and 0.86, respectively.
9. The rocking core acted as a strongback in the system, eliminating the risk of soft-story formation and controlling the movement pattern during earthquakes. As a result, the system

predominantly behaved in a first-mode pattern with a uniform (normalized linear) drifting response.

10. To enhance the response and further minimize residual drifts, it is essential to balance the energy dissipation capacity contributed by the dampers with the tendon size, post-tension force, and optimized rocking frame size, as all these factors must be fine-tuned to improve the system's self-centering capability.

6.11 Future Studies

The findings represented in this paper are obtained based on theoretical studies and numerical simulations performed with computers. Therefore, it is considered as a prelude to further studies. In this regard, a set of experimental tests on real prototypes are essentially required to support the theoretical output and better investigate the characteristics and performance of the system. To improve the sustainability in the proposed system, it is intended to replace the fuse joints with damage-free connections, designed with rotational springs or friction devices. Optimization of tendon size, post-tensioning force, and rocking frame dimensions, considering the energy dissipation capacity, is also recommended to achieve a higher level of performance.

6.12 Appendix I:

Table 6-3: Sections used in Truss Frames

Storey ID	Diagonal	Brace	Chord	Vertical	Column
7	2C150x15.6	2C75x5.2	2C200x17.1	2C100x9.3	W360x262
6	2C150x15.6	2C75x5.2	2C200x20.5	2C100x9.3	W360x262
5	2C150x15.6	2C75x5.2	2C200x20.5	2C100x9.3	W360x287
4	2C150x15.6	2C75x5.2	2C230x22	2C100x9.3	W360x287
3	2C150x15.6	2C75x5.2	2C230x22	2C100x9.3	W360x287
2	2C150x15.6	2C75x5.2	2C230x22	2C100x9.3	W360x314
1	2C150x15.6	2C75x5.2	2C230x22	2C100x9.3	W360x314
9-Storey					
	Diagonal	Brace	Chord	Vertical	Column
9	2C150x15.6	2C75x5.2	2C200x17.1	2C100x9.3	W360x287
8	2C150x15.6	2C75x5.2	2C200x20.5	2C100x9.3	W360x287
7	2C150x15.6	2C75x5.2	2C200x20.5	2C100x9.3	W360x287
6	2C150x15.6	2C75x5.2	2C230x22	2C100x9.3	W360X314
5	2C150x15.6	2C75x5.2	2C230x22	2C100x9.3	W360X314
4	2C150x15.6	2C75x5.2	2C230x22	2C100x9.3	W360X314
5	2C150x15.6	2C75x5.2	2C230x22	2C100x9.3	W360x382
2	2C150x15.6	2C75x5.2	2C230x22	2C100x9.3	W360x382
1	2C150x15.6	2C75x5.2	2C230x30	2C100x9.3	W360x382
12-Storey					
	Diagonal	Brace	Chord	Vertical	Column
12	2C150x15.6	2C75x5.2	2C200x17.1	2C100x9.3	W360x314
11	2C150x15.6	2C75x5.2	2C200x20.5	2C100x9.3	W360x314
10	2C150x15.6	2C75x5.2	2C200x20.5	2C100x9.3	W360x314
9	2C150x15.6	2C75x5.2	2C200x20.5	2C100x9.3	W360x347
8	2C150x15.6	2C75x5.2	2C230x22	2C100x9.3	W360x347
7	2C150x15.6	2C75x5.2	2C230x22	2C100x9.3	W360x347
6	2C150x15.6	2C75x5.2	2C230x22	2C100x9.3	W360x382
5	2C150x15.6	2C75x5.2	2C230x22	2C100x9.3	W360x382
4	2C150x15.6	2C75x5.2	2C230x22	2C100x9.3	W360x382
3	2C150x19.3	2C75x5.2	2C230x22	2C100x9.3	W360x463
2	2C150x19.3	2C75x5.2	2C230x22	2C100x9.3	W360x463
1	2C150x19.3	2C75x5.2	2C230x30	2C100x9.3	W360x463

Table 6-4: Sections used in Rocking core, Link and Grade Beams

7-Storey				
Vertical Elements Rocking Core	Horizontal Elements Rocking Core	Diagonal Elements Rocking Core	Link Beams	Grade beams
W360x421	W360x262	W360x110	W360x262	W310x283
9-Storey				
Vertical Elements Rocking Core	Horizontal Elements Rocking Core	Diagonal Elements Rocking Core	Link Beams	Grade beams
W360x551	W360x287	W360x110	W360x287	W310x283
12-Storey				
Vertical Elements Rocking Core	Horizontal Elements Rocking Core	Diagonal Elements Rocking Core	Link Beams	Grade beams
W360x744	W360x347	W360x122	W360x347	W310x375

6.13 References

Ajrab, J. J., Pekcan, G., & Mander, J. B. (2004). Rocking wall–frame structures with supplemental tendon systems. *Journal of Structural Engineering, 130*(6), 895-903.

Chao, S.-H., Jiansinlapadamrong, C., Simasathien, S., & Okazaki, T. (2020). Full-scale testing and design of special truss moment frames for high-seismic areas. *Journal of Structural Engineering, 146*(3), 04019229.

Christopoulos, C., Tremblay, R., Kim, H.-J., & Lacerte, M. (2008). Self-centering energy dissipative bracing system for the seismic resistance of structures: development and validation. *Journal of Structural Engineering, 134*(1), 96-107.

De Luca, A., & Guidi, L. G. (2019). State of art in the worldwide evolution of base isolation design. *Soil DynamicsEarthquake Engineering 125*, 105722.

Deierlein, G., Krawinkler, H., Ma, X., Eatherton, M., Hajjar, J., Takeuchi, T., Kasai, K., & Midorikawa, M. (2011). Earthquake resilient steel braced frames with controlled rocking and energy dissipating fuses. *Journal of Steel Construction, 4*(3), 171-175.

Eatherton, M. R., Ma, X., Krawinkler, H., Deierlein, G. G., & Hajjar, J. F. (2014). Quasi-static cyclic behavior of controlled rocking steel frames. *Journal of Structural Engineering, 140*(11), 04014083.

Eatherton, M. R., Ma, X., Krawinkler, H., Mar, D., Billington, S., Hajjar, J. F., & Deierlein, G. G. (2014). Design concepts for controlled rocking of self-centering steel-braced frames. *Journal of Structural Engineering, 140*(11), 04014082.

Faraji, K., & Tremblay, R. (2019). *Multi-story truss moment frames equipped with friction dampers and self-centering system for enhanced seismic performance*. Paper presented at the The Evolving Metropolis-IABSE Congress, New York, New York-USA.

Federal Emergency Management Agency. (2009). Quantification of Building Seismic Performance Factors (FEMA P695). In. USA: Federal Emergency Management Agency

Garlock, M. E., & Li, J. (2008). Steel self-centering moment frames with collector beam floor diaphragms. *Journal of Constructional Steel Research, 64*(5), 526-538.

Grigorian, M. (2021). Resiliency and post-earthquake realignment. *30*(5), e1836. doi:https://doi.org/10.1002/tal.1836

Grigorian, M., & Grigorian, C. E. (2018). Sustainable earthquake-resisting system. *Journal of Structural Engineering, 144*(2), 04017199.

Grigorian, M., Moghadam, A. S., & Mohammadi, H. (2017). Advances in rocking core-moment frame analysis. *Bulletin of Earthquake Engineering, 15*(12), 5551-5577.

Grigorian, M., Sedighi, S., Targhi, M. A., & Targhi, R. A. (2023). Sustainable earthquake-resistant mixed multiple seismic systems. *Journal of Structural Engineering, 149*(3), 04023002.

Jiansinlapadamrong, C., Park, K., Hooper, J., & Chao, S.-H. (2019). Seismic design and performance evaluation of long-span special truss moment frames. *Journal of Structural Engineering, 145*(7), 04019053.

Lai, J.-W., & Mahin, S. A. (2015). Strongback system: A way to reduce damage concentration in steel-braced frames. *Journal of Structural Engineering, 141*(9), 04014223.

Lignos, D. G., & Krawinkler, H. (2011). Deterioration modeling of steel components in support of collapse prediction of steel moment frames under earthquake loading. *Journal of Structural Engineering, 137*(11), 1291-1302.

Ma, X. (2010). *Seismic design and behavior of self-centering braced frame with controlled rocking and energy-dissipating fuses.* Stanford University,

MacRae, G. A., Kimura, Y., & Roeder, C. (2004). Effect of column stiffness on braced frame seismic behavior. *Journal of Structural Engineering, 130*(3), 381-391.

Mahin, S. A. (1998). Lessons from damage to steel buildings during the Northridge earthquake. *Engineering structures, 20*(4-6), 261-270.

Martin, A., Deierlein, G. G., & Ma, X. (2019). Capacity design procedure for rocking braced frames using modified modal superposition method. *Journal of Structural Engineering, 145*(6), 04019041.

Mohammadi, R. K., El Naggar, M., & Moghaddam, H. (2004). Optimum strength distribution for seismic resistant shear buildings. *International Journal of Solids and Structures, 41*(22-23), 6597-6612.

Pan, P., Zamfirescu, D., Nakashima, M., Nakayasu, N., & Kashiwa, H. (2005). Base-isolation design practice in Japan: introduction to the post-Kobe approach. *Journal of Earthquake Engineering, 9*(01), 147-171.

Qu, Z., Wada, A., Motoyui, S., Sakata, H., & Kishiki, S. (2012). Pin-supported walls for enhancing the seismic performance of building structures. *Earthquake Engineering & Structural Dynamics 41*(14), 2075-2091.

Ricles, J. M., Sause, R., Garlock, M. M., & Zhao, C. (2001). Posttensioned seismic-resistant connections for steel frames. *Journal of Structural Engineering, 127*(2), 113-121.

Simpson, B. G., & Mahin, S. A. (2018). Experimental and numerical investigation of strongback braced frame system to mitigate weak story behavior. *Journal of Structural Engineering, 144*(2), 04017211.

Steele, T. C., & Wiebe, L. D. (2016). Dynamic and equivalent static procedures for capacity design of controlled rocking steel braced frames. *Earthquake Engineering &Structural Dynamics, 45*(14), 2349-2369.

The American Institute of Steel Construction. (2016). Specification for Structural Steel Buildings-ANSI/AISC 360-16. In. American Institute of Steel Construction, Chicago, IL: AISC.

The American Society of Civil Engineers. (2022). Minimum Design Loads and Associated Criteria for Buildings and Other Structures (ASCE 7-2022). In. USA: The American Society of Civil Engineers,.

The World Bank. (2023). Earthquake Damage in Türkiye Estimated to Exceed $34 billion: World Bank Disaster Assessment Report. (PRESS RELEASE NO: 2023/ECA/66).

Tremblay, R., & Faraji, K. (2019). *Steel truss moment frames with self-centring energy dissipation mechanisms for enhanced seismic performance*. Paper presented at the 12th Canadian

Conference on Earthquake Engineering, Quebec City, June 17-20, 2019, Quebec City- QC-Canada.

Wang, W., Fang, C., Yang, X., Chen, Y., Ricles, J., & Sause, R. (2017). Innovative use of a shape memory alloy ring spring system for self-centering connections. *Engineering structures, 153*, 503-515.

Wiebe, L., & Christopoulos, C. (2009). Mitigation of higher mode effects in base-rocking systems by using multiple rocking sections. *Journal of Earthquake Engineering, 13*(S1), 83-108.

Wu, Y., Song, X., Gu, X., & Luo, L. (2018). Dynamic performance of a multi-story traditional timber pagoda. *Engineering structures, 159*, 277-285.

CHAPTER 7 CONCLUSION AND RECOMMENDATIONS

7.1 General

This final chapter includes the principal findings and conclusions of this research performed during the PhD program. Recommendation for future studies is included in this chapter.

The primary original contributions of this thesis work, which manifest the achievements of this PhD Program, are delineated as follows:

1- Two novel earthquake resistant and repairable low damage systems, FT-TMF and RF-TMF, were introduced and studied.
2- A practical and reliable analysis and force based design procedure for each systems with respect to both Canadian and American standards and provisions were developed.
3- The seismic performance of the proposed systems was verified by means of robust and precise computational simulation and numerical analyses.
4- The effectiveness of the applied energy dissipation devices and the self-centering mechanism, in improving both systems' performance under seismic events, were verified.
5- The compatible and satisfactory functionality of the friction dampers and elastic tendons in the FT-TMF system during seismic events was confirmed.
6- The compatibility of the two employed truss moment frames (F-TMF) and the post-tensioned rocking frame (R) in the hybrid RT-TMF system were proved.
7- The findings and numerical results are a solid base for future experimental studies on the proposed structural systems.

7.2 Summary of the studies and findings:

This study proposed two practical earthquake resistant systems which were developed based on the STMF system. The main objective in development of the new systems including FT-TF and RF-TMF, was to employ a damage-free energy dissipation device with a self-centering mechanism in a structural system to achieve an improved response and higher level of resistance and resilience during intense seismic events. These systems were expected to maintain their post-event operability with minimal required repair adhering to structural sustainability concept.

The first studied system, named FT-TMF, was a truss moment frame enhanced with friction dampers and steel tendons. A detailed step by step analysis and design method was developed for this system and it was examined in a group of representative 4-, 7- and 12-storey buildings located in Vancouver, BC. The buildings under investigation underwent 15 nonlinear time history analyses each, to numerically simulate earthquake conditions and investigate their seismic behaviour. The analytical results showed that the buildings with FT-TMF system maintained their global stability and the ground motions did not cause any collapse in any of the buildings. The largest inter-storey drifts of the buildings with FT-TMF; occurred in the 12-storey model and were about 2.8%, while they were diminished to 2.1% by augmenting the tendons sizes in the model by 30% so that it verified the effectiveness of the tendons in controlling the drifting. Moreover, the resulting strain in the tendons were at least 50% less than ultimate capacity which guaranteed the elastic response and a reliable self-centering reaction in tendons. The 12-storey model, with the worst severe P-Δ effect, exhibited the highest residual drifts of about 0.8% while a 30% increase in the tendon size the residual drift were limited to 0.5%. The resulted residual drift values confirmed that the archetypal buildings could maintain post-event serviceability. Since the structural members such as the columns experienced seismic demands less than their capacity, it was perceived that they remain elastic. All friction dampers performed very well, and tendons worked elastically as expected.

To better understand the behaviour of the system it was subjected to a collapse capacity evaluation analyses, based on FEMA P-695, to quantify the strength and resilience of this system under intense seismic events. The representative model buildings were considered to be located in Los Angeles Area, CA, USA. They were subjected to a series of Incremental Dynamic Analyses (IDA) by application of 44 far-field strong ground motions. The IDA results revealed that the 4-, 7- and 12-storey buildings demonstrated median collapse intensities $\hat{S}_{CT}(g)$ approximately equal to 1.85g, 1.78g, and 1.22g, respectively.

A 30% increase in the tendon's size in the 12-story model, which showed the weakest collapse resilience, led to about 28% enhancement expressed as $\hat{S}_{CT}(g) = 1.56g$.

The system-level uncertainty, which were qualitatively ranked as "superior", "good", "fair", or "poor" was included in the analyses to study the effect of this parameter in the system's resistance against collapse. The collapse probability in all models with the worst level of uncertainty (poor

level) was less than 10% subjected to the MCE level that met the FEMA P-695 criteria for an acceptable structural system.

The second proposed system (RF-TMF) was a hybrid system composed of truss moment frames equipped with friction damper inter-connected to a post tensioned rigid rocking frame via link beams and fuse connections. In this system a set of support-level grade beams were attached to the columns through repairable fuse connections as well.

This system was examined in a set of 7-, 9- and 12-storey archetypes which were considered to be in Los Angeles area, CA,USA. A set of non-linear dynamic time history analyses under 22 strong ground motions, were employed to capture their seismic response. The output of the analyses showed that in all archetypes the lateral drift followed a normalized linear pattern through the heigh, and the average of drifts were limited to about 1.5%. The mean residual drifts were also limited to 0.5%, which represented the satisfactory performance of the rocking system. The friction force in the dampers exactly matched the pre-defined design slip-force and the largest strain in the tendons installed on the rocking frame was limited to about 0.35% which proved their elastic action. In all archetypes the seismic demand in the structural elements such as columns remained less than the capacity and they remained intact during the earthquakes. Some of the fuses accommodated in the link beams experienced plastic deformations, however due to the post-yielding hardening in steel they kept their strength until the end of the events.

All in all, this study proposed two earthquake resistant systems. Both proposed systems exhibited satisfactory seismic performance as confirmed through rigorous numerical analyses. Notably, when subjected to ground motions at the design level, both systems exhibit either minimal damage or none at all, allowing them to remain operational. This study was considered a prelude and an initial step towards further advanced studies including experimental tests on the proposed system.

7.3 Recommendations for future studies

To improve the proposed FT-TMF and RF-TMF systems' seismic resilience, the fuse connection installed in the grade and the link beams can be replaced by rotational springs or friction dampers which can limit the induced force without any damage and remain operational.

An optimization study is recommended to determine and match the size of the steel tendons, the post-tensioning force, and the number and size of rocking frames, considering the energy dissipation capacity in the truss frames with friction damper, in the RF-TMF system to achieve a more elevated response.

A set of experimental tests including quasi-static cyclic and shake table tests, on prototype models is essentially required to determine the behaviour of the systems and their components practically.

7.4 Limitations:

This study was limited to numerical analyses and simulations, which were based on mathematical methods and performed by computer. Mathematical technics and computational simulations inherently include some approximation and simplifications that can affect the analytical results. Therefore, advanced experimental tests are required to better study the proposed systems and validate the numerical results.

REFERENCES

Ajrab, J. J., Pekcan, G., & Mander, J. B. (2004). Rocking wall–frame structures with supplemental tendon systems. *Journal of Structural Engineering, 130*(6), 895-903.

Al-Shawwa, N., & Lignos, D. (2023). Web-Based Interactive Tools for Performance-Based Earthquake Engineering. Retrieved from https://resslabtools.epfl.ch/index.php

Aslam, M. (1978). Earthquake rocking response of rigid bodies.

Basha, H. S., & Goel, S. C. (1994). *Seismic Resistant Truss Moment Frames with Ductile Vierendeel Segment*: Department of Civil Engineering, University of Michigan.

Basha, H. S., & Goel, S. C. (1995). Special truss moment frames with Vierendeel middle panel. *Engineering structures, 17*(5), 352-358.

Chao, S.-H., & Goel, S. C. (2008). Performance-based plastic design of special truss moment frames. *Engineering journal, 45*(2), 127.

Chao, S.-H., Jiansinlapadamrong, C., Simasathien, S., & Okazaki, T. (2020). Full-scale testing and design of special truss moment frames for high-seismic areas. *Journal of Structural Engineering, 146*(3), 04019229.

Chen, L., Tremblay, R., & Tirca, L. (2019). Practical seismic design procedure for steel braced frames with segmental elastic spines. *Journal of Constructional Steel Research, 153*, 395-415.

Christopoulos, C., Filiatrault, A., Uang, C.-M., & Folz, B. (2002). Posttensioned energy dissipating connections for moment-resisting steel frames. *Journal of Structural Engineering, 128*(9), 1111-1120.

Christopoulos, C., Tremblay, R., Kim, H.-J., & Lacerte, M. (2008). Self-centering energy dissipative bracing system for the seismic resistance of structures: development and validation. *Journal of Structural Engineering, 134*(1), 96-107.

Clayton, P. M., Dowden, D. M., Li, C.-H., Berman, J. W., Bruneau, M., Lowes, L. N., & Tsai, K.-C. (2016). Self-centering steel plate shear walls for improving seismic resilience. *Frontiers of Structural, 10*(3), 283-290.

Computers&Structures Inc. (2023). SAP2000 (Version 21): CSI. Retrieved from https://www.csiamerica.com/

De Luca, A., & Guidi, L. G. (2019). State of art in the worldwide evolution of base isolation design. *Soil Dynamics Earthquake Engineering 125*, 105722.

Deierlein, G., Krawinkler, H., Ma, X., Eatherton, M., Hajjar, J., Takeuchi, T., Kasai, K., & Midorikawa, M. (2011). Earthquake resilient steel braced frames with controlled rocking and energy dissipating fuses. *Journal of Steel Construction, 4*(3), 171-175.

Dowden, D. M., & Bruneau, M. (2016). Dynamic shake-table testing and analytical investigation of self-centering steel plate shear walls. *Journal of Structural Engineering 142*(10), 04016082.

Eatherton, M. R. (2010). *Large-scale cyclic and hybrid simulation testing and development of a controlled-rocking steel building system with replaceable fuses*: University of Illinois at Urbana-Champaign.

Eatherton, M. R., Ma, X., Krawinkler, H., Deierlein, G. G., & Hajjar, J. F. (2014). Quasi-static cyclic behavior of controlled rocking steel frames. *Journal of Structural Engineering, 140*(11), 04014083.

Eatherton, M. R., Ma, X., Krawinkler, H., Mar, D., Billington, S., Hajjar, J. F., & Deierlein, G. G. (2014). Design concepts for controlled rocking of self-centering steel-braced frames. *Journal of Structural Engineering, 140*(11), 04014082.

Erochko, J., Christopoulos, C., & Tremblay, R. (2015). Design and testing of an enhanced-elongation telescoping self-centering energy-dissipative brace. *Journal of Structural Engineering 141*(6), 04014163.

Faraji, K., & Tremblay, R. (2019). *Multi-story truss moment frames equipped with friction dampers and self-centering system for enhanced seismic performance*. Paper presented at the The Evolving Metropolis-IABSE Congress, New York, New York-USA.

Federal Emergency Management Agency (2009). Quantification of Building Seismic Performance Factors (FEMA P695). In. USA: Federal Emergency Management Agency

Federal Emergency Management Agency. (2018). Seismic Performance Assessment of Buildings (FEMA P-58-1). In. USA: Federal Emergency Management Agency.

Garlock, M. E., & Li, J. (2008). Steel self-centering moment frames with collector beam floor diaphragms. *Journal of Constructional Steel Research, 64*(5), 526-538.

Garlock, M. M., Sause, R., & Ricles, J. M. (2007). Behavior and design of posttensioned steel frame systems. *Journal of Structural Engineering, 133*(3), 389-399.

Ger, J.-F., Cheng, F. Y., & Lu, L.-W. (1993). Collapse behavior of Pino Suarez building during 1985 Mexico City earthquake. *Journal of Structural Engineering, 119*(3), 852-870.

Gilbert, C. F., & Erochko, J. (2019). Development and testing of hybrid timber-steel braced frames. *Journal of Engineering Structures, 198*, 109495.

Goel, S., Leelataviwat, S., & Stojadinovic, B. (1997). Steel moment frames with ductile girder web opening. *ENGINEERING JOURNAL-AMERICAN INSTITUTE OF STEEL CONSTRUCTION INC, 34*(4), 115-125.

Goel, S., Rai, d. C., & Basha, S. (1998). *Special Truss Moment Frame*. Retrieved from

Goel, S. C., & Itani, A. M. (1994). Seismic-resistant special truss-moment frames. *Journal of Structural Engineering, 120*(6), 1781-1797.

Grigorian, C. E., & Grigorian, M. (2015). Performance control and efficient design of rocking-wall moment frames. *Journal of Structural Engineering, 142*(2), 04015139.

Grigorian, M. (2021). Resiliency and post-earthquake realignment. *30*(5), e1836. doi:https://doi.org/10.1002/tal.1836

Grigorian, M., & Grigorian, C. E. (2018). Sustainable earthquake-resisting system. *Journal of Structural Engineering, 144*(2), 04017199.

Grigorian, M., Moghadam, A. S., & Mohammadi, H. (2017). Advances in rocking core-moment frame analysis. *Bulletin of Earthquake Engineering, 15*(12), 5551-5577.

Grigorian, M., Sedighi, S., Targhi, M. A., & Targhi, R. A. (2023). Sustainable earthquake-resistant mixed multiple seismic systems. *Journal of Structural Engineering, 149*(3), 04023002.

Hanson, R., Martin, H., & Martinez-Romero, E. (1986). *Performance of steel structures in the September 19 and 20, 1985 Mexico City earthquakes.* Paper presented at the The National Engineering Conf., AISC.

Ireland, R. C. (1997). *Special truss moment frames in low to moderate seismic regions with wind*: University of Michigan.

Itani, A. M., & Goel, S. C. (1991). *Earthquake resistance of open web framing systems*: Department of Civil Engineering, University of Michigan.

Jiansinlapadamrong, C. (2018). *Seismic performance of double-channel and double-HSS sections, special truss moment frame with buckling restrained braces, and long span Special Truss Moment Frame.*

Jiansinlapadamrong, C., Park, K., Hooper, J., & Chao, S.-H. (2019). Seismic design and performance evaluation of long-span special truss moment frames. *Journal of Structural Engineering, 145*(7), 04019053.

Kim, H.-J., & Christopoulos, C. (2008). Friction damped posttensioned self-centering steel moment-resisting frames. *Journal of Structural Engineering, 134*(11), 1768-1779.

Kim, J., Lee, J., & Kang, H. (2016). Seismic retrofit of special truss moment frames using viscous dampers. *Journal of Constructional Steel Research, 123*, 53-67.

Lai, J.-W., & Mahin, S. A. (2015). Strongback system: A way to reduce damage concentration in steel-braced frames. *Journal of Structural Engineering, 141*(9), 04014223.

Latour, M., D'Aniello, M., Zimbru, M., Rizzano, G., Piluso, V., & Landolfo, R. (2018). Removable friction dampers for low-damage steel beam-to-column joints. *Journal of Soil Dynamics & Earthquake Engineering, 115*, 66-81.

Lignos, D. G., & Krawinkler, H. (2011). Deterioration modeling of steel components in support of collapse prediction of steel moment frames under earthquake loading. *Journal of Structural Engineering, 137*(11), 1291-1302.

Ma, X. (2010). *Seismic design and behavior of self-centering braced frame with controlled rocking and energy-dissipating fuses.* Stanford University,

Ma, X., Borchers, E., Pena, A., Krawinkler, H., Billington, S., & Deierlein, G. (2010). Design and behavior of steel shear plates with openings as energy-dissipating fuses. *John A. Blume Earthquake Engineering Center Technical Report,*.

MacRae, G. A., Kimura, Y., & Roeder, C. (2004). Effect of column stiffness on braced frame seismic behavior. *Journal of Structural Engineering, 130*(3), 381-391.

Mahin, S. A. (1998). Lessons from damage to steel buildings during the Northridge earthquake. *Engineering structures, 20*(4-6), 261-270.

Martin, A., Deierlein, G. G., & Ma, X. (2019). Capacity design procedure for rocking braced frames using modified modal superposition method. *Journal of Structural Engineering, 145*(6), 04019041.

Mckenna, F., Fenves, G. L., Scott, M. H., and Jeremic, B. . (2020). Open system for earthquake engineering simulation (OpenSees) (Version 3.2.1). Berkeley (CA). Retrieved from https://opensees.berkeley.edu/

Mohammadi, R. K., El Naggar, M., & Moghaddam, H. (2004). Optimum strength distribution for seismic resistant shear buildings. *International Journal of Solids and Structures, 41*(22-23), 6597-6612.

Momeni, S., Aoudia, A., Tatar, M., Twardzik, C., & Madariaga, R. (2019). Kinematics of the 2012 Ahar–Varzaghan complex earthquake doublet (M w6. 5 and M w6. 3). *Geophysical Journal International, 217*(3), 2097-2124.

National Research Council of Canada. (2015). National Building Code of Canada (NBCC 2015),. In. Canada: National Research Council of Canada.

Osteraas, J., & Krawinkler, H. (1989). The Mexico earthquake of September 19, 1985—Behavior of steel buildings. *Journal of Earthquake Spectra, 5*(1), 51-88.

Pan, P., Zamfirescu, D., Nakashima, M., Nakayasu, N., & Kashiwa, H. (2005). Base-isolation design practice in Japan: introduction to the post-Kobe approach. *Journal of Earthquake Engineering, 9*(01), 147-171.

Pekcan, G., Linke, C., & Itani, A. (2009). Damage avoidance design of special truss moment frames with energy dissipating devices. *Journal of Constructional Steel Research, 65*(6), 1374-1384.

Peterson, I. (1986). Mexico City's Earthquake: Lessons in the Ruins. *Science News, 129*, 36-36.

Potter, S. H., Becker, J. S., Johnston, D. M., & Rossiter, K. P. (2015). An overview of the impacts of the 2010-2011 Canterbury earthquakes. *International Journal of Disaster Risk Reduction, 14*, 6-14.

Qu, Z., Wada, A., Motoyui, S., Sakata, H., & Kishiki, S. (2012). Pin-supported walls for enhancing the seismic performance of building structures. *Earthquake Engineering & Structural Dynamics 41*(14), 2075-2091.

Ricles, J. M., Sause, R., Garlock, M. M., & Zhao, C. (2001). Posttensioned seismic-resistant connections for steel frames. *Journal of Structural Engineering, 127*(2), 113-121.

Simpson, B. G., & Mahin, S. A. (2018). Experimental and numerical investigation of strongback braced frame system to mitigate weak story behavior. *Journal of Structural Engineering, 144*(2), 04017211.

Steele, T. C., & Wiebe, L. D. (2016). Dynamic and equivalent static procedures for capacity design of controlled rocking steel braced frames. *Earthquake Engineering & Structural Dynamics, 45*(14), 2349-2369.

Steele, T. C., Wiebe, L. D., & Dynamics, S. (2017). Collapse risk of controlled rocking steel braced frames with different post-tensioning and energy dissipation designs. *46*(13), 2063-2082.

The American Institute of Steel Construction. (2016a). Seismic Provisions for Structural Steel Buildings, ANSI/AISC 341-16. In: American Institute of Steel Construction, Chicago, IL.

The American Institute of Steel Construction. (2016b). Specification for Structural Steel Buildings-ANSI/AISC 360-16. In. American Institute of Steel Construction, Chicago, IL: AISC.

The American Society of Civil Engineers. (2017). Seismic Evaluation and Retrofit of Existing Buildings ASCE/SEI 41-17. In. USA: ASCE.

The American Society of Civil Engineers. (2022). Minimum Design Loads and Associated Criteria for Buildings and Other Structures (ASCE 7-2022). In. USA: The American Society of Civil Engineers,.

The Canadian Standards Association. (2019). Design of steel structures CSA S16:19. In: CSA Group.

The World Bank. (2023). Earthquake Damage in Türkiye Estimated to Exceed $34 billion: World Bank Disaster Assessment Report. (PRESS RELEASE NO: 2023/ECA/66).

Tremblay, R. (1993). *Seismic behavior and design of friction concentrically braced frames for steel buildings.* University of British Columbia,

Tremblay, R., & Faraji, K. (2019). *Steel truss moment frames with self-centring energy dissipation mechanisms for enhanced seismic performance*. Paper presented at the 12th Canadian Conference on Earthquake Engineering, Quebec City, June 17-20, 2019, Quebec City- QC-Canada.

Vamvatsikos, D., & Cornell, C. A. (2002). *The incremental dynamic analysis and its application to performance-based earthquake engineering.* Paper presented at the 12th European Conference on Earthquake Engineering.

Vamvatsikos, D., & Cornell, C. A. (2004). Applied incremental dynamic analysis. *Earthquake Spectra, 20*(2), 523-553.

Wang, W., Fang, C., Yang, X., Chen, Y., Ricles, J., & Sause, R. (2017). Innovative use of a shape memory alloy ring spring system for self-centering connections. *Engineering structures, 153*, 503-515.

Wiebe, L., & Christopoulos, C. (2009). Mitigation of higher mode effects in base-rocking systems by using multiple rocking sections. *Journal of Earthquake Engineering, 13*(S1), 83-108.

Wiebe, L., Christopoulos, C., Tremblay, R., & Leclerc, M. (2013). Mechanisms to limit higher mode effects in a controlled rocking steel frame. 1: Concept, modelling, and low-amplitude shake table testing. *Earthquake Engineering & Structural Dynamics 42*(7), 1053-1068.

Wongpakdee, N., & Leelataviwat, S. (2017). Performance-based design of mid-rise buckling-restrained knee braced truss moment frames. *SURANAREE JOURNAL OF SCIENCE TECHNOLOGY, 24*(4), 445-454.

Wongpakdee, N., Leelataviwat, S., Goel, S. C., & Liao, W.-C. (2014). Performance-based design and collapse evaluation of buckling restrained knee braced truss moment frames. *Engineering structures, 60*, 23-31.

Wu, Y., Song, X., Gu, X., & Luo, L. (2018). Dynamic performance of a multi-story traditional timber pagoda. *Engineering structures, 159*, 277-285.

Yang, T., Li, Y., & Goel, S. C. (2015). Seismic performance evaluation of long-span conventional moment frames and buckling-restrained knee-braced truss moment frames. *Journal of Structural Engineering*, *142*(1), 04015081.

Yang, T., Li, Y., & Leelataviwat, S. (2014). Performance-based design and optimization of buckling restrained knee braced truss moment frame. *Journal of Performance of Constructed Facilities*, *28*(6), A4014007.

Zhang, A.-l., Zhang, Y.-x., Li, R., & Wang, Z.-y. (2016). Cyclic behavior of a prefabricated self-centering beam–column connection with a bolted web friction device. *Engineering structures*, *111*, 185-198.